2011 Arctic-Yukon-Kuskokwim Sustainable Salmon Initiative Project Final Product[1]

Landscape Predictors of Coho Salmon

by:

Kelly M. Burnett[2], Daniel J. Miller[3], Rick Guritz[4], Mark A. Meleason[5], Ken Vance-Borland[6], Rebecca Flitcroft[2], Matthew J. Nemeth[7], Justin Priest[7], Nicholas A. Som[8], and Christian E. Zimmerman[9]

2USFS, Pacific Northwest Research Station, 3200 SW Jefferson Way, Corvallis, Oregon 97331
3 Earth Systems Institute, 3040 NW 57th St., Seattle, Washington 98107
4 Geophysical Institute, University of Alaska Fairbanks, 903 Koyukuk Dr., Fairbanks, Alaska 99775
5 Oregon Department of Forestry, Salem Headquarters, 2600 State Street, Salem, Oregon 97310,
6 Oregon State University, Forest Ecosystems and Society, Corvallis, Oregon 97331
7 LGL Alaska Research Associates, Inc., 1101 East 76th Ave, Suite B, Anchorage, Alaska 99518
8US Fish and Wildlife Service, Arcata Fish and Wildlife Office, 1655 Heindon Road, Arcata, California 95521
9 USGS Alaska Science Center, 4210 University Dr., Anchorage, Alaska 99508

14 February 2013

1 Final products of AYK Sustainable Salmon Initiative-sponsored research are made available to the Initiatives Partners and the public in the interest of rapid dissemination of information that may be useful in salmon management, research, or administration. Sponsorship of the project by the AYK SSI does not necessarily imply that the findings or conclusions are endorsed by the AYK SSI.

I. ABSTRACT

Habitat quality and quantity are key abiotic variables driving the abundance and distribution of salmon in freshwater, but understanding about how these variables affect salmon is minimal in the Arctic-Yukon-Kuskokwim (AYK) region. This diminishes opportunities to predict effects of habitat change on salmon or to know whether freshwater factors are related to observed changes in salmon returns. Recent research indicates that statistical methods using geographically limited field surveys and spatially extensive landscape data (e.g., stream, terrain, and vegetation) can reliably estimate habitat characteristics and salmon abundance in freshwater over large areas. The objectives of this study were to: 1) develop and evaluate high-resolution terrain and hydrogeomorphic attributes, directly through remote sensing data, and indirectly through information inferred from spatial patterns in the remote sensing data; and 2) relate juvenile coho salmon abundances to hydrogeomorphic and landscape attributes to identify factors that potentially affect coho salmon distribution and productivity. The study was conducted in the Nome River of northwestern Alaska, USA. This research demonstrated the feasibility of creating highly accurate, high-resolution data over a large area of the AYK, and developed new algorithms and approaches for doing so. For the Nome River basin, we derived from ALOS PRISM satellite data a seamless ortho-rectified optical image mosaic and a 2.5-m Digital Elevation Model (DEM) mosaic (5-m vertical accuracy) that meets National Map Accuracy Standards for Alaska. We also developed processing algorithms to automate DEM production and accuracy evaluation using satellite laser altimetry data – an effective and less expensive alternative to LiDAR data. Until data from the Alaska Statewide Digital Mapping Initiative become available for the AYK region, ALOS PRISM data are a relatively low-cost source of DEMs and ortho-imagery with accuracies and resolutions sufficient to benefit fisheries management. To illustrate, we combined newly created DEMs and field data for the Nome River to delineate a highly resolved stream network along with 14 modeled attributes (e.g., stream gradient, valley-floor width, drainage area) for all channels that support salmonids. By varying the contributing-area threshold and linking to a water mask we developed from PRISM optical imagery, our algorithms produce more spatially and structurally accurate networks than other common tools for delineating streams from DEMs. Although some attributes were derived with existing approaches, we developed new methods for attributes that describe floodplain complexity, indicative of off-channel and complex edge habitats that are important for rearing juvenile salmonids. The extent to which streams freeze during winter, potentially contracting space for egg incubation and juvenile rearing, is another aspect considered. We acquired, terrain-corrected, and geo-coded a time series of Synthetic Aperture Radar (TerraSAR-X) data to classify open water and ice in the Nome River. Field data were also collected during the winter to support a supervised classification. Given the ability to visually identify open water and ice on images from the TerraSAR-X data, we are optimistic about ongoing efforts to develop a statistical model for ice classification on the Nome River, as has been done with SAR data on larger rivers. A new technique we developed allowed linking field data for summer habitat, summer snorkel counts of fish, and winter ice to the 14 DEM-derived attributes and then geo-referencing to nodes in the delineated stream network. We found that juvenile coho salmon were not randomly distributed at any spatial resolution we considered, from the micro-habitat to the tributary scale. Juvenile coho using stream margins were often concentrated around the bank dens of beaver, a link that has not been well described in past studies. More juvenile coho salmon were observed than any other age-class or species of fish in the Nome River basin, consistent with the high coho salmon intrinsic potential we modeled throughout the basin. The channel length in slow-water habitat unit types varied inversely with DEM-derived channel gradient, which may help identify high-capacity stream reaches. Densities of juvenile coho salmon were much greater in slow-water than fast-water habitats, but snorkelers observed no fish in many of the slow-water habitats. This suggests that differences in fish abundance may arise from factors affecting whether or not fish occupy a unit as well as those affecting abundance in occupied units. We are exploring statistical tools necessary to model relationships between the zero-inflated juvenile coho salmon data and hydrogeomorphic and landscape characteristics as well as presence of adult salmonids as potential predators of juvenile coho salmon.

Key Words: Nome River, Norton Sound, landscape characterization, remote sensing, digital elevation models, stream delineation, habitat models, coho salmon, *Oncorhynchus kisutch*

II. Table of Contents

List of Figures

List of Tables

III. INTRODUCTION

Habitat quality and quantity are key abiotic variables driving the abundance and distribution of salmon in freshwater (e.g., Lister and Genoe 1970; Reeves et al. 1989; Burnett 2001), but understanding about how these variables affect salmon is minimal in the Arctic-Yukon-Kuskokwim (AYK) region (AYK SSI 2006). This diminishes opportunities to predict effects of habitat change on salmon or to know whether freshwater factors are related to observed changes in salmon returns. Field surveys, critical to develop needed understanding, are practical for only a small portion of salmon-bearing streams in the AYK.

Recent research indicates that statistical methods using geographically limited field surveys and spatially extensive landscape data (e.g., stream, terrain, and vegetation) can reliably estimate habitat characteristics and salmon abundance in freshwater over large areas. Statistical models have been applied to estimate salmon habitat or relative abundance in regions outside the AYK (e.g., Steel et al. 2004; Burnett et al. 2006; Wissmar et al. 2010; Andrew and Wulder 2011; Anlauf et al. 2011; Woll et al. 2011). Such modeling has contributed to regional salmon conservation and management programs, for instance, by identifying factors affecting production (e.g., Lee et al. 1997), helping establish production goals for basins across a region (e.g., Lawson et al. 2005; Lindley et al. 2006), and evaluating and planning for restoration (e.g., Sheer and Steel 2006; Fullerton et al. 2011).

Despite successes elsewhere that suggest that statistical techniques linking landscape attributes with habitat and fish production are feasible and can benefit salmon management, few examples are available for AYK. Modeling approaches from other regions can transfer directly to AYK streams, as illustrated by relationships linking stream length and coho salmon production applied to two Norton Sound rivers (Nemeth et al. 2009). Additionally, statistical relationships have been developed between moderate-scale hydrogeomorphic attributes and fine-scale salmon habitats with data from selected rivers in the AYK (Whited et al. 2013). Models also need to incorporate the specific ways in which the AYK differs from other regions, including the extent to which streams freeze during winter, potentially contracting space for egg incubation or juvenile rearing (Bradford et al. 2001; NSSTC 2002).

The size and remoteness of the AYK limit availability of extensive high-resolution landscape data as inputs to statistical models of salmon habitat or abundance. A geospatial database of hydrogeomorphic attributes for basins across the North Pacific Rim was developed from moderate-resolution data (Luck et al. 2010). However, these data may be insufficient to resolve stream-adjacent landscape characteristics or streams smaller than fourth order (Luck et al. 2010), which provide considerable salmonid habitat. Landscape data available throughout the entire AYK region include the 1:63,000-scale National Elevation Data (NED) and the National Hydrographic Data (NHD) developed from high-altitude aerial photographs acquired in the 1950s. These terrain and hydrogeomorphic data lack the accuracy and attributes for detailed mapping and

modeling of salmon and their habitats (Clarke and Burnett 2003; Clarke et al. 2008), especially for areas of low topographic relief in the AYK region. Recent technological advances demonstrated that high-quality digital elevation models (DEMs) can be generated from space-borne sensors (e.g., Atwood et al. 2007). The DEMs produced from Shuttle Radar Topography Mission (SRTM) imagery are a prime example, but these exclude areas below 60 degrees north latitude and thus most of the AYK region (Rabus et al. 2003). Interest is growing in satellite sensors for directly classifying areas as water (Luck et al. 2010) and for quantifying the amount of overwintering habitat for fish (Wirth 2012). Such new geospatial data could facilitate attempts to develop statistical relationships for estimating variability in salmon productivity in the AYK region

The project is relevant to Framework 3, Theme 4 of the Arctic-Yukon-Kuskokwim Salmon Research and Restoration Plan (AYK SSI 2006). "Escapement goal setting to ensure sustainable fisheries can best be accomplished by using stock-recruitment models in combination with life-history and habitat-based modeling." Specifically, the research addressed the 2008 RFP Question of Special Concern, "What are the abiotic and biotic variables driving the abundance and distribution of smolts and juvenile salmon in AYK watersheds?" To approach the Question of Special Concern, the research was intended to explore the development of high-resolution terrain and hydrogeomorphic predictor variables, and the relationships of juvenile coho salmon abundances to hydrogeomorphic and landscape predictors. The intent is to yield models that use field and remotely sensed data to estimate fish abundances and the potential of streams to provide high-quality habitat. These models could ultimately help quantify the spatial variability of production potential at a relatively high resolution within and between basins throughout Norton Sound.

IV. OBJECTIVES

Objective 1. Determine the feasibility, accuracy, and costs of developing high-resolution terrain and hydrogeomorphic predictor variables over a large area, directly through remote sensing data, and indirectly through information inferred from spatial patterns in the remote sensing data.

Objective 2. Determine relationships of juvenile coho salmon abundances to hydrogeomorphic and landscape characteristics that can predict juvenile coho salmon abundances and identify factors that potentially affect coho salmon distribution and productivity over large areas.

All originally proposed components for Objective 1 of the project were met. Most components for Objective 2 were accomplished during the period funded by the AYK SSI (21 October 2008 – 31 March 2011). To continue modeling of coho salmon under Objective 2, we secured a grant from another source and hired a postdoctoral research associate. The grant funded work through December 2012. Three issues extended the anticipated time required for project completion:

1) Delays in negotiating and processing contracts postponed budget authority for expenditures under both Statements of Work for approximately nine months;

2) Overcoming challenges during data processing before fish modeling and ice classification could begin. This required developing a new, more flexible tool for geo-referencing field data to a digital stream network and waiting for engineers at the Alaska Satellite Facility, who were not supported by this grant, to enable the terrain correction and geo-coding functions of the MapReady software for TerraSAR-X before we could process the imagery; and

3) Obstacles during analysis that required exploration of novel methods, such as two-phase hurdle modeling to accommodate the highly patchy distribution of juvenile coho salmon. Modeling of open water from the TerraSAR-X imagery and of juvenile coho salmon is ongoing.

V. METHODS

Study Area

The study was conducted in the Nome River basin of northwestern Alaska, USA (Figure 1). The Nome River flows primarily north to south, entering Norton Sound 5 km east of the town of Nome, Alaska (64°30'14"N latitude; 165°23'58" W longitude). The Nome River basin (415 km^2) is in the Bering Tundra ecoregion (Nowacki et al. 2001) and is similar to other Norton Sound basins in climate, landform, vegetation, and salmonid assemblage.

The climate of the Nome River basin is moist polar, with bitterly cold winter temperatures and typically cool summer temperatures. Elevations range from sea level to approximately 946 m at the northern drainage divide. Coastal lowlands and hills with broad valleys comprise most landforms in the basin, which is underlain by a mosaic of sedimentary, metamorphic, and volcanic rocks. Soils tend toward wet, shallow, and organic because of permafrost occurring in thin to moderately thick layers. Vegetation in the Nome River basin is characterized by moist sedge-tussock tundra with willow (*Salix* spp.), birch (*Betula* spp.), alder (*Alnus* spp.), and ericaceous species typically located in protected areas (swales) or better drained riparian and floodplain soils.

The estimated mean discharge in the Nome River is 6.5 m^3/sec. Peak stream flows occur in June from snowmelt and in late summer from rainfall. Low flows typically occur during March. Ice covers much of the upper Nome River from November to May, with areas in the lower river periodically thawing and refreezing during this period. Based on the ratio of estuary area to drainage area (Bottom and Jones 1990), the Nome River estuary can be characterized as river-dominated. River-dominated estuaries tend to have relatively high energy, narrow floodplains, and low salinity. The outlet and downstream reaches of the Nome River are tidally influenced, with sporadic mixing of fresh and marine waters in the lower river (Nemeth et al. 2005).

The Nome River and its tributaries provide approximately 72 km of spawning and rearing habitat for native coho salmon (O. *kisutch*), which is the salmon species with the longest freshwater rearing period in the basin (Nemeth et al. 2004). Coho salmon spawning habitat is reported to be concentrated on the Nome River between Osborne Creek and Hobson Creek (Gaboury et al. 2005). The Alaska Department of Fish and Game has monitored adult coho salmon escapement into the Nome River basin since 2001(Menard et al. 2011) (Table 1). Twenty-two fish species other than coho salmon have been reported in the basin, including Chinook salmon (*O. tshawytscha*), chum salmon (*O. keta*), pink salmon (*O. gorbuscha*), sockeye salmon (*O. nerka*), arctic grayling (*Thymallus arcticus*), Dolly Varden (*Salvelinus malma*), and whitefish (*Coregonus nasus*) (Nemeth et al. 2005).

Table 1. Estimated escapement of adult salmon by year as source of, and context for, our estimates of juvenile coho salmon in the Nome River, AK during August 2009. Adult salmon escapement data were estimated at a weir by ADF&G (Menard et al. 2011).

	Adult salmon escapement for the Nome River basin					Parental year class for juvenile coho salmon in this study		
Year	Coho	Pink	Chum	Chinook	Sockeye	Age 0	Age 1	Age 2
2001	2,418	3,138	2,859	7	55			
2002	3,418	35,057	1,720	7	29			
2003	548	11,402	1,957	12	47			
2004	2,283	1,051,146	3,903	51	114			
2005	5,848	285,759	5,584	69	381			
2006	8,308	578,555	5,677	43	188			x
2007	2,437	24,395	7,034	13	534		x	
2008	4,605	1,186,554	2,607	28	90	x		
2009	1,370	16,490	1,565	10	103			

The majority of land in the study area is in either State of Alaska or Native Corporation ownership; the remainder is in scattered parcels of private ownership ('Generalized Land Status' BLM-Alaska Spatial Data Management System http://sdms.ak.blm.gov/isdms/imf.jsp?site=sdms). Gold mining and transportation corridors are the primary source of anthropogenic alteration in the Nome River basin. The Nome River and tributaries have been periodically influenced by placer mining, beginning in the early 1900s. Concurrently, three major ditches were constructed on the west slopes of the basin to provide water needed for gold mining. These ditches, sporadically operated and maintained until the mid-1950s, cross several tributaries and run roughly parallel to the main river (Smith 1997). In 1906, a narrow-gauge railroad was completed between Nome and the Kougarok area along most of the Nome River valley. Although evidence remains of the railroad, it was replaced in 1960 by the Nome-Taylor Highway. Some of the tributaries appear to be used as transportation corridors (e.g., Buster Creek and Darling Creek) (Gaboury et al. 2005). Stream channels in the basin have been scoured and aggraded by hydraulic and dredge mining, quarried for gravel for road

construction, simplified by vehicle use, and constrained by the highway. Rural residential uses may influence stream morphology, water quality, and flows, but likely with localized effects. The Nome River basin ranks relatively high among Norton Sound river basins regarding the potential for human effects on streams (http://rap.ntsg.umt.edu/humanfootprintrank).

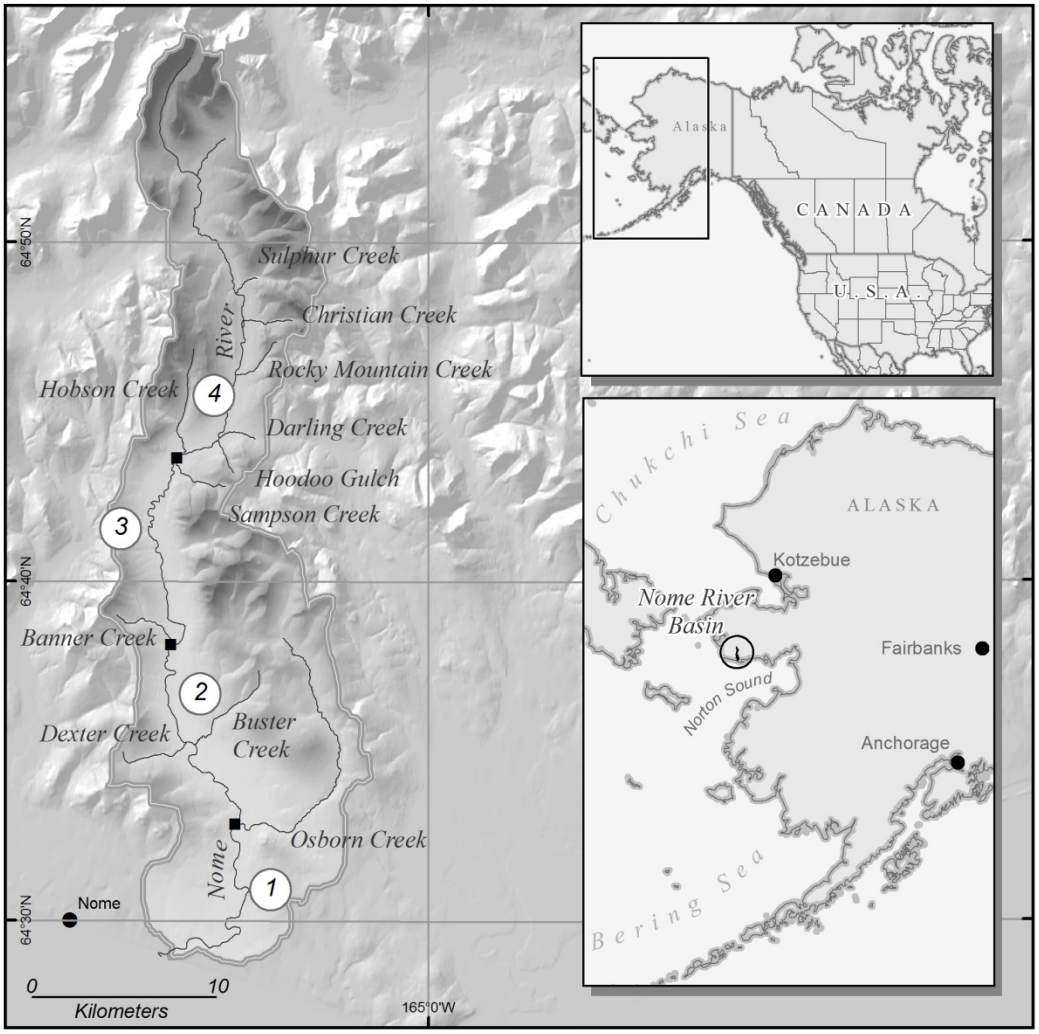

Figure 1. Location and map of the Nome River basin, Alaska. Streams are mapped from the National Hydrography Dataset (NHD) at 1:63,000 scale. Stream segments surveyed on the Nome River during August 2009 are numbered.

Deriving Terrain and Hydrogeomorphic Landscape Predictor Variables

Digital elevation data

To derive DEMs, which are the foundation for much of this study, two types of high-resolution ALOS satellite imagery were acquired from the Japanese Space Agency (JAXA). The ALOS imagery was: 1) PALSAR L-band Synthetic Aperture Radar (SAR) data; and 2) PRISM optical stereo data. We acquired ALOS PALSAR L-Band SAR data: three pairs in fine-beam single polarization mode (between 11 January 2007 and 26 February 2007, 14 January 2008 and 29 February 2008, and 16 January 2009 and 03 March 2009) and one pair in fine-beam dual polarization mode (between 29 August 2007 and 14 October 2007). The PRISM optical sensor generates 2.5-m resolution observations and is the first satellite to collect full stereo data with three coincident viewing geometries (backward, nadir, and forward) in a single pass. All available 2.5-m resolution PRISM optical imagery was examined for the study area, and three relatively cloud-free scenes were acquired (27 May 2007; 08 September 2008; 13 September 2009).

Elevation data to develop and evaluate accuracies of the DEMs were obtained in the field and from the Geoscience Laser Altimeter System (GLAS) instrument onboard NASA's Ice, Cloud, and Land Elevation Satellite (ICESat). The ICESat laser altimetry was demonstrated to be a reliable source of geodetic control (Atwood et al. 2007). Dates for ICESat elevations ranged from 2003 to 2007. We collected the field elevation and location data during September 2008 for 16 geodetic control points (Figure 2 and Table 2).

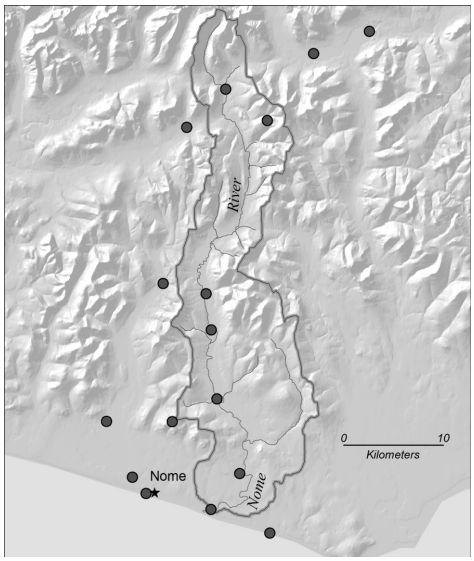

Figure 2. Map of geodetic control points for which GPS coordinates and elevation were collected in the field for the Nome River basin and adjacent areas. Points are shown on a hillshade of the 60-m NED.

The field data were used to anchor the 'floating' satellite imagery to known ground elevations in the Nome River basin as well as to evaluate DEM accuracies for ALOS PALSAR and PRISM and the 60-m National Elevation Data (NED).

Table 2. Data for geodetic control points were obtained with a highly accurate 1-sec data collection frequency Global Positioning System (GPS) (Trimble GeoXT) and were augmented with 1-sec data collection frequency, which we requested from the three nearby University NAVSTAR Consortium (UNAVCO) permanent GPS base stations (AB11, AC07, and AC31). Data were collected for 16 of the 23 potential control points that were assigned an ID prior to going in the field, and are in orthometric heights with EGM96 as the vertical reference.

ID	Northing	Easting	Elevation (m)
1	7152766.552	479483.630	4.482
2	7154385.778	478108.520	10.990
3	7151165.394	485988.385	5.957
5	7154759.371	488874.790	4.635
7	7199150.584	501919.556	136.345
10	7162237.875	486599.595	25.999
11	7172791.537	485508.997	45.199
13	7173821.954	481195.596	48.032
14	7189502.267	483561.984	189.709
15	7193342.123	487479.274	173.697
16	7196900.252	496325.460	135.795
20	7190202.749	491651.057	546.425
21	7148770.702	491920.016	2.184
22	7159974.156	482103.779	341.263
23	7169174.674	486027.453	34.384

Generating DEMs

PALSAR-derived DEMs

High-resolution DEMs were produced with phase and amplitude measurements from four pairs of PALSAR fine-beam data with SAR interferometry using the Gamma Remote Sensing software package (Release 22-Jan-2009, www.gamma-rs.ch). The temporal baseline of selected pairs was one cycle or 46 days. A detailed processing flow was developed from several example scripts provided with the software. The SAR data obtained for a particular location but at different times were combined to overcome problems due to tropospheric water vapor. Each PALSAR DEM covered the entire Nome River basin, and so mosaic processing was not required.

PRISM-derived DEMs

Data were derived from three swaths (ordered and processed from seven-frame products) of the triplet ALOS-PRISM images available for the study area. Two software packages were explored for producing stereo DEMs and ortho-rectified photos from the PRISM optical imagery: 1) the PCI Geomatics OrthoEngine software (Geomatica V10.1); and 2) DSM and ORI Generation Software for ALOS-PRISM (DOGS-AP) (Takaku and Tadono 2009). The PCI OrthoEngine software is an established photogrammetric tool that can process stereo images from a variety of sensors. Stereogrammetry uses differences in the viewing angle of two images, or parallax, to determine distance from an airborne sensor, and thus surface elevation. The DOGS-AP software was optimized to the PRISM sensor model and processing of high-resolution triplet stereo imagery. Preliminary efforts to generate accurate DEMs and nadir-view ortho-rectified images to match the DEM demonstrated the advantages of DOGS-AP over the PCI Geomatics OrthoEngine software for processing the ALOS-PRISM data. For example, the stereo-matching technique used in the DOGS-AP software takes full advantage of the available PRISM image triplets and redundancy between backward-nadir and forward-nadir geometries. Correlating the nadir pairs provided greater accuracy than is possible from single-pair stereoscopic methods used in the OrthoEngine software.

Final PRISM-derived DEMs were produced with only the DOGS-AP software. Initial scene orientation was performed for each of the three dates of imagery by an automated tie-point identification process between the set of three stereo images for each date and applying the sensor model parameters. With these inputs, DOGS-AP refines scene orientation parameters, employing a number of unique characteristics of the image-matching algorithm for the most accurate results. Ground control was not used in stereo processing to ensure consistent products across the entire study area. Prior to processing, each stereo triplet was masked to remove regions of uncertainty due to the presence of cloud or cloud shadows.

We created a seamless large-scale mosaic from multiple swaths of the PRISM sensor, using the JPL Multi-Mosaic software (NASA Jet Propulsion Lab). Multi-Mosaic performs rigorous height and amplitude matching through Fast Fourier Transforms (FFTs) between independent, overlapping data to produce tie-point files that geometrically relate the overlapping products. To minimize noise and improve accuracy of this relationship, statistics-based culling is performed to remove outliers from the data. Geodetic control points were added to adjust the location of each individual swath, improving planimetric accuracy. This relates the geodetic coordinates given in latitude, longitude, and elevation of a GPS coordinate to a measured pixel in the DEM (or ortho-rectified image) as line, sample, and height. A bundle adjustment was performed with the geodetic control points using a three-dimensional affine transform in which like data are combined to reduce errors in a least squares sense. This process solves for allowed degrees of freedom including rotation, scale, and translation. Optimal affine transforms are determined for each input data set that are later used to re-

sample and combine multiple output products into a single seamless mosaic. The software provides a feathering capability for blending seams when necessary to produce the best quality product.

Evaluating DEMs

Accuracies of DEMs from each processing method and the 60-m NED were conducted for the Nome River basin. We assessed differences (minimum, maximum, mean, standard deviation, and root mean square error): 1) between elevations at each geodetic control point obtained from the field with a GPS and from each DEM; and 2) between the elevation at each NASA ICESat laser altimetry point and the mean elevation calculated from each DEM in a circle centered on the ICESat point. Each ICESat point is distributed as a single ground elevation value, which is the average over a 70-m diameter laser altimeter beam 'footprint' (GLA014). Thus, for accuracy evaluation, we selected and buffered each ICESat point coincident with our generated DEMs at a distance of 35 m, using ArcGIS (ESRI v9.3.1 2009). This produced a shapefile with 2477 circles of 70-m diameter centered on the ICESat points. We assigned a unique ID number to each circle and calculated zonal statistics using ArcGIS Spatial Analyst Tools to produce a table summarizing DEM elevation values within each 70-m circle (pixel count, area, and elevation min, max, mean, std, range, and sum).

Extracting a water mask

A water mask was deemed necessary to help guide flow directions when delineating stream channels from the DEM and to characterize channel configuration when generating hydrogeomorphic attributes as potential landscape predictor variables. We directly extracted a final water mask from only the ALOS PRISM 2.5-m ortho-rectified optical image mosaic because hydrographic features were insufficiently depicted with the PALSAR data.

Limited forest cover in the Nome River basin contributes to relatively high contrast between wet and dry areas in the PRISM optical imagery; areas inundated by water appear dark compared to the adjacent land. Capitalizing on this high contrast, we identified water bodies in the imagery by classifying pixels with intensity values below a variable threshold. Specifying a single threshold was not possible because contrast in intensity for wet and dry areas varied between images collected on different dates and at different places. Thus, the process we developed to classify water bodies accounted for these variations in image intensity.

In the first step, intensity contrast was normalized across each image so that all images had the same range of intensity values. Each image has a potential range spanning 0 to 255. However, the range of values in the final images was considerably smaller than this. So that all images started with the same range, we shifted the values in each image so that the minimum was at zero and multiplied the values so that the maximum was at 255. Next, water was distinguished from non-water in the normalized data by specifying threshold intensity

values, which varied with location as a function of the local mean intensity calculated over a circular window of 150-m radius. Then, any patch classified as water with a mean surface gradient exceeding 10% was filtered out. Gradients were estimated from the ALOS PRISM 2.5-m DEM over a 50-m radius. And, finally we developed and applied another filter to target the water mask on stream channels by considering the width-to-length ratio (A/L^2) of each delineated water patch in terms of the estimated surface area (A) (m^2) and linear extent (L) (m). Patches with $A/L^2 > 0.03$ tended to be associated with ponds or other dark areas on the ground and were filtered out.

Delineating streams

A spatially connected stream network was delineated from the DEM mosaics derived from the PALSAR and from the PRISM data. The stream network was necessary as the bridge linking DEM-generated hydrogeomorphic attributes with field data. Our automated extraction of the stream network from a DEM was based on algorithms, described elsewhere (Miller et al. 2003; Clarke et al. 2008), that determine surface-water flow directions and calculate specific contributing area to each DEM cell, then trace channels through all cells with a contributing area exceeding some threshold value. The upstream extent of each stream channel (i.e., initiation point) was determined according to Clarke et al. (2008) based on thresholds for specific contributing area and for plan curvature of isoheight contours (a topographic indicator of channel location). A centerline for each channel was then estimated using the downstream flow path from its initiation point.

Channel locations traced from flow paths inferred from the PALSAR-derived DEM, the PRISM-derived DEM, the National Elevation Data 60-m DEM (the most highly resolved publically available DEM), and from the 1:100,000 National Hydrography Data were visually compared to channels visible on the PRISM 2.5-m ortho-rectified images. This provided a qualitative accuracy assessment of channel location.

Based on our visual assessment of DEM-traced channel locations, we chose to guide flow directions in the final PRISM-derived 2.5-m DEM using the water mask because sufficient noise remained even in the highest-resolution terrain data to render flow directions in low-gradient areas ambiguous. We assumed that elevations in areas on the water mask identified as stream channels could be represented as monotonically decreasing downstream. To enforce this assumption in the DEM elevations, we used a ray-tracing algorithm to follow a constant-velocity wave front confined to the water mask polygons and initiating from the lowest-elevation point along the polygon edges. This wave front was then followed in reverse (moving downstream), and elevations were set not to exceed the lowest elevation encountered along the wave front to that point. To guide flow directions toward the center of the water mask, we lowered the cells within the water mask polygon by an amount proportional to the distance from the polygon edge. These adjustments to the DEM

were used solely in deriving flow direction; all other topographic attributes were calculated from the original, unaltered elevation values.

Deriving hydrogeomorphic attributes

We modeled a suite of hydrogeomorphic attributes thought to be important controls on salmon habitat. The channel centerlines in a stream network traced from DEM-inferred flow paths follow a series of points or channel nodes (Figure 3) spaced at the resolution of the DEM for which we modeled the hydrogeomorphic attributes (Table 3).

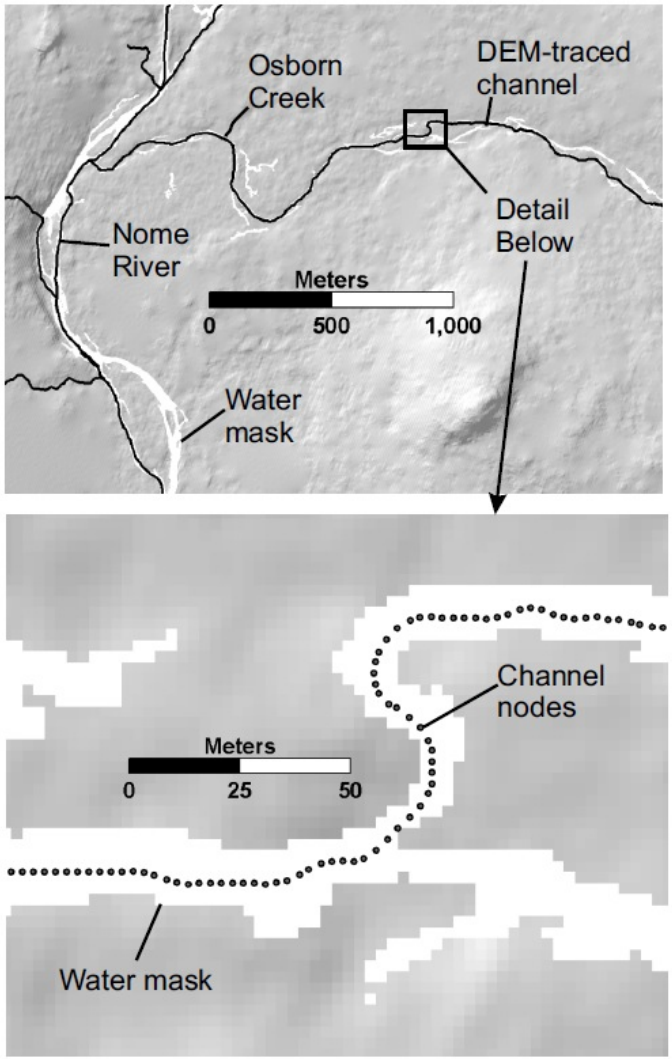

Figure 3. Illustration of the channel-node structure for deriving and storing data on hydrogeomorphic attributes. The centerline for primary channels is characterized at the spatial grain of the DEM from which flow paths are determined to delineate the stream layer. Each channel node is associated with a table containing hydrogeomorphic-attribute values.

Node spacing varies slightly at a given resolution because delineated channels were smoothed, rather than following straight-line segments from DEM grid point to grid point. Each attribute is specific to the location of the node, for example, contributing area increases with each node downstream. Nodes are spatially connected in that IDs for the upstream and downstream nodes are included in the data associated with each node.

Table 3. Description of hydrogeomorphic attributes as candidate predictor variables for statistically modeling observed abundances of juvenile coho salmon. Attributes were estimated from ALOS PRSIM 2.5-m DEMs and optical imagery for each channel node in the final stream layer. Methods are provided in the text for attributes lacking entries in the table.

Attribute description Methods	Possible relationship with channel characteristics as an indicator of:
Contributing drainage area (km^2) as described in Clarke et al. (2008)	Channel size and geomorphic type (e.g., Montgomery and Buffington 1997)
Elevation (m) above sea level	Channel location, climate, and used to calculate gradient.
Flow distance to ocean (m) from the downstream end of the channel segment	Travel distance for spawning adult fish and out-migrating smolts.
Mean annual precipitation (m) for the contributing area to the downstream end of each channel segment estimated from the Parameter-elevation Regressions on Independent Slopes Model (PRISM) (Daly et al. 1994; Simpson et al. 2002) interpolated to rainfall data from 1961-1990	Channel size.
Mean annual flow (m^3/sec) at the downstream end of the channel segment estimated from an Alaskan state-wide regression equation to *contributing drainage area* and *mean annual precipitation* (Parks and Madison 1985)	Channel size and stream power.
Active-channel width (m) averaged over the length of the channel segment estimated from a regression of field-measured values in the Nome River basin to *mean annual flow* (Leopold et al. 1964)	Channel size and used to determine representative channel lengths when deriving other attributes, such as sinuosity.
Wetted channel depth (m) averaged over the length of the channel segment from regression of field-measured values for non-pool units in the Nome River basin to *mean annual flow* (Leopold et al. 1964)	Channel size and used to delineate valley-floor extent.
Channel gradient from fitting a 2^{nd}-order polynomial over a centered window of channel node *elevations* along the traced channel centerline for each channel node. Window length varied from 500 m over high-gradient (>0.2) channels to 1500 meters for low-gradient (< 0.01) channels. Channel gradient is reported as the average of channel gradients (calculated over the specified window length) for all the nodes in the channel segment.	Geomorphic stream type and stream power.

Attribute description Methods	Possible relationship with channel characteristics as an indicator of:
Maximum channel gradient downstream the largest node-based (not segment averaged) *channel gradient* encountered downstream of each segment.	Allows mapping of stream reaches upstream of gradient thresholds.
Sinuosity ratio of channel flow-path length to straight-line distance over a channel flow-path of 40 active channel widths in length. Calculated for each DEM channel node, and then averaged over all nodes in a segment for a mean channel-segment value	Geomorphic stream type.
Water-mask area per channel length (m)	Total channel width, which increases with presence of side channels and alcoves.
Water-mask edge length per channel length	Total channel edge length, which increases with presence of side channels and alcoves.
Valley width (m)	Channel confinement and variations in hyporheic flow where valley width changes abruptly.
Intrinsic potential for coho salmon from the geometric mean of indexed *channel gradient*, channel constraint (*area-based valley width* calculated at an elevation of 5 channel depths above the channel divided by *active channel width*), and *mean annual flow* (Burnett et al. 2007).	Potential to develop high-quality habitat for juvenile coho salmon.

Attributes that must be determined over a specified length, such as channel gradient, are calculated for a channel length centered at each node. Using established methods (Clarke et al. 2008), we evaluated modeled characteristics of channel length and gradient by correlation with the field habitat data collected in the Nome River basin during the summer of 2009. Following the general approach in Leopold et al. (1964), we empirically derived equations for active channel width and wetted channel depth, excluding field data collected from complex channels. Values of active channel width were used to provide a channel-size-dependent length scale for subsequent calculations of channel sinuosity and for averaging valley width measures. Values of wetted channel depth were used to provide a channel-size-dependent elevation scale for subsequent calculations of valley floor area, from which valley width is estimated.

Most hydrogeomorphic attributes were derived using existing approaches (e.g., Burnett et al. 2007; Clarke et al. 2008); however, we developed new methods for attributes describing channel configuration based on the water mask and valley width based on the delineated valley floor.

Channel configuration

The attributes of water-mask area per channel length and edge length per channel length describe channel configuration and indicate availability of off-channel habitats and complex edge habitats, which are important to rearing juvenile coho salmon (e.g., Nickelson et al. 1992; Beechie et al. 1994). Channel edges can provide specific habitat types, depending on the degree of bank undercutting and overhanging vegetation. Both channel configuration attributes are sensitive to channel size, which varies systematically with contributing area and mean annual precipitation, as well as the degree of channel anastomosing and constraints imposed by valley-floor geometry, vegetation, and infrastructure (e.g., roads)—all of which are reflected in the water mask. Features such as side channels and alcoves increase both the area and edge length of polygons in the water mask. To the extent that the water mask accurately and completely characterizes such features, the two water-mask-derived values should reflect the complexity of channel configuration.

To calculate the water-mask area per channel length for each channel node, DEM cells inside the water mask were associated with the closest channel node. The cumulative area of cells associated with all channel nodes within 20 active channel widths up- and down-stream of a node was then divided by a length equal to 40 times the active-channel-width.

A similar procedure was used to calculate the water-mask edge length per channel length. The lengths of DEM cell edges along the edge of the water mask were summed for cells associated with nodes within 20 active channel widths upstream and downstream of each specific channel node. The summed length was divided by the value equal to 40 active channel widths.

Valley width

To estimate valley width required delineation of the valley floor, thus we associated each valley-floor DEM cell to a single channel node. Valley-floor cells are those within a user-specified elevation of the channel elevation. Cells are associated to the "closest" channel node, with closest defined using the straight-line distance weighted by a function of the highest elevation encountered between the cell and the channel node. The weighting (w) is as follows:

$$w = (1-R/R_{MAX})^{\alpha} * (1-\delta e/\delta e_{MAX})^{\beta}.$$

A weight w is calculated for every DEM cell within a search radius R_{MAX} of each channel node, and each DEM cell was assigned to the channel node for which it had the largest weight.

The first term $(1-R/R_{MAX})^{\alpha}$ provides a weight that decreases with distance from the channel node, where R is the straight-line distance from the channel node to the DEM cell. The exponent α determines how rapidly the weighting decreases with distance from the channel node. In applying the equation, we used a search radius R_{MAX} = 2500 m and an exponent value α = 10. A radius of 2500 m was large enough to span the valley floor for all points along the channel centerline and still allowed the program to complete at a reasonable rate. Distance weighting varies from a value of one at R = 0 (at the channel) to zero at a distance of R_{MAX} or greater from the channel. Setting α at one gives a linear decrease. The larger α is set, the more rapidly the weight decreases with distance from a channel node. We set α = 10 so that cells would tend to be associated very strongly with the nearest channel node.

The second term $(1-\delta e/\delta e_{MAX})^{\beta}$ provides a weight that decreases with the height of topography encountered between the node and the DEM cell. Here, δe is the maximum elevation difference encountered along the straight-line path between the node and the cell and δe_{MAX} is the maximum specified elevation difference. The value of β determines how rapidly the weighting decreases with increasing elevation differences between the channel node and the DEM cell. We used a value for δe_{MAX} of 20 wetted channel depths and a value for β of 3. A value of 20 provides adequate leeway for exploring relationships between valley floor extent and elevation above the channel while balancing the time necessary to run the program. The weighting value varies from a value of one when the DEM cell and channel node are at the same elevation to a value of zero when the maximum elevation difference (plus or minus) encountered between the channel node and the DEM cell is equal to or larger than δe_{MAX}. By setting β larger than one, valley-floor DEM cells tend to be associated more closely with channel nodes having no intervening topography.

We experimented to find coefficient values for the weighting equation that provided reasonable results for valley width as compared to the PRISM optical imagery, but we do not have field data with the accuracy necessary to verify valley-width estimates. We adjusted the values of α and β in the weight equation to give valley-floor zones that generally matched what we would have drawn by eye based on contour lines.

Although assigning each valley-floor DEM cell to a specific channel node simplifies data logistics, in reality the channel has a zone of influence over the valley floor, and vice-versa, the extent of which varies with stream discharge. Hence, to assign a height above the channel to each DEM cell, we used the mean of elevation difference (between the cell and channel node) for all channel nodes within the search radius, weighted by the value of w defined above. Use of a large value for α (relative to the value of β) preferentially

weights cells closer to each node. Once the height-above-the-channel is estimated for each valley-floor DEM cell, the area within a user-specified height of the channel can be determined.

To obtain a valley-width value for a single channel node, we sum the number of cells associated with nodes inside a specified channel-flow distance 20 active channel widths upstream and downstream of the node, multiply by the area of a single cell, and divide by the total length of the channel segment (40 active channel widths). Note that only cells within the specified height-above-the-channel limit are included. We can specify a height limit based either on a number of channel depths, which provides a channel-size-dependent estimate of valley extent, or an explicit value (e.g., 2 meters). This procedure provides an estimated valley width for every channel node, based on valley geometry over a length scale of 40 active channel widths. The valley width assigned to a stream segment is the average over all channel nodes contained in the segment.

Classifying open water as an indicator of potential overwintering habitat

Field data collection

Field data to support a supervised classification of water and ice from SAR data and/or DEM data were collected in the Nome River during 25-28 March 2009 and 8-10 April 2009. Areas of open water, often influenced by exchange with warmer hyporheic or ground water, can be important for salmonid egg incubation and juvenile rearing (Reynolds 1997; Huusko et al. 2007). Starting transects for data collection were selected approximately every 0.5 km in the Nome River through a systematic sample. GPS coordinates for locations of starting sites in each center, starting transect (Figure 4) were obtained in the field with a highly accurate 1-sec data collection frequency Global Positioning System (Trimble GeoXT) and were augmented with 1-sec data collection frequency that we requested from the three nearby University NAVSTAR Consortium (UNAVCO) permanent GPS base stations (AB11, AC07, and AC31). Locations at other sample sites along the starting transect and along the two offset transects were obtained with hand-held GPS units (Figure 4). Depending on the width of the channel at the starting site, one to three sample sites were identified along each transect. All GPS coordinates were collected in UTM Zone 3N NAD1983.

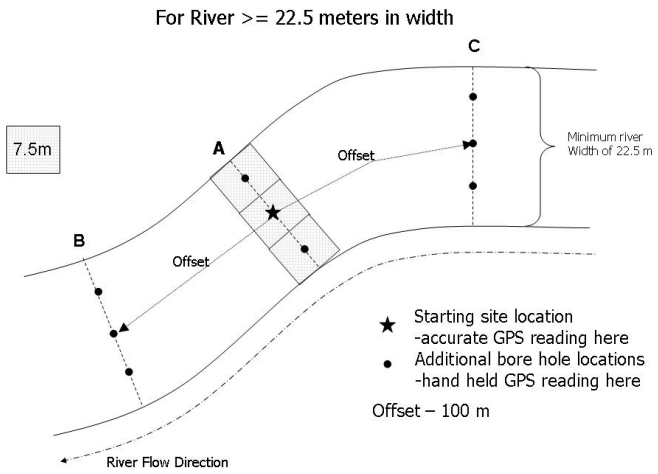

Figure 4. Schematic of data collection at randomly selected sample locations for use in ice classification, as illustrated for large channels in the Nome River basin.

Each site was identified in the field as ice, open water, ice over water, or water over ice. The length and width of open water and water over ice were measured to the nearest 0.01 m and water depths were measured, where feasible, to the nearest 0.01 m. To determine depths at a sample site of ice and of ice over water, snow was removed from the surface of the ice and a hole with diameter of either 6 cm or 20 cm was drilled through the ice. Snow thickness, ice thickness, and depth of water under ice (if present) were measured to the nearest 0.01 m.

Acquiring SAR data

We wrote a successful proposal to the German Aerospace Center (DLR) to acquire TerraSAR-X imagery. As with other SAR systems, TerraSAR-X transmits focused pulses of microwaves that strike the earth. Some of this energy is reflected back to a receiver on the satellite. Characteristics of objects reflecting the energy can be related to the magnitude of the returned signal. TerraSAR-X operates in the X-band with a frequency of 9.65 GHz. Ice has been classified in large river from SAR data, including TerraSAR-X data (e.g., Mermoz et al. 2009; South 2010). Classification takes advantage of variations in the amount of energy reflected to the satellite (backscatter), which is determined by surface interactions of air, ice, and water and volume properties of ice caused primarily by trapped air bubbles (Mermoz et al. 2008). Calm areas of open water appear dark in SAR images due to low backscatter; areas of turbulent water, snow, or ice produce greater backscatter, depending on dielectric properties, and so appear brighter.

Before submitting the final data acquisition plan to DLR, we consulted with experts in SAR classification of river ice and experimented with available data options for modes (single or dual), for transmit and receive polarizations (various combinations of horizontal (H) and vertical (V)), and for geometries (ascending or descending). We ultimately obtained, at no cost to the project, 34 TerraSAR-X polarimetric StripMap radar images (3-m resolution) with HH and VV polarizations at ascending and descending geometries.

Pre-processing SAR data

To prepare for ice classification, TerraSAR-X data were processed using software from PolSARPro (v 4.2, 2011) and the Alaska Satellite Facility's MapReady (v3.1.22, 2012). Each TerraSAR-X dataset was initially processed in PolSARPro to generate a grey-scale SPAN image combining return scatter from both the HH and VV polarimetric channels. With MapReady and the ALOS PRISM 2.5-m DEM, we radiometrically corrected terrain distortions in each SPAN image arising from the side-looking geometry of the TerraSAR-X data. These were geo-coded in the UTM Zone 3N NAD1983 map projection and converted to a floating point GeoTIFF image format.

To animate a time series of SPAN images, a window was clipped with map projection coordinates using gdal_translate. The brightness was adjusted for some of the images minimize the effect of temperature differences on SAR backscatter during the time series. The annotation was created and burned into each scene using ENVI. A MP4 file was created using ffmpeg.

Relating Juvenile Coho Salmon to Hydrogeomorphic Variables and Landscape Characteristics

Summer field data

Summer data were collected 13 - 24 August 2009 to target associations between rearing fish and habitat in the Nome River and selected tributaries. This period for data collection was based on Williams et al. (2010) to follow completion of the coho salmon smolt outmigration. Generally, a tributary was selected if the Anadromous Waters Catalogue (AWC) mapped it within the distribution of coho salmon (http://www.adfg.alaska.gov/sf/SARR/AWC/) or if Gaboury et al. (2005) reported observing coho salmon. Christian Creek met neither of these criteria, but the downstream end was surveyed. Although Dexter Creek met both criteria, it was not surveyed due to active gravel mining. Despite occurring in the AWC, Sulfur Creek was not surveyed given time constraints.

Before field data collection, the Nome River was divided into segments (Table 4) (*sensu* Frissell et al. 1986) that are relatively homogeneous lengths of stream (10^2–10^3 m) bounded by abrupt changes in drainage area or

valley gradient. All GPS coordinates for latitude and longitude were obtained with hand-held units in decimal degrees.

Table 4. Characteristics of stream segments where field data were collected during August 2009 in the Nome River and selected tributaries. Start coordinates are latitude and longitude in decimal degrees (easting and northing UTM Zone 3N NAD1983). The extent of coho salmon distribution was obtained from the Anadromous Waters Catalogue (http://www.adfg.alaska.gov/sf/SARR/AWC/). Other attributes were estimated based on the ALOS PRISM 2.5-m DEMs, with drainage area and distance to the ocean obtained at the downstream most location in the stream segment.

Stream Segment	Start coordinate	Drainage area (km^2)	Valley gradient (%)	Coho salmon distribution (km)	Distance to ocean (km)
Nome 1	64.4826, -165.3063	415.7	0.3	14.3	0.0
Nome 2	64.5474, -166.2236	367.9	0.1	15.1	14.6
Nome 3	64.6352, -165.2946	206.9	0.2	15.6	30.1
Nome 4	64.7299, -165.2842	145.9	0.4	12.8	44.2
Osborn Creek	64.5474, -166.2236	81.7	0.4	1.5	14.6
Buster Creek 61	64.5882, -165.2762	15.2	0.9	3.2	21.6
Lillian Creek 71	64.5997, -165.2455	6.1	1.0	0	24.2
Darling Creek 65	64.7439, -165.2333	4.8	1.3	2.1	47.8
Sampson Creek 66	64.7259, -165.2904	5.2	1.9	1.3	44.2
Hobson Creek 67	64.7299, -165.2842	15.7	1.5	0	45.3
Rocky Mountain Creek 68	64.7681, -165.2217	3.4	2.7	2.0	51.9
Christian Creek 78	64.7921, -165.2146	5.6	3.7	0	54.9

Habitat

Stream habitat data were collected at the channel-unit scale (*sensu* Frissell et al. 1986) for several habitat characteristics thought important to rearing juvenile coho salmon. Channel units in primary channels were defined as at least as long as the estimated mean active channel width (10^0 - 10^1 m). The mean active channel width corresponds approximately to scour from a 1.5-yr flow event (Gaboury et al. 2005). The minimum

length of channel units in secondary channels and alcoves (no surface flow at the upstream end) was scaled to the mean wetted channel width. Using a simple census design, information was gathered at every primary channel unit, including the primary channel in multichannel complexes. Due to time constraints, habitat data were obtained for channel units in secondary channels and alcoves (connected only at the downstream end to another channel) in a random sample of multichannel complexes. This allowed us to assess potential differences in habitat between primary channels and secondary channels / alcoves.

Two-person crews gathered information on channel units. Channel units were identified by habitat type as slow water (pool or glide), fast water (Hawkins et al. 1993), or beaver pond and by location as primary channel, secondary channel, or alcove; assigned to a dominant substrate class of silt/sand/fine organics (< 2 mm), gravel (2 - 64 mm), cobble (64 -256 mm), boulder (>256 mm), or bedrock; characterized as having no, low (chewed sticks), or high (dam/bank lodge) beaver activity; and assessed for percentage of over-hanging cover and other cover types for juvenile coho salmon. Whether or not a secondary channel or alcove entered or exited a primary channel unit was recorded.

Crews measured the thalweg length and mean wetted width of all channel units, or following the approach of Hankin and Reeves (1988), at every 15th channel unit for which these dimensions were estimated. In either case, the thalweg length was obtained to the nearest 0.1 m, wetted width to the nearest 0.1 m averaged across three transects at 25%, 50% and 75% of the unit length, and depth to the nearest 0.01 m for pools (at the deepest point and at the tail crest) and for other habitat unit types as the mean across the three width transects. All lengths and widths were measured with an Impulse 200 laser range finder (Laser Technology, Inc.). A separate calibration ratio was developed from the subset ($n \geq 20$) of channel units with paired measured and estimated values for each person estimating dimensions. All estimated lengths and widths were multiplied by the appropriate calibration ratio, and only the calibrated values were used in subsequent analyses.

At approximately every 15th primary channel unit, crews measured the active channel width to the nearest 0.1 m and stream slope to the nearest 1% with a laser range finder. Field crews also estimated the dominant class within 100 m of the wetted channel for riparian vegetation (none, grasses/forbs, shrubs, or deciduous trees), land use (rural residential, mining, none, or other), and whether the valley form was unconstrained (valley width > 4 times the active channel width) or constrained (valley width < 4 times the active channel width) (Hall et al. 2007) by a landform (terrace or hillslope) or by landuse such as a road.

To help spatially reference data in a GIS, GPS coordinates were obtained for field landmarks (e.g., bridge or named tributary) shown on maps and at either the up- and/or downstream end point for a subset of channel units in the primary channel.

Size at age for juvenile coho salmon

Minnow traps were placed in sampling locations throughout the Nome River (21–24 August 2009) to establish a relationship between size and age class of juvenile coho salmon. Sampling locations were concentrated in side channels, eddies, and beaver ponds because juvenile coho salmon typically prefer such slow-water habitats, but other habitat types were sampled. At a sampling location, two to four traps were placed and GPS coordinates were obtained for each trap. A trap was baited with 1 Tbsp of salmon eggs sterilized in a 1:100 iodine:water solution and fished from 3 to 6 hours but never more than 10 hours. Upon pulling a trap, fish were counted by species. Up to 30 randomly selected juvenile coho salmon from each location were placed in water containing Alka-Seltzer® for anesthesia and then measured for fork length to the nearest 1 mm. For 10 of these fish (≥45 mm), a sample for age analysis of 4 – 6 scales was taken from above the lateral line and in-line with the posterior ends of the dorsal and anal fins. Fish recovered in a freshwater bath before being released at the site of capture. Fish scales were prepared and analyzed by C. Lidstone of Birkenhead Scale Analysis (Lone Butte, British Columbia). In-season growth of scale circuli was rounded down to the next annuli (i.e., fish with in-season growth [1+] were analyzed with other one year-old fish).

Relative fish abundance

A subset of channel units was snorkeled to estimate relative fish abundances. For primary channels and habitat-typed secondary channels, a systematic sample of every 5th pool and glide was identified to snorkel for each stream segment in the Nome River and each tributary. Sampling extended upstream in Nome 4 and the tributaries until no coho salmon were observed in three consecutive channel units. A random sample of beaver ponds and alcoves was also snorkeled. To confirm that juvenile coho salmon targeted slow water habitats, as expected (Bisson et al. 1988), all channel units, including fast water, in the first reach (the length equal to 20 times the active channel width) of each Nome River stream segment and in the two largest tributaries (Osborne Creek and Buster Creek) were snorkeled.

At each selected channel unit, one to five snorkelers, depending on the size of the unit, moved upstream whenever possible, counting fish (juvenile coho by size class, adult coho, chum, pink, and sockeye salmon, as well as Dolly Varden, whitefish, and grayling that were >100 mm). Size classes of juvenile coho salmon, based on previous sampling in the Nome River as reported in Williams et al. (2010), were chosen to approximate fish at age 0 (<70 mm), age 1 (75 – 95 mm), and age 2+ (> 100 mm). Data were collected at each snorkeled unit also on water clarity*;* cover characteristics; air and water temperature; and other incidental factors that

may have affected fish counts. At the upstream and downstream end of each snorkeled unit, GPS coordinates were obtained. Snorkeling counts were not calibrated with electroshocking estimates of fish abundance in a departure from Hankin and Reeves (1988). Consequently, estimates from snorkeling counts are assumed to be negatively biased (Rodgers et al. 1992; Thompson and Lee 2000) but to provide measures of relative abundance.

Developing and applying statistical relationships for juvenile coho salmon

Linking field and DEM-derived data

To link field data with the DEM-derived attributes, summer and winter field-survey locations were geo-referenced to the final stream network delineated from the ALOS PRISM 2.5-m DEM. In the context of the channel-node data structure previously described, we established a one-to-one correspondence between each channel node (over the extent of the channel network in the summer field survey) and units in the primary channel. For the subset of primary channel units where GPS coordinates were obtained, these points were associated (snapped) to the nearest node in the appropriate section of the final stream network. Each channel unit in the primary channel had a field-measured length, from which to calculate the total channel length between GPS points and the proportion of that length occupied by each channel unit. The DEM-delineated channel lengths and the field-measured channel lengths correspond well but do not match exactly (Figure 5), so each node along the traced channel between snapped GPS points was linked to a particular channel unit based on the proportional distance between points.

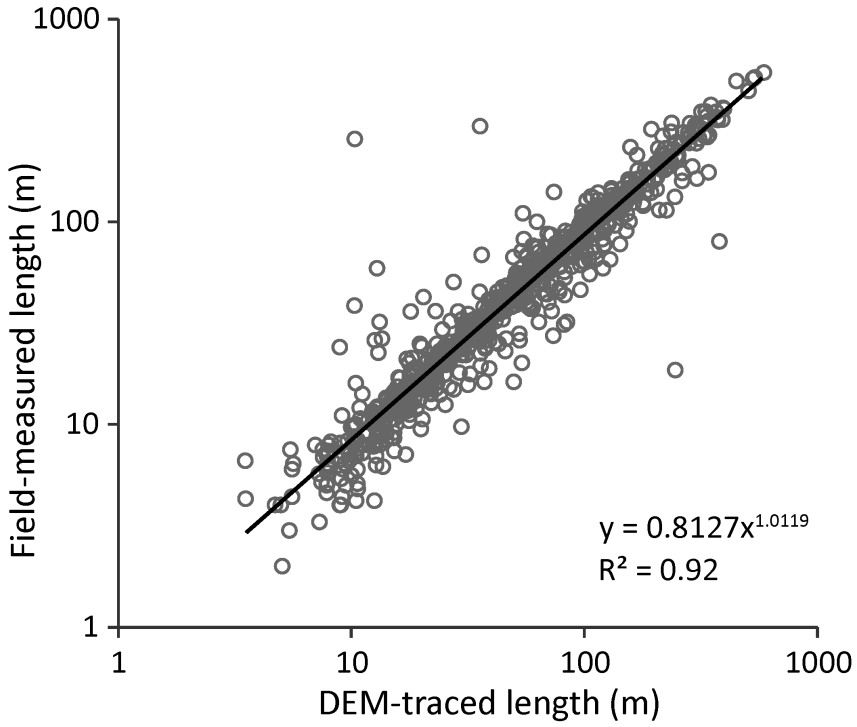

Figure 5. Plot of field-measured habitat-unit lengths against habitat-unit lengths from the ALOS PRISM 2.5-m DEM-delineated stream layer for the Nome River and its tributaries. Field data are from all surveyed habitats in the primary channel. The dark line shows the best-fit regression (df = 812; $p < 0.0001$).

With this procedure, each surveyed unit in the primary channel was linked to a set of DEM-traced channel nodes. Thus, each node has an associated set of field-measured attributes along with its DEM-derived hydrogeomorphic attributes. Field data for the small set of secondary and alcove units included in the summer survey were geo-referenced to the final stream network by snapping a GPS point for the unit to the nearest primary channel node (for all secondary and alcove units where GPS points were collected). The GPS coordinates of each site in winter surveys for ice classification were snapped to the nearest primary channel node on the final stream network.

Spatial patterns

We used three approaches to evaluate spatial patterns in the distribution of juvenile coho salmon in the Nome River. In the first, we plotted the cumulative frequency of fish counts by age class against the river distance from the downstream start of the snorkel survey. We were also interested in the distribution of channel units where no fish were observed. And so in the second approach, we plotted a histogram of the channel unit-scale counts by age class against the river distance from the downstream start of the snorkel survey.

To evaluate whether channel-unit scale observations of juvenile coho salmon counts were spatially autocorrelated, a robust stream-network semivariogram was estimated using methods detailed in Ganio et al.

(2005). Empirical semivariograms plot half the mean squared pairwise difference between points (semivariance) against the binned distance between pairs of points (separation distance), which we calculated at the centroids of habitat units. Following the methods of Ganio et al. (2005), we measured separation distance along the stream network rather than Euclidean distance (e.g., shortest distance a fish would swim rather than a crow would fly). For cases that included one unit on the Nome River and the other on Osborne Creek, separation distance was calculated from the unit centroid along the Nome River to the junction with Osborne Creek plus the distance from the junction to the centroid of the unit in Osborne Creek. We calculated semivariance by age class of coho salmon from the ln (number counted in a habitat unit +1) and the separation distance between pairs of snorkeled habitat units in primary channels for the Nome River and Osborne Creek.

The empirical stream-network semivariogram was compared with the 2.5th and 97.5th percentiles for each separation distance of semivariograms generated from 100 random permutations of our data. The separation distance corresponding to a peak or asymptote in the semivariance above the randomization 97.5th percentile (Rossi et al. 1992) indicates the dominant spatial scale of correlation in fish counts. No spatial autocorrelation is suggested at separation distances where the empirical semivariance falls between the randomization 2.5th and 97.5th percentiles.

Comparing coho salmon densities by metrics, after excluding units without fish, and among habitat types

Median linear densities (number per 100 m) and median areal densities (number per 100 m^2) of coho salmon were compared by age class (age 0, age 1, and age 2) for primary channel pools and glides in the Nome River and Osborne Creek using the Kruskal-Wallis one-way ANOVA on ranks test. P-values were converted from Kruskal-Wallis multiple-comparison Z-value test (Dunn's Test). The six groups were compared in two separate sets of tests: one that included all snorkeled units and another that excluded units where no fish were observed. All densities were transformed as ln (density +1). These analyses enabled us to inform subsequent modeling decisions by assessing whether: 1) results were likely to be affected by how fish density is expressed, 2) median densities of juvenile coho salmon were likely to reflect processes affecting fish occupancy, and 3) age classes of juvenile coho salmon were similarly distributed among habitat types.

Because only a sample of habitats in secondary channels / alcoves was surveyed and snorkeled due to time and logistical constraints, we wanted to assess whether relative densities of juvenile coho salmon in these habitats differed from those in primary channels. Thus, the median fish density was compared by channel and habitat type for the three age classes of juvenile coho salmon in the Nome River and Osborne Creek. The Kruskal-Wallis one-way ANOVA on ranks test for ln (density + 1) was used. The p-values were converted

from Kruskal-Wallis multiple-comparison Z-value test (Dunn's Test). Secondary channel pools excluded beaver ponds.

Intrinsic Potential

We applied a spatial model to estimate the intrinsic potential of streams to provide high-quality rearing habitat for juvenile coho salmon (Burnett et al. 2007). Intrinsic potential reflects species-specific associations between fish use and persistent stream attributes, which for coho salmon were mean annual stream flow, valley constraint, and channel gradient. As described in Burnett et al. (2007), these attributes were produced from DEMs in conjunction with the final stream network and then translated into index scores based on empirical evidence from published studies regarding the relationship between a stream attribute and juvenile fish use. Intrinsic potential for each stream node was calculated as the geometric mean of the un-weighted index scores. This approach reflects the assumption that the three stream attributes are of approximately equal importance and only partially compensatory, and that the smallest index score has the greatest influence on the intrinsic potential. The index scores and intrinsic potential can range from zero to one; larger values indicate a greater potential for providing high-quality rearing habitat. Stream reaches are considered to have a high species-specific intrinsic potential when the calculated value exceeds 0.75.

VI. RESULTS

Deriving Terrain and Hydrogeomorphic Variables

High-resolution DEMs

Both ALOS sensors provided data from which we could develop relatively high-resolution DEMs. The Gamma Remote Sensing package yielded four interferograms and coherence images from the ALOS PALSAR data for the study area. Despite the long wavelength of L-Band SAR data and lack of forest cover in the study area, only moderate coherence was obtained due to winter scenes with snow events between data acquisitions. One of the pairs of ALOS PALSAR data, however, did yield a 10-m DEM (horizontal resolution). By combining multiple swaths of the PRISM imagery, a final seamless 2.5-m DEM mosaic (32 bit floating point elevations) and an optical image mosaic (8 bit amplitude nadir imagery) were derived. These were converted to GeoTIFF image format, which supports rapid ingest of the data into most GIS software packages.

The final DEMs produced from the ALOS PRISM data are more highly resolved and accurate than the highest resolution publicly available National Elevation Data for the Nome River basin (Figure 6 and Tables 5 and 6).

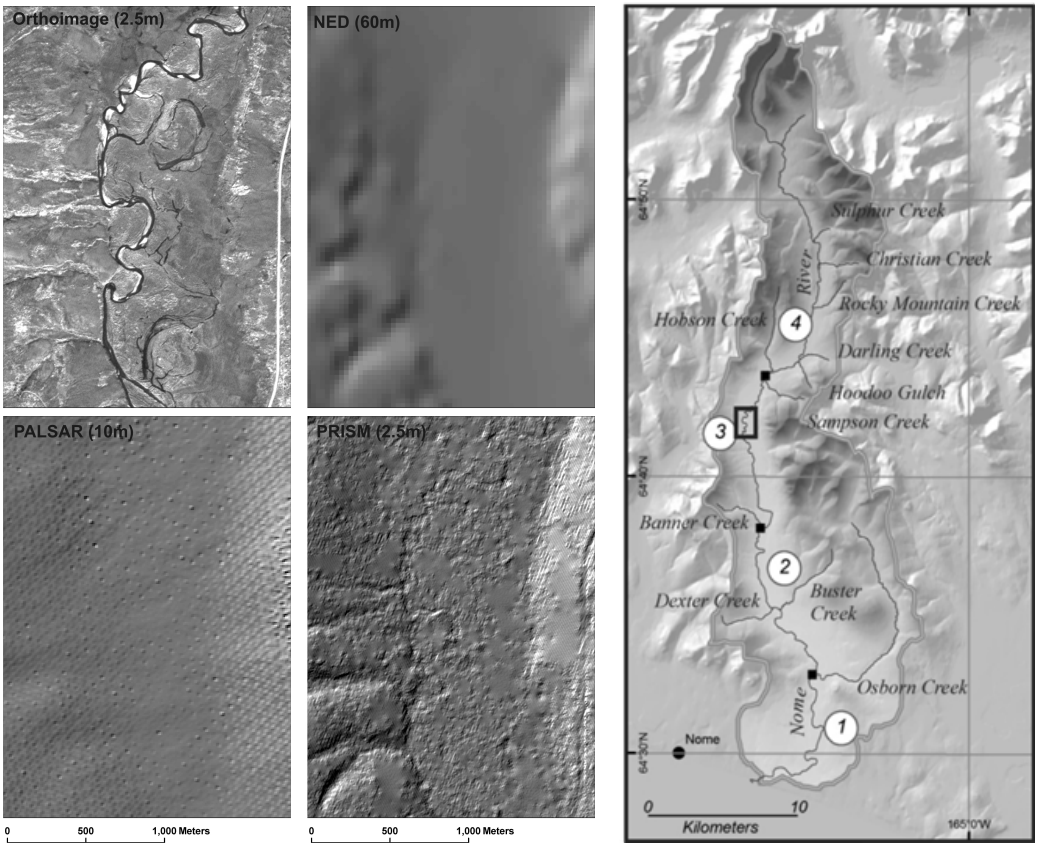

Figure 6. Comparing ALOS PRISM 2.5-m digital ortho-rectified imagery with hillshades produced from the 60-m National Elevation Data, 10-m PALSAR-derived DEMs, and PRISM-derived 2.5-m DEMs for an area in the Nome River basin, shown by the rectangle near Section 3 in the map.

Table 5. Differences for the Nome River basin between the elevation at each NASA ICESat laser altimetry point and the mean elevation calculated from each DEM in a 70-m diameter circle centered on the ICESat point.

Difference (m)	National Elevation Data 60-m DEM	ALOS PALSAR 10-m DEM	ALOS PRISM 2.5-m DEM
Min	-50.1	-49.0	-12.6
Max	50.0	46.4	20.6
Mean	-7.9	-11.5	6.8
Std Dev	18.1	12.4	2.3
RMSE	19.8	16.9	7.2

The PRISM DEMs were of greater vertical accuracy than PALSAR DEMs (Tables 5 and 6). We had intended to create a single 'best' composite DEM by combining final mosaics from the two ALOS sensors, but chose not to do so given the relatively low accuracy of the PALSAR DEMs.

The PALSAR DEMs were more accurate than the National Elevation Data DEMs when compared to elevations from the NASA ICESat laser altimetry data, but not to those from the geodetic control points. This is surprising because the geodetic control points were incorporated when developing both the ALOS PALSAR and PRISM DEM mosaics. Thus, accuracy evaluations based on these points could be expected to exhibit a bias in favor of the ALOS products, but this does not appear to be true at least for the PALSAR DEMs.

Table 6. Differences for the Nome River basin between elevations at geodetic control points obtained in the field with a GPS and from each DEM.

Difference (m)	National Elevation Data 60-m DEM	ALOS PALSAR 10-m DEM	ALOS PRISM 2.5-m DEM
Min	-25.8	-38.4	-5.2
Max	8.8	19.7	3.8
Mean	-3.9	-1.7	0.3
Std Dev	8.2	14.6	2.4
RMSE	9.1	14.7	2.4

Water mask

The method we developed used differences in image intensity between areas of water and non-water to automate extraction of a water mask directly from the ALOS PRISM 2.5-m ortho-rectified optical image. The final water mask targeted the corridor along Nome River and its tributaries (Figure 7) but under-represented very small tributaries apparent on the PRISM 2.5-m image. This resulted because we filtered out areas with surface gradients exceeding 10% to reduce the chance of incorrectly classifying areas as water. Patches in the water mask with width-to-length ratios less than 0.03 tended to be associated with river channels.

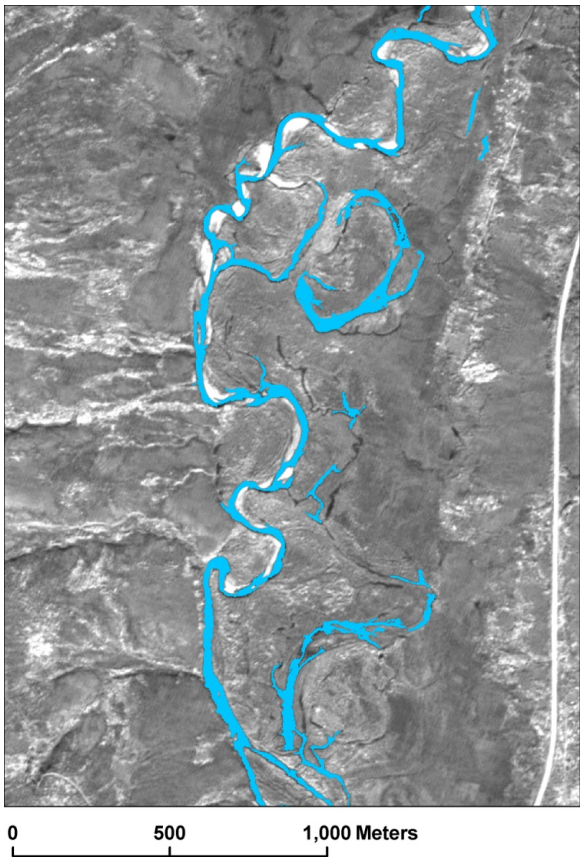

Figure 7. The ALOS PRISM 2.5-m digital ortho-rectified imagery overlain with the water mask for the same area of the Nome River basin shown in Figure 6. The water mask was created using an automated process that capitalizes on differences in image intensity between areas identified as water and non-water.

Streams

We delineated a spatially connected stream network from the highest-resolution publicly available DEMs (60-m NED), the PALSAR-derived 10-m DEMs, and the final PRISM-derived 2.5-m DEMs. Each network consists of a single-thread center-line flow path for all DEM-identified streams, but which may not include all actual stream channels. When compared to stream channels visible on the ALOS PRISM 2.5-m ortho-rectified optical image mosaic, both the PALSAR and PRISM stream networks were more accurate than the NED stream network (Figure 8a, b, and c). The 60-m resolution of the NED provided insufficient topographic detail along wide valley floors to discern channel locations, so delineated streams tend to follow the midpoint of the valley. Delineated streams follow flow paths in the PALSAR- and PRISM-derived DEMs between connected topographic low points, but in many cases, these represented locations of former or secondary channels. The PRISM-derived DEMs yielded a somewhat more accurate stream network than the PALSAR-derived DEMs. This is likely due to the higher resolution and accuracy of PRISM-derived DEMs. Adding the capacity to link DEM-inferred flow paths to a water mask from the same original imagery further improved the quality of the PRISM stream network (Figure 8c and d). This produced a stream layer from the

PRISM-derived DEM that faithfully followed primary channels on the 1:100,000 NHD (Figure 8d and e). Hereafter, the water-mask-guided PRISM stream network is referenced as the ALOS PRISM 2.5-m DEM-derived stream network or more simply as the final stream network.

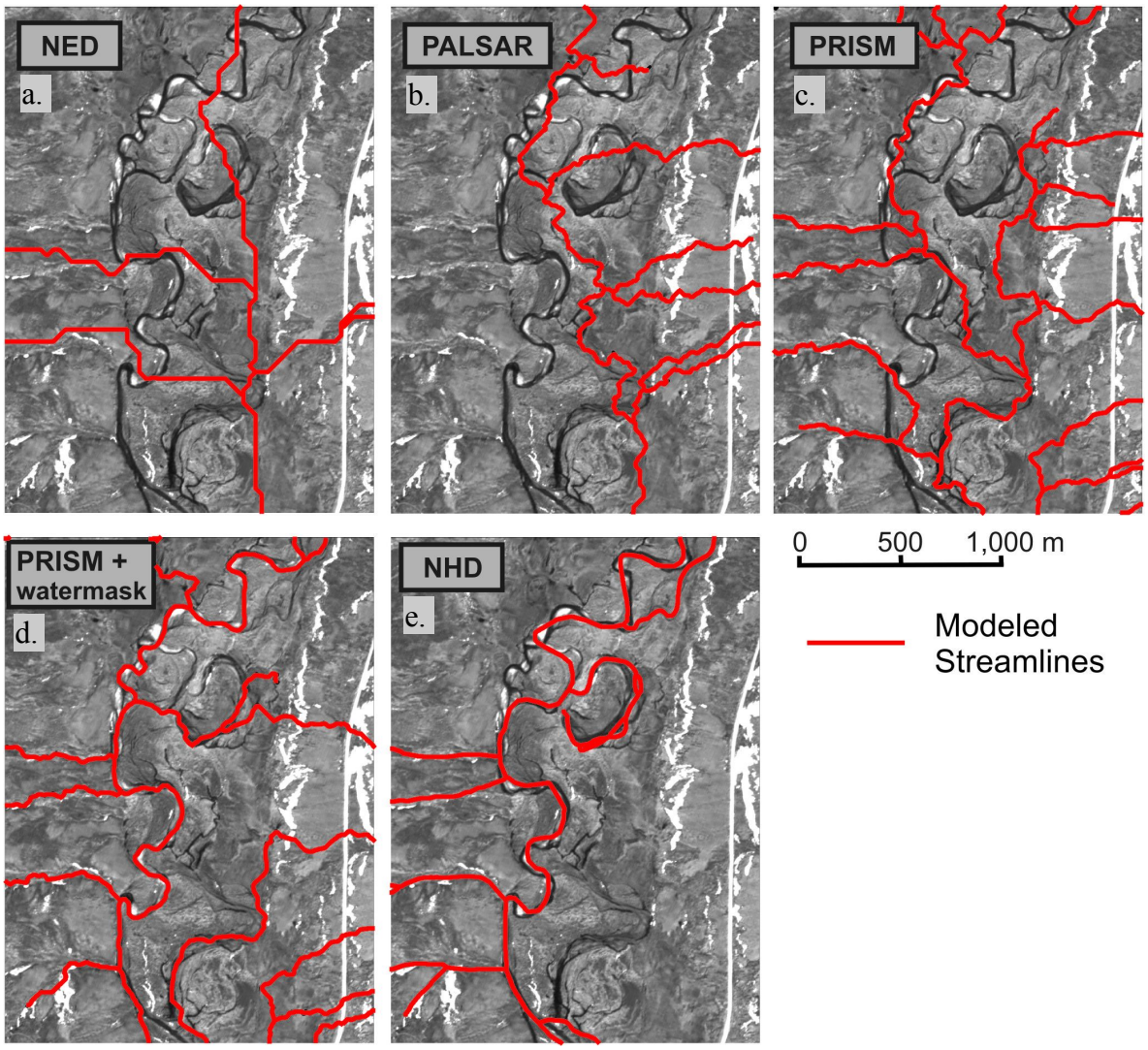

Figure 8. The PRISM 2.5-m digital ortho-rectified imagery for an area in the Nome River basin overlain with streams from different sources: generated from (a) 60-m National Elevation Data (NED) DEMs; (b) 10-m PALSAR-derived DEMs; (c) 2.5-m PRISM-derived DEMs without the PRISM water mask; (d) 2.5-m ALOS PRISM-derived DEMs with guidance from the PRISM water mask; and (e) the 1:100,000-scale National Hydrography Data (NHD).

The upstream extent of each stream channel (i.e., initiation point) in the final stream network for the Nome River basin was identified based on two empirically determined thresholds (Table 7). These are: 1) the AS^2 threshold is the specific contributing area (contributing area divided by the contour length crossed by flow out of a DEM cell) multiplied by the square of surface slope; and 2) the plan curvature threshold needed to

be met or exceeded for a flow distance of at least 60 m to qualify as a channel initiation point. The surface slope and plan curvature were calculated over a 50-m radius.

Table 7. Thresholds for stream channel initiation used to delineate the final stream network for the Nome River basin. The AS2 threshold is the specific contributing area (contributing area divided by the contour length crossed by flow out of a DEM cell) multiplied by the square of surface slope. For surface slopes between 0.25 and 0.4, thresholds were determined by linear interpolation.

Surface slope	AS^2 (m)	Plan curvature
<0.25	300	0.00175
>0.4	600	0.00275

Hydrogeomorphic attributes

We modeled the 14 hydrogeomorphic attributes listed in Table 3 for each channel node in the final stream layer for the Nome River basin. Although stored in a channel-node-based structure at the resolution of the ALOS PRISM 2.5-m DEM, data for hydrogeomorphic attributes can be summarized at any coarser spatial resolution.

Following the general equations in Leopold et al. (1964), we derived the empirical equation (Figure 9) to predicted active channel width (m) (W_a) in the Nome River:

$$W_a = 3.8827Q^{0.4976},$$

(Figure 9) where Q is mean annual flow (m^3/sec), obtained from a state-wide regression equation for Alaska (Parks and Madison 1985).

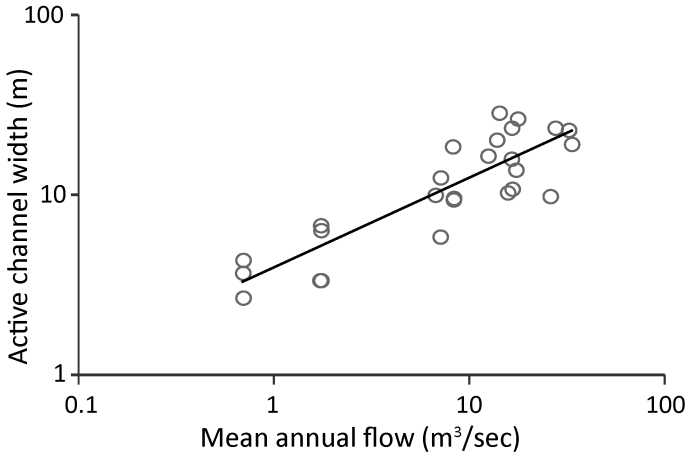

Figure 9. Field-measured active channel width as a function of mean annual flow for the Nome River and its tributaries. Field data are from the subset of surveyed primary-channel habitats where active channel width was measured. Mean annual flow is calculated according to Parks and Madison (1985). The dark line shows the best-fit regressions to mean annual flow for log-transformed values ($R^2 = 0.75$; df = 25; $p < 0.0001$).

Similarly, our empirically derived equation for wetted channel depth (D) (m) is:

$$D = 0.1378Q^{0.2825},$$

as graphed in Figure 10.

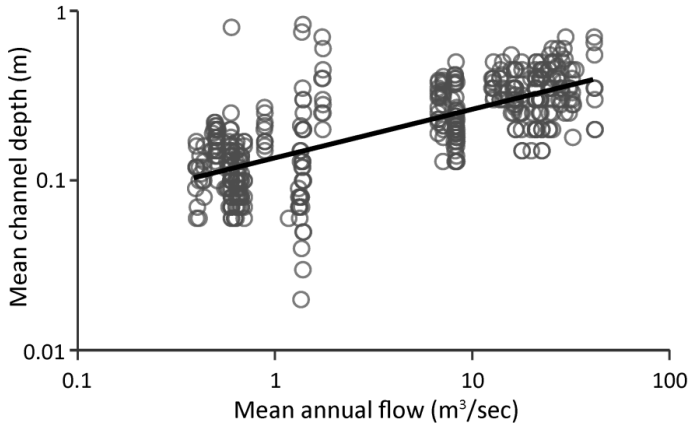

Figure 10. Field-measured active channel depth as a function of mean annual flow for the Nome River and its tributaries. Field data are from all surveyed primary-channel riffle and glide habitats. Mean annual flow is calculated according to Parks and Madison (1985). The dark line shows the best-fit regression to mean annual flow for log-transformed values ($R^2 = 0.51$; df = 429; $p < 0.0001$).

We applied the equations to estimate values of mean active channel width and mean wetted channel depth for each channel node in the final stream layer.

Stream gradients for channel units in the field survey ranged from 0% to 3.9%. The DEM was able to resolve gradients across this entire range but less reliably resolved differences in gradient less than 1% (Figure 11).

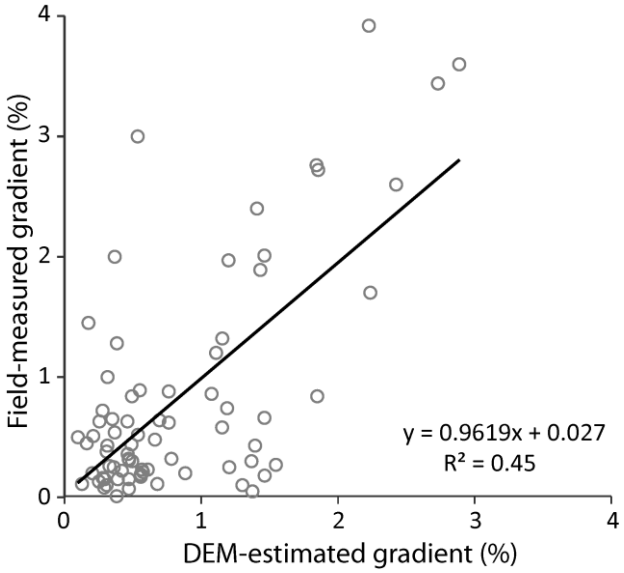

Figure 11. Field-measured stream gradients as a function of stream gradients estimated from the ALOS PRISM 2.5-m DEM-derived stream layer for the Nome River and its tributaries. Field data are from the

subset of surveyed primary-channel habitats where stream gradient was measured. The dark line shows the best-fit regression (df = 73; $p < 0.0001$).

The DEM clearly reflects apparent spatial variations in valley extent with increasing elevation above the channel, as illustrated in Figure 12. This spatial variation in valley extent is captured by the algorithm developed to estimate valley width. Longitudinal variation along the channel is also clearly evident in maps of other modeled hydrogeomorphic attributes as illustrated in Figure 13.

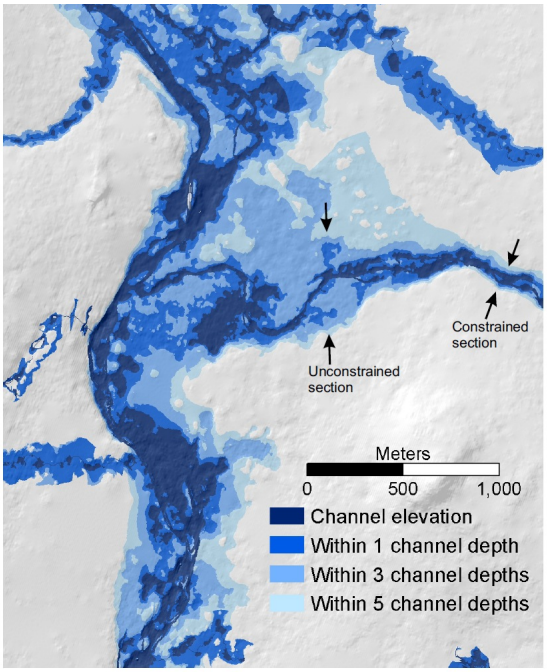

Figure 12. Map of valley extent for an area near the confluence of Osborn Creek with the Nome River, AK. Valley extent is shown at elevations equal to 1, 3, and 5 wetted channel depths above the channel.

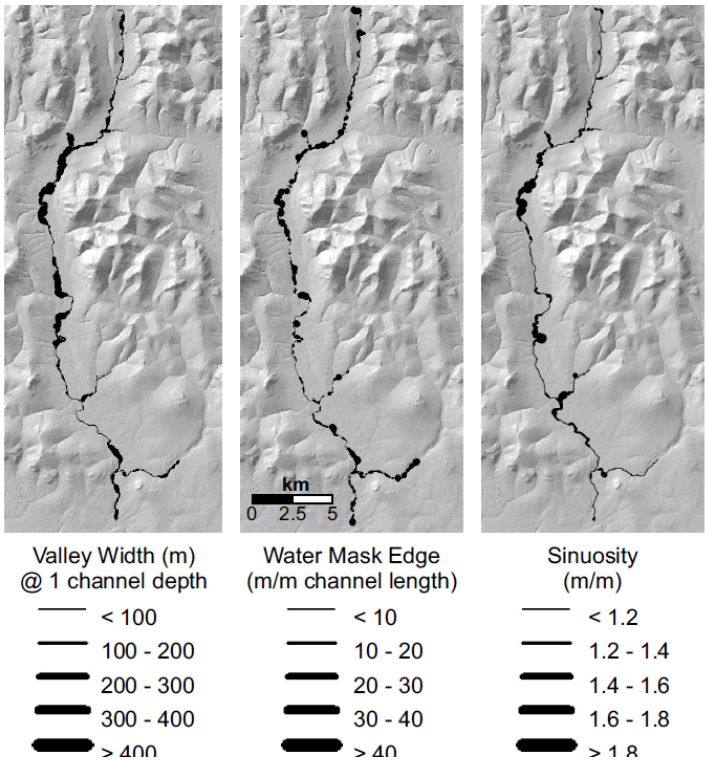

Figure 13. Map of longitudinal variation in three hydrogeomorphic attributes as examples for the Nome River and its tributaries. Attributes were modeled for each channel node in conjunction with the ALOS PRISM 2.5-m DEM-derived stream layer.

Newly developed algorithms allowed us to exploit the water mask in estimating channel area per channel length and edge length per channel length, which reflect the abundance of secondary channels and alcoves and contribute to habitat complexity.

Classifying open water as an indicator of potential overwintering habitat

Data for GPS coordinates and depth (cm) of snow, water, and ice were collected at sample sites identified in the field as ice (n = 35), open water (n = 16), ice over water (n =17), and water over ice (n = 2) (Figure 14). All of the open-water sites on the Nome River occurred downstream of the junction with Sampson Creek. This suggested that in 2009 substantial areas of overwintering rearing habitat for coho salmon were unlikely for areas draining less than 146 km^2, which would have included the Nome 4 stream segment and the tributaries. Areas that were identified in the field as solid ice were distributed along the entire sampled length of the Nome River.

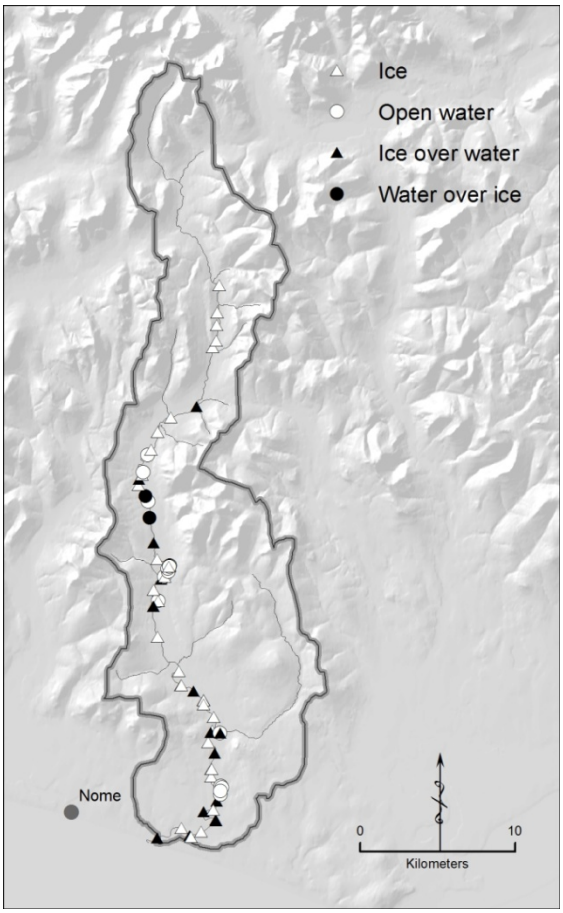

Figure 14. Map of 72 sample sites where field data for ice classification were collected for the Nome River and Osborne Creek, Alaska. Sites are coded by symbols according to field-determined class from data collected 25-28 March 2009 and 8-10 April 2009.

To attempt to classify open water, we acquired a time series for the Nome River basin of 29 TerraSAR-X single and dual polarization (HH-VV) datasets between 3 November 2008 and 18 April 2009 (Table 8). The 5 TerraSAR-X datasets acquired in July 2009 provide a baseline to help classify open water during winter.

Table 8. Description of TerraSAR-X datasets for the Nome River basin. The daily low and high air temperatures for the acquisition dates were obtained from the weather station at Nome, Alaska. Field data for ice classification were collected 25-28 March 2009 and 8-10 April 2009.

Dataset	Date Acquired	Polarization	Geometry	Range	Temperature (C) Low	High
203407836	03 Nov 2008	VV			-6.11	-3.89
203407882	04 Nov 2008	VV			-8.33	-5.00
203407924	09 Nov 2008	VV			-14.44	-6.11
203410007	10 Nov 2008	HH-VV	Ascending	Near	-7.22	-2.22
203424753	14 Nov 2008	HH-VV	Descending	Near	-16.67	-5.56
203424769	15 Nov 2008	VV			-16.67	-5.00
203424786	20 Nov 2008	HH-VV	Descending	Far	-26.11	-12.78
203512731	01 Dec 2008	HH-HV	Descending	Far	-18.33	-12.22
203589111	17 Dec 2008	VV			-8.33	0.56

Dataset	Date Acquired	Polarization	Geometry	Range	Temperature (C) Low	High
203589147	18 Dec 2008	VV			-0.56	0.56
203646099	20 Jan 2009	VV			-22.78	-3.89
203665433	25 Jan 2009	HH			-7.22	-4.44
203669901	26 Jan 2009	HH-HV	Ascending	Near	-13.33	-6.11
203676923	30 Jan 2009	HH-VV	Descending	Far	-31.67	-16.67
203676959	31 Jan 2009	HH			-27.78	-18.33
203708485	10 Feb 2009	HH-HV	Descending	Far	-35.00	-20.56
203708522	11 Feb 2009	VV			-30.56	-20.00
203738169	21 Feb 2009	HH-VV	Descending	Far	-23.33	-6.11
203738205	22 Feb 2009	HH-VV	Ascending	Near	-7.22	0.56
203767446	04 Mar 2009	HH-VV	Descending	Far	-9.44	-5.56
203767393	05 Mar 2009	HH-VV	Ascending	Near	-13.33	0.56
203792104	15 Mar 2009	HH-VV	Descending	Far	-30.00	-18.33
203792140	16 Mar 2009	HH-VV	Ascending	Near	-25.56	-16.67
203792195	22 Mar 2009	HH-VV	Ascending	Near	-18.89	-10.56
203813666	27 Mar 2009	HH-VV	Ascending	Near	-21.67	-13.89
203813702	02 Apr 2009	HH-VV	Ascending	Near	-26.67	-13.89
203863454	06 Apr 2009	HH-VV	Descending	Far	-6.67	-2.78
203863495	07 Apr 2009	HH-VV	Ascending	Near	-8.89	-1.11
203904273	18 Apr 2009	HH-VV	Ascending	Near	-17.22	-6.11
204089868	03 Jul 2009	HH-VV	Descending	Far	8.33	22.78
204089938	04 Jul 2009	HH-VV	Ascending	Near	7.78	10.56
204089974	09 Jul 2009	HH-VV	Descending	Near	6.11	8.33
204090010	14 Jul 2009	HH-VV	Descending	Far	8.33	11.67
204090046	15 Jul 2009	HH-VV	Ascending	Near	7.22	10.56

After preliminary exploration, we pursued classification with just the dual polarization (HH - VV) TerraSAR-X data. We radiometrically terrain corrected and produced grey-scale SPAN images from 24 of the TerraSAR-X datasets. For each pixel, a SPAN image quantifies the total power received by the four polarimetric channels. Such SPAN images are usually sufficiently sensitive to identify areas of open water, which appear darker due to specular reflection of the SAR energy away from the satellite (Mermoz et al. 2009a). The minimum and the maximum daily air temperatures in the Nome River basin were both less than 0°C on 08 October 2008. As shown in the first SPAN image for the lower Nome River after this date, high backscatter values are from frozen water which appear bright compared to ice or land (Figure 15a). Bubbles that were frozen in the ice caused scattering, and the rough interface between ice and water produced a strong signal and bright return.

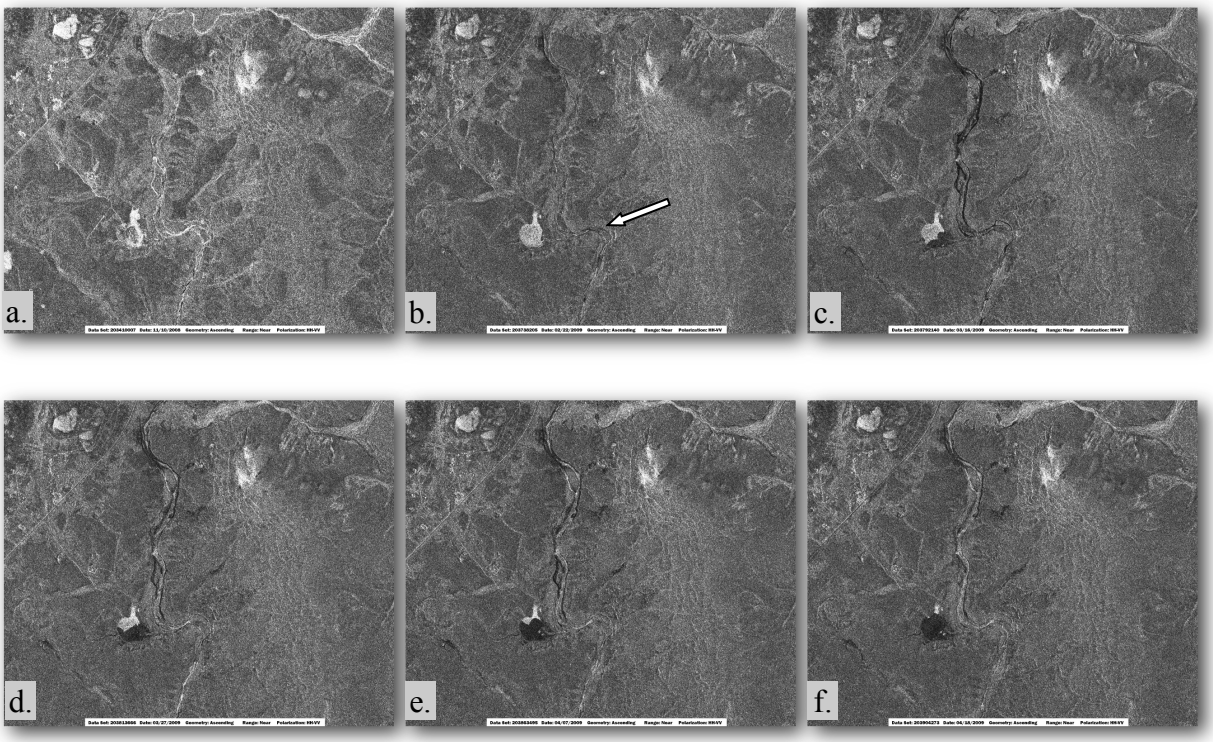

Figure 15. A time series of TerraSAR-X SPAN images for the lower Nome River. Datasets and dates in the time series are: a) 203410007, 10 Nov 2008; b) 203738205, 22 Feb 2009; c) 203792140, 16 Mar 2009; d) 203813666, 27 Mar 2009; e) 203863495, 07 Apr 2009; and f) 203904273, 18 Apr 2009. The arrow in b) identifies an area of open water just to the right of the pond.

Variations in brightness between SPAN images generated from a time series of TerraSAR-X data, a subset of which is in Figure 15, seem to indicate thawing and progressive freezing. The maximum daily air temperature remained below freezing until 20 April 2009 except for brief periods: 1) 17 - 20 December 2008; 2) 16-17 January 2009; 3) 13 February 2009; 4) 22-23 February 2009; 5) 5 March 2009. Consistent with this, the image from 22 February 2009 shows darker areas on the river just to the right of the pond, likely due to thawing (Figure 15b). During the period of extremely cold temperatures after 5 March, as the pond and deeper areas of the river freeze toward the bottom, some of the return SAR energy is scattered, diminishing the signal and producing darker values in subsequent images (Figure 15c - f).

The location of the Nome River in the processed SPAN image from 15 July 2009 was consistent with the water mask derived from the ALOS PRISM 2.5-m digital ortho-rectified imagery (Figure 16). This indicated that terrain distortions were successfully removed and that PolSARPro products could be clipped to the water mask for confining classification to the river channel. Both outcomes are prerequisites for reasonable accuracy in statistical classification of river ice from open water.

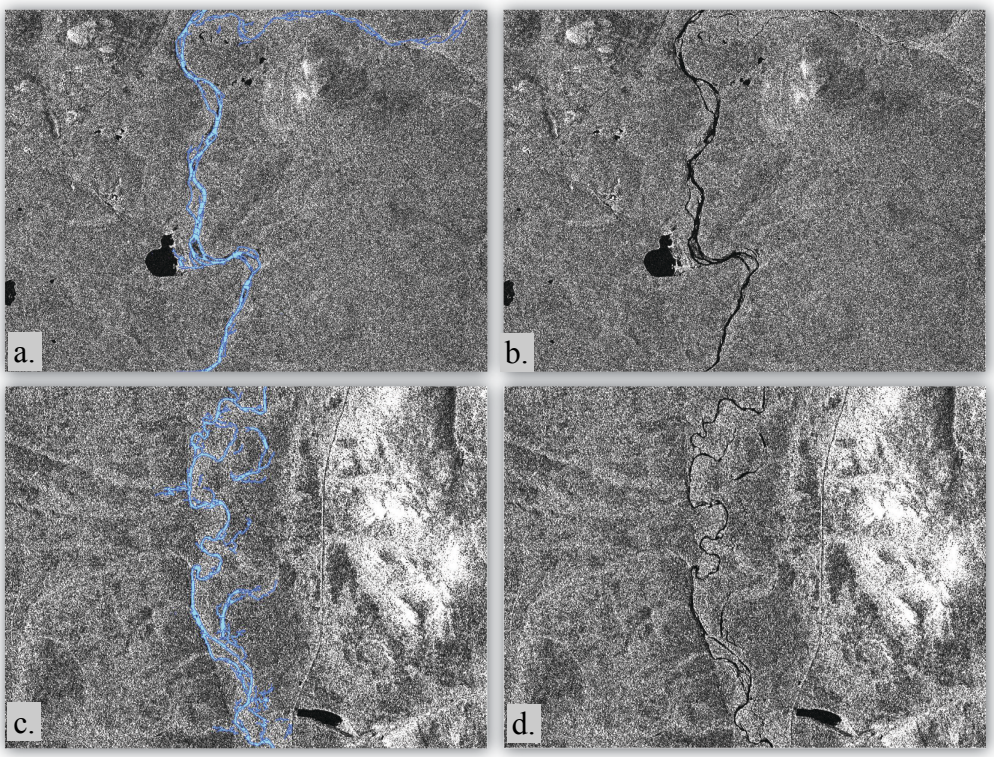

Figure 16. Overlay of SPAN image for the Nome River with the water mask from the ALOS PRISM 2.5 digital ortho-rectified imagery (in blue) for areas in segment 1, a) with, and b) without the water mask, and segment 3, c) with, and d) without the water mask. The SPAN image was produced from the 15 July 2009 TerraSAR-X dataset (204090046).

Relating Juvenile Coho Salmon to Hydrogeomorphic and Landscape Characteristics

Summer habitat and fish

Habitat

Data were collected at the channel-unit scale in primary channels, secondary channels, and alcoves across the 49 km of the Nome River and 13 km of its tributaries (Tables 9 and 10). The habitat survey started approximately 10 km upstream of Norton Sound and encompassed the extent of coho salmon distribution in the wadeable portion of the Nome River.

Considering only primary channels, pools comprised at least 30% of both the length and the area for each Nome River stream segment except Nome 4 (Table 9). Pools were 42% of the primary channel length in Osborne Creek and from 5% to 57% of the primary channel length in other surveyed tributaries. Of all stream segments surveyed, only Buster Creek contained beaver dams in the primary channel. Thus in Table 8, Buster Creek pools are heavily weighted toward beaver ponds, with these comprising 0.95 km of the pool length and 5.50 ha of the pool area.

Table 9. Length and area of habitat units by stream segment and type from a census of the primary channel in the Nome River and its tributaries.

	Unit length (km)					Unit wetted area (ha)				
Stream segment	%Pool	Pool	Glide	Fast water	Total length	%Pool	Pool	Glide	Fast water	Total Area
Nome 1	41.3	1.58	1.45	0.80	3.83	43.9	7.04	5.54	3.46	16.05
Nome 2	32.3	4.83	7.72	2.16	14.70	30.2	11.51	20.82	5.75	38.09
Nome 3	42.7	5.58	3.63	3.87	13.08	38.5	10.13	7.86	8.31	26.30
Nome 4	10.8	1.22	3.61	6.42	11.25	9.4	2.32	8.21	14.12	24.65
Osborne	41.9	2.23	1.94	1.16	5.32	46.3	2.83	2.03	1.25	6.11
Buster	44.1	1.50	0.61	1.29	3.40	87.3	5.73	0.27	0.56	6.56
Lillian	36.0	0.09	0.03	0.12	0.25	37.5	0.03	0.01	0.04	0.08
Darling	15.2	0.19	0.30	0.75	1.25	15.9	0.07	0.10	0.28	0.44
Sampson	57.1	0.20	0.08	0.07	0.35	72.7	0.08	0.02	0.01	0.11
Hobson	15.7	0.22	0.15	1.02	1.40	14.5	0.11	0.06	0.60	0.76
Rocky Mt	9.3	0.09	0.08	0.80	0.97	9.7	0.03	0.02	0.26	0.31
Christian	5.3	0.01	0.05	0.13	0.19	16.7	0.01	0.01	0.04	0.06

In our sample of secondary channels and alcoves, we stratified the data for slow-water habitats into pools, glides, and beaver ponds (Table 10). No more than 2.3 km of secondary channels and alcoves were sampled in any stream segment. This was a small but unknown percentage of the total length for Nome River and Osborne Creek. These channel types were rare or absent in the other tributaries.

Table 10. Length and area of habitat units by stream segment and type from a sample of secondary channels and alcoves in the Nome River and its tributaries. NA indicates no secondary channel or alcove units were sampled in that segment.

	Unit length (km)					Unit wetted area (ha)				
Stream segment	Pool	Glide	Fast water	Beaver pond	Total length	Pool	Glide	Fast water	Beaver pond	Total Area
Nome 1	0.19	0.43	0.01	0.29	0.93	0.13	0.84	0.02	0.30	1.29
Nome 2	1.08	0.40	0.10	0.12	1.70	1.20	0.28	0.09	0.10	1.65
Nome 3	0.89	0.34	0.30	0.00	1.53	0.54	0.21	0.17	0.00	0.92
Nome 4	0.63	0.52	1.03	0.15	2.33	0.33	0.51	0.75	0.13	1.72
Osborne	0.41	0.29	0.28	0.02	0.99	0.20	0.17	0.20	0.02	0.59
Buster	0.00	0.02	0.07	0.00	0.09	0.00	0.01	0.02	0.00	0.03
Lillian	NA									
Darling	0.04	0.00	0.02	0.00	0.06	0.01	0.00	0.00	0.00	0.01
Sampson	0.01	0.00	0.00	0.00	0.01	0.00	0.00	0.00	0.00	0.00
Hobson	0.01	0.00	0.00	0.00	0.01	0.01	0.00	0.00	0.00	0.01
Rocky Mt	NA									
Christian	NA									

A total of 1020 habitat units were surveyed: of these, 82% were in primary channels, 13% were in secondary channels, and 5% were in alcoves. In primary channels, over 40% of all units in Nome River stream segments were complex (Table 11), as these were identified in the field to contain an entrance or an exit to a secondary channel or alcove. By this metric, channel complexity was relatively low in the tributaries, ranging from 0% to 19%. A greater percentage of habitat units were complex in Hobson Creek and Buster Creek than in other tributaries. These two tributaries also had a large percentage of primary channel units with signs of beaver activity. For Nome River stream segments, the percentage of primary channel units with signs of beaver activity decreased moving in the upstream direction. Either gravel or cobble was the dominant substrate in all primary channel units for each stream segment in the Nome River and tributaries. None of these channel units had boulders or bedrock as the dominant substrate. Mean residual pool depth generally increased with drainage area.

Table 11. Summary by stream segment of data on all habitat attributes collected in the field for each channel unit in primary channels and a sample of units in secondary channels and alcoves of the Nome River and its tributaries. Percentages are out of the total number of units surveyed, reflecting units with an entrance or exit to a secondary channel or alcove as complex channel, any level of beaver activity, and the dominant substrate as cobble, gravel, or sand. Residual pool depth (m) is the difference between maximum pool depth and pool crest depth. Overhead cover is the percent of cover provided along both banks. NA indicates not in the sample for the stream segment.

Stream segment	Number of units surveyed	% Complex channel	% Beaver activity	% Dominant Substrate			Mean residual pool depth (SD)	Mean overhead cover (SD)
				Cobble	Gravel	Sand		
Primary Channels								
Nome 1	25	52.0	28.0	0.0	92.0	8.0	0.98 (0.1)	37.6 (16.7)
Nome 2	91	48.4	8.8	0.0	95.6	4.4	0.93 (0.3)	35.2 (15.6)
Nome 3	162	42.0	8.6	6.2	91.4	2.5	0.95 (0.2)	10.7 (13.5)
Nome 4	130	51.6	0.8	70.8	28.5	0.8	0.80 (0.3)	35.3 (16.7)
Osborne	121	11.6	3.3	36.4	63.6	0.0	0.45 (0.2)	1.4 (1.9)
Buster	118	6.8	8.5	25.4	57.6	14.4	0.42 (0.2)	20.0 (21.4)
Lillian	19	10.5	0.0	21.1	78.9	0.0	0.15 (0.1)	42.9 (19.5)
Darling	76	2.6	0.0	2.6	93.4	2.6	0.34 (0.1)	9.3 (13.1)
Sampson	18	5.6	0.0	0.0	100.0	0.0	0.33 (0.1)	50. 6 (20.0)
Hobson	26	19.2	26.9	34.6	61.5	0.0	0.48 (0.2)	51.9 (21.6)
Rocky Mt	39	0.0	0.0	74.4	25.6	0.0	0.30 (0.2)	36.2 (30.3)
Christian	12	0.0	0.0	100.0	0.0	0.0	0.77 (0.7)	35.0 (23.3)
Total	837							
Secondary channels and alcoves								
Nome 1	9	0.0	88.9	0.0	44.4	44.4	0.70 (0.2)	53.8 (19.2)
Nome 2	33	12.1	9.1	0.0	81.8	18.2	0.67 (0.3)	38.5 (18.3)
Nome 3	30	0.0	16.7	0.0	70.0	30.0	0.52 (0.3)	16.2 (15.7)
Nome 4	64	7.8	4.7	26.6	68.8	4.7	0.44 (0.3)	44.9 (22.4)
Osborne	35	0.0	5.7	0.0	88.6	5.7	0.31 (0.2)	4.08 (6.2)
Buster	4	0.0	0.0	0.0	100.0	0.0	NA	2.3 (2.1)

Lillian	NA							
Darling	6	0.0	0.0	0.0	66.7	33.0	0.26 (0.0)	18.3 (14.4)
Sampson	1	0.0	0.0	0.0	100.0	0.0	0.40	95.0
Hobson	1	0.0	0.0	100.0	0.0	0.0	0.20	50.0
Rocky Mt	NA							
Christian	NA							
Total	183							

In our sample of secondary channel and alcove units, only a few units contained an entrance or an exit to a smaller channel or alcove and all of these were in either the Nome 2 or Nome 4 stream segments (Table 11). Surveyed secondary channel and alcove units had signs of beaver activity for stream segments only in the Nome River and Osborne Creek. Except for Nome 1, cobble or gravel was the dominant substrate for most secondary channel and alcove units in each stream segment.

Fish

Minnow traps were set at 37 freshwater locations from 1 to 52 km upstream of the Nome River outlet to Norton Sound. Of the 660 juvenile coho salmon captured in minnow traps, 332 were selected to determine length-at-age (Table 12). Non-targeted fish species caught in minnow traps included Dolly Varden (*Salvelinus malma*), Alaska blackfish (*Dallia pectoralis*), threespine stickleback (*Gasterosteus aculeatus*), and sculpin (*Cottus* spp.). Captured juvenile coho salmon ranged in length from 43 to 117 mm and in age from 0 to 2 yr; no fish older than age-2 was caught (Table 12). Based on the mean length for each age class, we interpreted the size classes of < 70 mm, 75 – 95 mm, and >100 mm by which juvenile coho salmon were counted during snorkeling, respectively as age 0, age 1, and age 2.

Table 12. Mean length of juvenile coho salmon by age class in the Nome River during August 2009. Age was determined from circuli on scales removed from the lateral line of sampled fish (n).

Age (yr)	*n*	Length (mm)			
		Mean	Min	Max	95% CI
0	170	61.9	43	91	1.7
1	110	85.6	62	116	1.8
2	7	98.6	82	117	9.0
Total	332	73.0	43	117	1.7

Relative abundances of fish were estimated through snorkel counts for the Nome River in 112 primary channel units and in 79 secondary channel and alcove units. For the tributaries, relative fish abundances were estimated in 67 primary channel units and in 25 secondary and alcove units. Approximately 30% of the habitat surveyed in the Nome River and its tributaries was snorkeled; this is true when expressed as percentage of the total number of units, habitat area, or habitat length.

Considering adults, Dolly Varden was the most widely distributed species in the Nome River basin and the only species observed in the tributaries (Table 13). Adults of one species or another were seen in every Nome River stream segment; all but pink salmon were scarce. Coho salmon was the only salmon species for which adults were observed in all four Nome River stream segments.

Table 13. Mean (standard deviation) for densities of adults (number/100 m) by stream segment for snorkeled channel units (n) in primary channels and in secondary channels and alcoves of the Nome River and its tributaries. Data are summarized across all habitat types from a random sample of channel units. NA indicates no secondary channel or alcove units were sampled in that segment.

Stream segment	*n*	Coho	Chum	Pink	Sockeye	Dolly Varden	Whitefish	Grayling
Primary channels								
Nome 1	6	0.2 (0.3)	0.2 (0.3)	9.6 (12.4)	0.0 (0.0)	0.7 (1.3)	0.1 (0.1)	0.1 (0.3)
Nome 2	25	0.2 (0.5)	1.2 (4.7)	5.1 (6.6)	0.0 (0.0)	2.0 (2.5)	0.0 (0.2)	0.8 (1.1)
Nome 3	46	0.3 (0.6)	0.2 (0.6)	1.8 (4.5)	0.3 (1.0)	2.3 (5.1)	1.1 (2.4)	1.8 (4.6)
Nome 4	35	0.1 (0.3)	0.0 (0.0)	0.0 (0.0)	0.0 (0.0)	0.6 (2.3)	1.2 (2.8)	0.5 (1.2)
Osborne	31	0.0 (0.0)	0.0 (0.0)	0.9 (2.4)	0.0 (0.0)	0.3 (1.2)	0.0 (0.0)	0.0 (0.0)
Buster	7	0.0 (0.0)	0.0 (0.0)	0.0 (0.0)	0.0 (0.0)	0.0 (0.0)	0.0 (0.0)	0.0 (0.0)
Lillian	0							
Darling	14	0.0 (0.0)	0.0 (0.0)	0.0 (0.0)	0.0 (0.0)	0.7 (2.8)	0.0 (0.0)	0.0 (0.0)
Sampson	0							
Hobson	5	0.0 (0.0)	0.0 (0.0)	0.0 (0.0)	0.0 (0.0)	0.0 (0.0)	0.0 (0.0)	0.0 (0.0)
Rocky Mt	7	0.0 (0.0)	0.0 (0.0)	0.0 (0.0)	0.0 (0.0)	20.6 (13.3)	0.0 (0.0)	0.0 (0.0)
Christian	3	0.0 (0.0)	0.0 (0.0)	0.0 (0.0)	0.0 (0.0)	1.9 (3.9)	0.0 (0.0)	0.0 (0.0)
Secondary channels and alcoves								
Nome 1	6	0.0 (0.0)	0.0 (0.0)	0.0 (0.0)	0.0 (0.0)	0.1 (0.2)	0.0 (0.0)	0.0 (0.0)
Nome 2	26	0.0 (0.0)	0.1 (0.3)	0.4 (2.2)	0.0 (0.0)	0.0 (0.0)	0.0 (0.0)	0.0 (0.0)
Nome 3	15	0.0 (0.0)	0.0 (0.0)	0.8 (3.0)	0.0 (0.0)	0.0 (0.0)	0.0 (0.0)	0.1 (0.4)
Nome 4	32	0.0 (0.0)	0.0 (0.0)	0.0 (0.0)	0.0 (0.0)	0.2 (0.9)	0.0 (0.0)	0.0 (0.2)
Osborne	20	0.0 (0.0)	0.0 (0.0)	0.0 (0.0)	0.0 (0.0)	0.3 (1.1)	0.0 (0.0)	0.0 (0.0)
Buster	0							
Lillian	NA							
Darling	4	0.0 (0.0)	0.0 (0.0)	0.0 (0.0)	0.0 (0.0)	0.0 (0.0)	0.0 (0.0)	0.0 (0.0)
Sampson	0							
Hobson	1	0.0	0.0	0.0	0.0	0.0	0.0	0.0
Rocky Mt	NA							
Christian	NA							

Although adults occurred in many stream segments, we observed more juvenile coho salmon than adults of any species (Figure 17). Juvenile coho salmon were seen in each Nome River stream segment and in Osborne Creek and Darling Creek tributary stream segments.

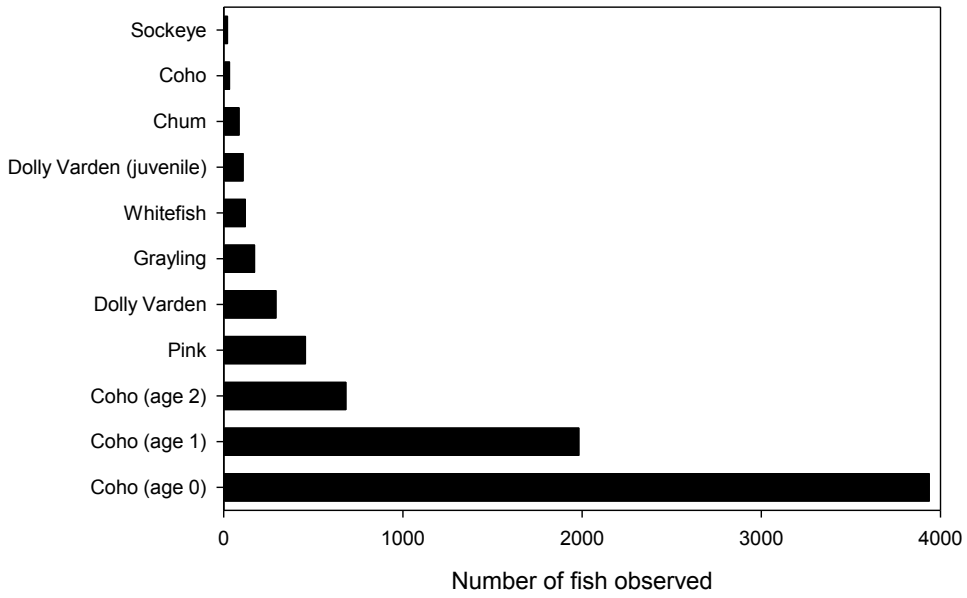

Figure 17. Total number of fish (n = 7899) observed by species and age class for some species during snorkeling in a random sample of channel units for the Nome River and selected tributaries.

Despite much of the primary channel being in fast-water habitats, we found juvenile coho salmon in only two snorkeled riffles, both in the Nome River. This was from our sample of 16 riffles that covered 790 m of primary channel in the Nome River and its two largest tributaries, Osborne Creek, and Buster Creek. Fish numbers were not estimated for fast-water units in the stream segment Nome 1 because these shallow habitats were too wide to reasonably snorkel. Thus in the other Nome River stream segments, estimated density over the 700 m of riffles sampled was 0.1, 1.4, and 0.0 fish per 100 m, respectively for age 0, age 1, and age 2 coho salmon.

For slow-water habitat types, juvenile coho were patchily distributed, with no fish observed in many habitat units (Tables 14 and 15). This was particularly true for age 2 coho salmon. Evidence was also provided for patchy distributions, given that the standard deviation exceeded the mean density of coho salmon (number/100 m) for each age class in each stream segment (Tables 14 and 15).

Table 14. Mean (standard deviation) for densities of juvenile coho salmon (number of fish/100 m) by stream segment, age class, and slow-water habitat types in primary channels of the Nome River and its tributaries. Age is in years. The number of snorkeled units is n. Data are from a systematic sample of habitat units.

	Pool					Glide				
			Coho salmon (# / 100 m)					Coho salmon (#/ 100 m)		
Stream segment	*n*	% Length Sampled	Age 0	Age 1	Age 2	*n*	% Length Sampled	Age 0	Age 1	Age 2
Nome 1	3	48.9	10.1 (17.5)	27.1 (23.7)	25.4 (30.9)	3	27.4	36.8 (60.5)	44.8 (67.2)	11.9 (17.1)
Nome 2	1 5	56.8	8.0 (8.9)	8.1 (18.9)	1.2 (2.1)	7	17.5	5.5 (6.7)	3.1 (5.9)	0.0 (0.0)
Nome 3	3 2	50.8	61.1 (122.6)	18.6 (40.9)	3.0 (10.1)	11	29.5	14.7 (45.7)	17.2 (50.2)	0.7 (1.9)
Nome 4	1 7	95.4	27.1 (41.1)	3.2 (6.3)	1.1 (2.2)	15	26.7	24.7 (41.0)	2.0 (4.9)	1.4 (3.0)
Osborne	1 9	58.7	13.6 (34.7)	20.1 (46.8)	6.5 (15.0)	9	14.8	4.2 (8.6)	9.7 (25.5)	2.1 (4.2)
Buster	3	6.4	0.0 (0.0)	0.0 (0.0)	0.0 (0.0)	1	1.7	0.0	0.0	0.0
Lillian	0	0.0				0	0.0			
Darling	1 0	54.0	0.0 (0.0)	1.2 (3.8)	1.8 (5.7)	4	23.1	0.0 (0.0)	0.0 (0.0)	0.0 (0.0)
Sampson	0	0.0				0	0.0			
Hobson	3	22.5	0.0 (0.0)	0.0 (0.0)	0.0 (0.0)	2	18.3	0.0 (0.0)	0.0 (0.0)	0.0 (0.0)
Rocky Mt	4	39.8	0.0 (0.0)	0.0 (0.0)	0.0 (0.0)	3	31.7	0.0 (0.0)	0.0 (0.0)	0.0 (0.0)
Christian	2	100	0.0 (0.0)	0.0 (0.0)	0.0 (0.0)	1	35.3	0.0	0.0	0.0

Densities of coho salmon in both primary channel pools and in glides tended to be greater for age-0 and age-1 than for age-2 fish in each stream segment (Table 14). The highest densities of age-2 fish in primary-channel pools and glides were observed in Nome 1, the furthest downstream stream segment, and in Osborne Creek, which joins the Nome River at Nome 1.

Densities of juvenile coho salmon in secondary channels and alcoves were similarly distributed to those in primary channels (Tables 14 and 15). To illustrate, Nome 2 had the lowest observed densities of age-0 fish in pools both for primary channels and for secondary channels and alcoves. Although only five beaver ponds were snorkeled due to human health concerns and visibility issues, estimated densities of juvenile coho

salmon for each age class were generally higher than in other habitat types in the same stream segment (Tables 14 and 15).

Table 15. Mean (standard deviation) for densities of juvenile coho salmon (number of fish /100 m) by age class, stream segment, and slow-water habitat type in secondary channels and alcoves of the Nome River and its tributaries. Age is in years. The number of snorkeled units is n. Data are from a random sample of habitat units. NA indicates no secondary channel or alcove units were sampled in that segment.

Pool					Glide				Beaver Pond			
Stream segment	*n*	Coho salmon (# / 100 m) Age 0	Age 1	Age 2	*n*	Coho salmon (# / 100 m) Age 0	Age 1	Age 2	*n*	Coho salmon (#/ 100 m) Age 0	Age 1	Age 2
Nome 1	2	24.4 (34.5)	43.9 (62.1)	39.8 (56.3)	2	2.2 (3.1)	5.8 (8.1)	0.4 (0.5)	2	152.4 (215.6)	219.5 (310.4)	48.8 (69.0)
Nome 2	13	5.1 (7.3)	7.7 (17.1)	1.5 (2.8)	11	38.1 (66.6)	2.9 (6.8)	1.0 (3.4)	2	32.9 (11)	22.5 (31.8)	0.7 (1.0)
Nome 3	12	67.8 (72.4)	16.7 (48.6)	1.0 (2.0)	2	101.8 (144.0)	9.0 (12.7)	0.0 (0.0)	NA			
Nome 4	21	64.2 (90.2)	9.7 (21.7)	4.8 (12.4)	11	14.0 (22.6)	0.4 (1.0)	0.0 (0.0)	0			
Osborne	11	36.4 (26.1)	19.5 (23.1)	17.7 (33.5)	8	19.1 (30)	3.0 (6.7)	0.3 (0.9)	1	113.6	17.0	11.4
Buster	NA				0				NA			
Lillian	NA				NA				NA			
Darling	3	0.0 (0.0)	0.0 (0.0)	0.0 (0.0)	1	0.0	0.0	0.0	NA			
Hobson	1	0.0	0.0	0.0	NA				NA			
Sampson	0				NA				NA			
Rocky Mt	NA				NA				NA			
Christian	NA				NA				NA			

Landscape attributes

Based on 84 field observations, obtained at approximately every 15th primary channel unit, the dominant class of riparian vegetation, landuse, and valley form were determined at the segment scale. The dominant riparian vegetation for each stream segment was shrubs, including willows. Mining and roads were components of the dominant landuse only for a few tributary stream segments. Rural residential uses were not among the dominant landuses for any stream segment. In stream segments where 'rural residential' was a subdominant landuse class, the dominant landuse class was 100% 'none' (Table 16). This suggests that rural residential areas in the Nome River basin are segregated from mining and roads. Given the gentle terrain, few stream

segments were identified as constrained, with the majority constrained by a feature related to human landuse, such as road, rather than a natural landform, such as a hillslope or terrace.

Table 16. Summary of field-estimated landscape attributes by valley segment for the Nome River and its tributaries. The number of channel units at which these attributes were estimated is n. The percentage this represents of the total number of primary channel units is %. Dominant and sub-dominant landuse were estimated within 100 m of the wetted channel. No data for %sub-dominant landuse were collected for Christian Creek. Constrained valley form: 1) if valley width > 4 times the active channel width, then "None" is the % of constrained units; 2) if valley width < 4 times the active channel width, then % of units constrained by landform or by landuse.

			% Dominant landuse			% Sub-dominant landuse				% Constrained		
Segment	*n*	%	None	Mining	Road	None	Mining	Road	Residential	None	Landform	Landuse
Nome 1	1	4	100	0	0	100	0	0	0	100	0	0
Nome 2	10	11	100	0	0	0	0	0	100	100	0	0
Nome 3	13	8	100	0	0	77	0	0	23	54	0	46
Nome 4	26	20	100	0	0	100	0	0	0	100	0	0
Osborne	8	7	62	38	0	100	0	0	0	75	25	0
Buster	7	6	14	29	57	42	29	29	0	71	0	29
Lillian	0	0										
Darling	6	8	0	0	100	17	83	0	0	17	33	50
Sampson	3	17	100	0	0	0	0	0	100	100	0	0
Hobson	5	19	100	0	0	0	0	0	100	100	0	0
Rocky Mt	3	8	0	67	33	0	67	33	0	0	0	100
Christian	2	17	0	100	0	-	-	-	-	0	0	100

Developing and applying statistical relationships for juvenile coho salmon

Linking field and DEM-derived data

The new technique that we developed allowed field data to be associated with nodes in a DEM-derived stream network, which affords efficiency in data processing and flexibility in data analysis.

The summer field data were geo-referenced to the final ALOS PRISM 2.5-m DEM-derived stream layer for the Nome River basin using a subset of the 686 field-obtained GPS coordinates. Field data for all habitat units were successfully geo-referenced to primary channels of every field surveyed valley segment.

The digital stream network with geo-referenced channel units was ultimately written to a GIS vector file in the ESRI shapefile format (ESRI 1998) as illustrated in Figure 18 for densities of juvenile coho salmon. The shapefile contains tabular data with one record for each channel unit; each record includes values for all field-measured attributes and all DEM-derived hydrogeomorphic attributes.

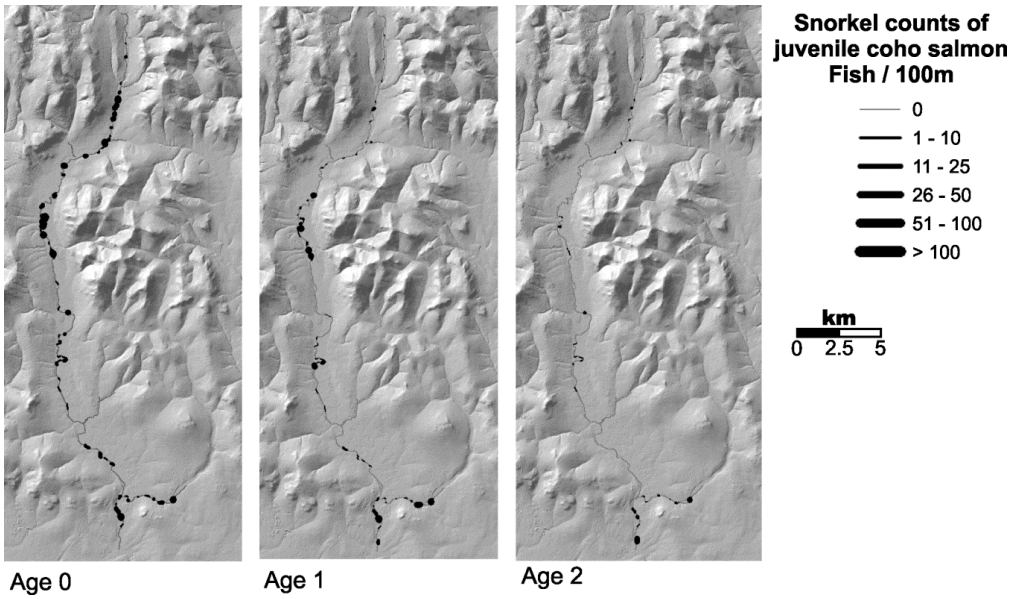

Figure 18. Density of juvenile coho salmon by age class from snorkel counts in the Nome River basin.

Coordinates for each of the 72 winter sample sites were snapped to the nearest channel node on the final stream network. Fifty-six of the winter sample sites were within the portion of the channel network that was subsequently included in the summer habitat and snorkel surveys. Data for these 56 sample sites are linked to specific channel units. Because the ice-drilling protocol involved drilling at three points for each sample site, many of the channel units contain more than one ice-drilling point. All 72 of the winter sample sites have DEM-derived channel attributes. This information is contained within GIS vector point files, with one record for each ice-drilling point.

Spatial patterns of fish abundances

Estimated abundances of juvenile coho salmon exhibited some spatial structure within the Nome River as indicated in plots of fish counts by river distance (Figures 19 and 20) and but this was generally not evidenced in a quantitative assessment of semivariance (Figure 21).

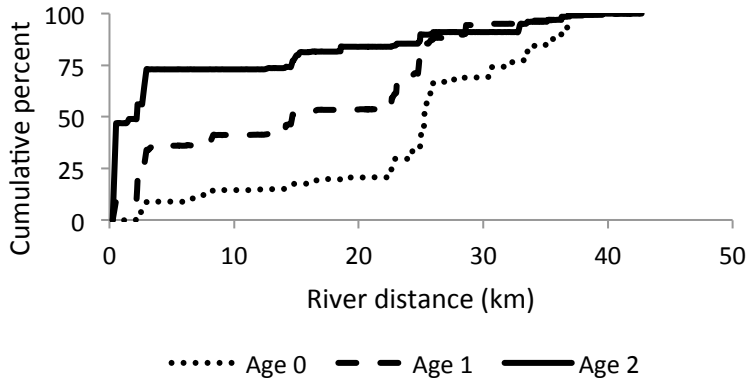

a.

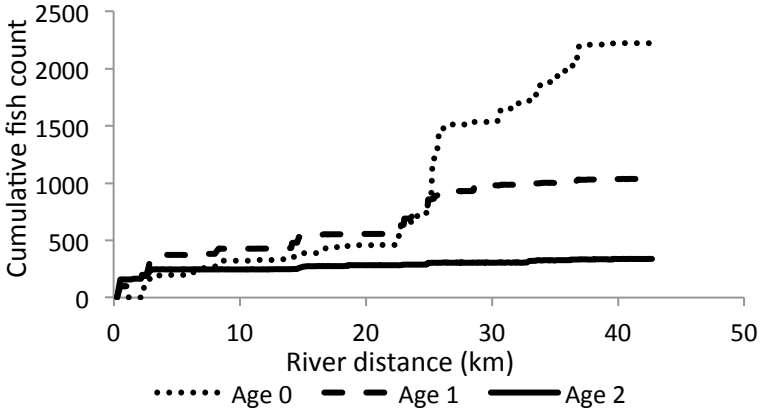

b.

Figure 19. Longitudinal distribution of juvenile coho salmon by age class for surveyed primary channel units in the Nome River presented as the: a) cumulative percent of the fish count by survey distance, and b) cumulative fish count by survey distance.

For age-2 juvenile coho salmon in the Nome River, 75% of the counted fish were observed in the downstream-most 5km of snorkeled habitat (Figure 19a). Upstream of this, age-2 fish contributed marginally to the observed abundance of juvenile coho salmon (Figure 19b). In contrast, cumulative counts of age-0 and age-1 fish increased gradually until 23 km and then increased sharply upstream over the next 3 km. Beyond this distance, age-1 fish were rarely observed. These patterns are demonstrated also by the locations of peaks in channel unit counts and of the many channel units where no fish were observed (Figure 20).

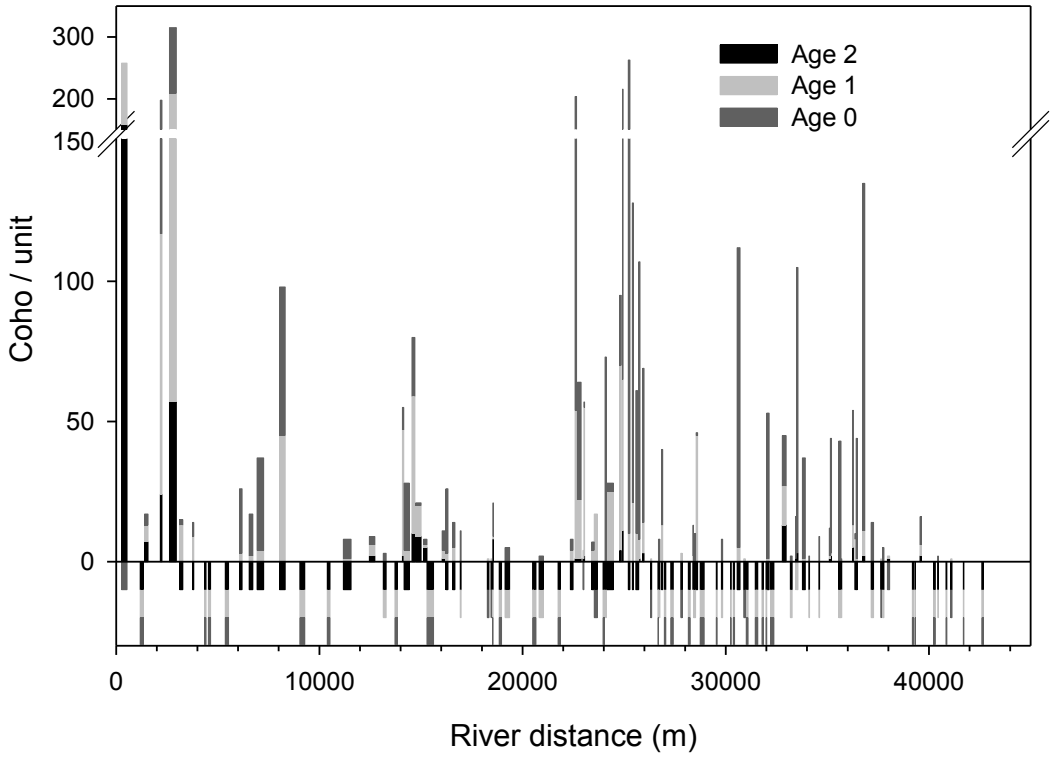

Figure 20. Longitudinal profile of the number of fish / unit for the three age classes of juvenile coho salmon in the primary channel of the Nome River. Each bar represents a snorkel count at the channel-unit scale. The width of a bar reflects the length of the unit sampled. Age classes in snorkeled units where no fish were observed are represented below zero on the y-axis such that the absence of an age class in a snorkeled unit is shown by the appropriate colored bar. Units not snorkeled are blank.

Based on empirical semivariograms, snorkel counts of juvenile coho salmon were either not spatially structured or were autocorrelated only at small spatial scales (Figure 21). We constructed empirical semivariograms using 100-m increments of primary stream length as categories for separation distance. Considering all habitat units at separation distances exceeding 100 m, we plotted semivariance for 20,306 pairs of habitat units. For age-0 and age-1 coho salmon counted in snorkeled habitat units, values of semivariance were low and increased to within the randomization 2.5th percentile at short separation distances and remained below the randomization 97.5th percentile at all larger separation distances. This suggested little spatial autocorrelation between habitat units further apart than 300 m for age-0 coho salmon (Figure 21a) and 100 m for age-1 coho salmon (Figure 21b). For age-2 coho salmon, values of semivariance were within the randomization 2.5th and 97.5th percentiles at all separation distances, indicating no spatial structuring in snorkel counts for this age class (Figure 21c).

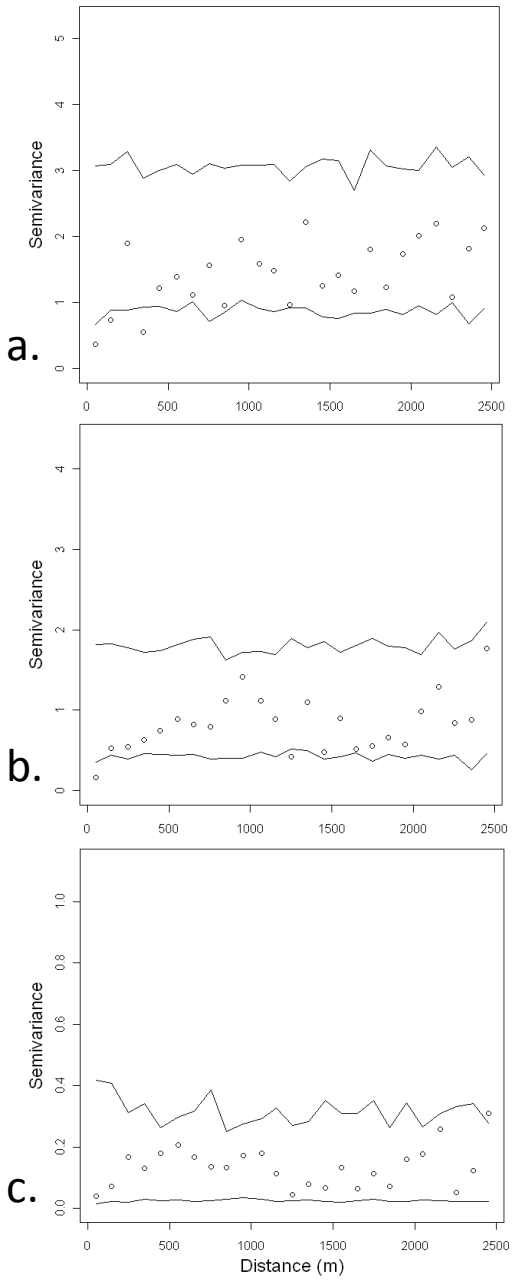

Figure 21. Empirical robust stream-network semivariogram for a) age-0, b) age-1, and c) age-2 juvenile coho salmon counted in snorkeled habitat units of primary channels of the Nome River and Osborne Creek. Circles represent semivariance values of ln (number of coho salmon counted in a habitat unit +1) for separation distances of 100-m stream length. Lines represent the 2.5 and 97.5 percentiles of 100 randomizations of the data to evaluate the observed semivariance against the null hypothesis of no spatially structured variance.

Linear or areal fish density?

Counts of juvenile coho salmon were not highly correlated ($r < |0.36|$) with the size of habitat units (Table 17). The only statistically significant correlations we found were between counts of age-1 coho salmon and lengths of habitat units for both pools and glides when all units were considered.

Table 17. Correlation (Spearman rho) between ranked counts of juvenile coho salmon and size of habitat units for primary channel units in the Nome River and Osborn Creek. * significant at □ = 0.05.

	All units			Units with fish observed		
	Age 0	Age 1	Age 2	Age 0	Age 1	Age 2
Pool						
Length	0.14	*0.22	0.13	-0.02	0.25	0.19
Area	0.14	0.17	0.11	-0.06	0.21	0.27
n	86	86	86	55	52	27
Glide						
Length	0.28	*0.36	-0.10	0.02	-0.14	0.19
Area	0.18	0.25	-0.17	-0.08	-0.15	0.10
n	45	45	45	24	18	11

Patterns of significance were similar when comparing medians based on linear fish density (number of fish per 100 m) and on areal fish density (number of fish per 100 m^2) (Table 18). The only difference we found was that the median linear density, but not the median areal density, of coho salmon in units where fish were observed differed between age-0 fish in pools and age-2 fish in glides.

Table 18. Comparison of median linear densities (number of fish per 100 m) and areal densities (number of fish per 100 m^2) of coho salmon by age class (age 0, age 1, and age 2) for primary channel pools and glides in the Nome River and Osborne Creek. Medians were compared using the Kruskal-Wallis one-way ANOVA on ranks test. Values in the table are p-values converted from Kruskal-Wallis multiple-comparison Z-value test (Dunn's Test). The six groups were compared in two separate tests: those above the diagonal included all snorkeled units and those below the diagonal excluded units with no fish observed. All densities were transformed as ln (density +1). The sample size (n) differed by the inclusion (all units) or exclusion of units where fish were not observed (fish observed). For reference the Bonferroni corrected p-value is < 0.0033 (0.05 / 15 comparisons).

	Age, unit type	Age 0, pool	Age 1, pool	Age 2, pool	Age 0, glide	Age 1, glide	Age 2, glide
Fish / 100 m	Age 0, pool	---	0.1507	<0.0001	0.1126	0.0014	<0.0001
	Age 1, pool	0.0142	---	0.0003	0.6923	0.0446	0.0002
	Age 2, pool	0.0061	0.4741	---	0.0092	0.3212	0.4809
	Age 0, glide	0.2686	0.4096	0.1833	---	0.1592	0.0039
	Age 1, glide	0.0801	0.9966	0.5794	0.5116	---	0.1386
	Age 2, glide	0.0280	0.4481	0.8188	0.2112	0.5125	---
Fish / 100 m^2	Age 0, pool	---	0.1953	<0.0001	0.0946	0.0012	<0.0001
	Age 1, pool	0.0358	---	0.0002	0.5498	0.0310	0.0003
	Age 2, pool	0.0090	0.3820	---	0.0134	0.3611	0.5556
	Age 0, glide	0.1748	0.7641	0.3158	---	0.1737	0.0075
	Age 1, glide	0.0571	0.6860	0.7503	0.5538	---	0.1897
	Age 2, glide	0.1123	0.7210	0.8037	0.5969	0.9835	---
n	all units	86	86	86	45	45	45
	fish observed	27	52	55	11	18	24

Given the strong correspondence between results for linear and areal density of juvenile coho salmon, that the only significant correlations between fish count and unit size were with length, and that snorkelers observed juvenile coho salmon concentrated along stream margins, we decided to use the linear metric in subsequent modeling of fish density.

Differences among habitat types for densities of juvenile coho salmon in primary channels

When all snorkeled units were considered, median linear densities of coho salmon (number of fish per 100 m) in pools were similar for age-0 and age-1 fish, but each of these densities was greater than that for age-2 fish (Figure 22 and Table 19). For coho salmon in glides, median linear densities were similar between age-0 and age-1 fish and between age-1 and age-2 fish, however densities of age-0 fish exceeded those of age-2 fish (Figure 22 and Table 19). Median linear densities were similar in pools and glides for age-0 fish and for age-2 fish yet were marginally greater in pools than in glides for age-1 fish (Figure 22 and Table 19). For the same set of previously described comparisons but conducted after excluding units where coho salmon were not observed by snorkelers, the only differences we found were that median linear densities (fish / 100 m) in pools were greater for age 0 than for either of the older age classes (Figure 22 and Table 19).

Differences among primary and secondary channels for densities of juvenile coho salmon

Median densities of age-0 and age-1 fish differed between some habitat types in primary and secondary channels. When all units were considered (Figure 22 and Table 19), median densities of coho salmon in primary channel pools were lower than in secondary channel pools for age-0 fish but similar in secondary channel pools for age-1 fish. Interestingly, just the opposite was found after excluding units where fish were not observed; median densities were similar in primary and secondary pools for age-0 fish, but median densities in primary channel pools were lower than in secondary channel pools. Median densities of age 2 coho salmon were similar for pools in primary and secondary channels regardless of whether units with no fish observed were excluded.

Median fish densities for all three age classes of juvenile coho salmon, when all units were considered, were lower in secondary channel glides than secondary channel pools but were similar for glides in secondary and primary channels (Figure 22 and Table 19). After excluding units where fish of a specific age class were not observed, relatively few secondary channel glides were considered in analysis. Small sample sizes may have masked any significant differences when comparing densities for each age class between secondary-channel glides and other habitat types.

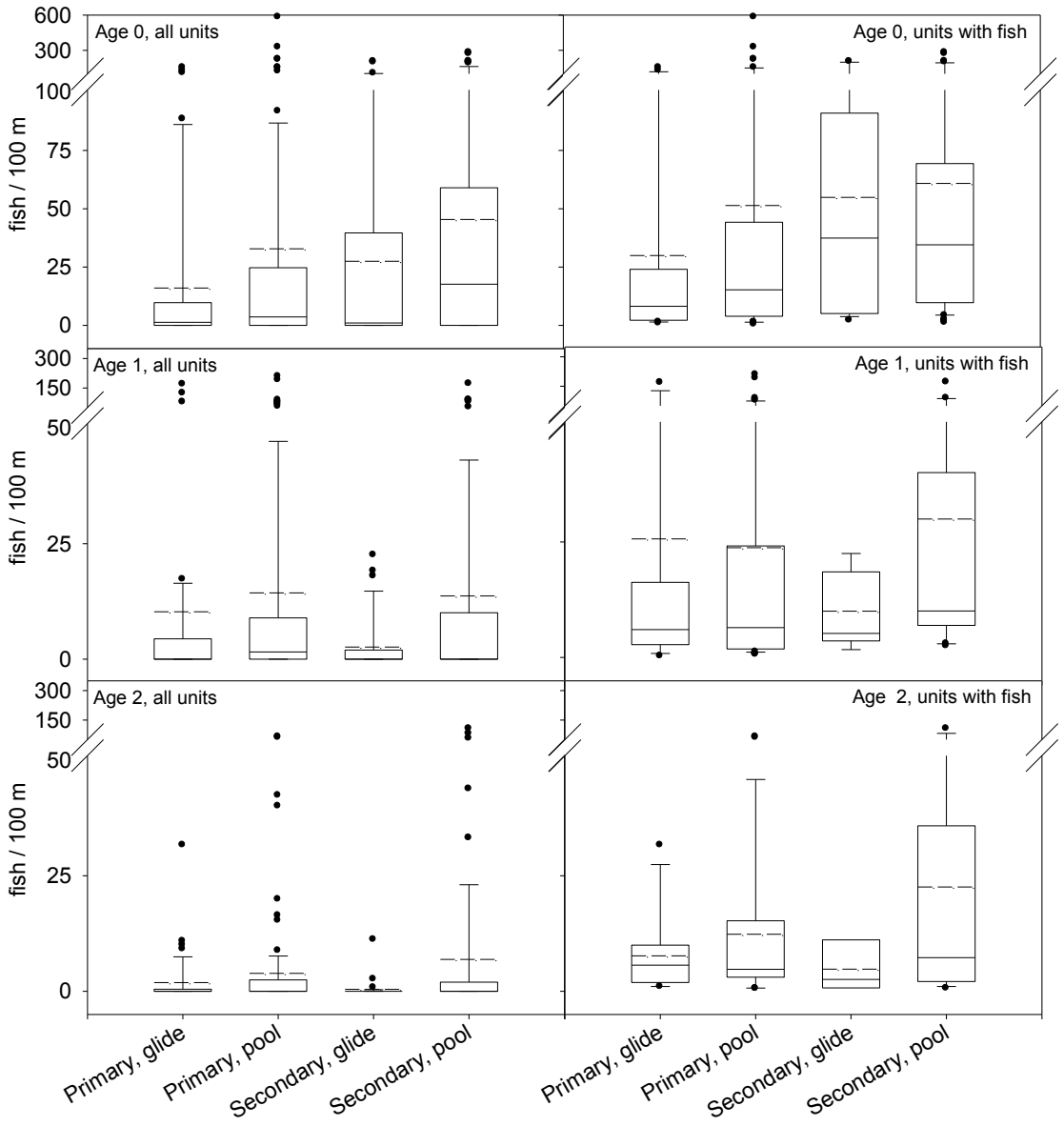

Figure 22. Graph of linear density (number of fish per 100 m) by channel and habitat type for the three age classes of juvenile coho salmon in the Nome River and Osborne Creek. Secondary channel pools excluded beaver ponds. Sample sizes in Table 18 are for the total number of channel units snorkeled (left panel) and for only the snorkeled units where juvenile coho salmon were observed (right panel). Whiskers represent the 5th and 95th percentile; dashed lines represent the mean value and solid lines represent the median value.

Table 19. Comparison of median density (fish per 100 m) by channel and habitat type for the three age classes of juvenile coho salmon in the Nome River and Osborne Creek. Secondary channels include alcoves. Beaver ponds are excluded from count of secondary channel pools. Medians were compared using the Kruskal-Wallis one-way ANOVA on ranks test for ln (1 + number of fish per 100 m). Values in the table are p-values converted from Kruskal-Wallis multiple-comparison Z-value test (Dunn's Test). The Bonferroni corrected p-value is ≤ 0.008 (0.05 / 6 comparisons). The four groups in each age class were compared in two separate tests: those above the diagonal included units with no fish observed and those below the diagonal excluded units with no fish observed. The sample size (n) is for the test that excluded units with no fish; the sample size for all tests that included all units were MG = 45, MP = 86, SG = 34, and SP = 59.

		n	Primary glide	Primary pool	Secondary glide	Secondary pool
Age 0	Primary glide	24	---	0.1352	0.6063	0.0012
	Primary pool	55	0.2658	---	0.4362	0.0310
	Secondary glide	17	0.0988	0.3657	---	0.0153
	Secondary pool	44	0.0100	0.0591	0.6471	---
Age 1	Primary glide	18	---	0.0445	0.3008	0.2296
	Primary pool	52	0.9700	---	0.0028	0.4354
	Secondary glide	9	0.8978	0.9071	---	0.0281
	Secondary pool	27	0.0598	0.0177	0.1763	---
Age 2	Primary glide	11	---	0.3876	0.1198	0.3874
	Primary pool	27	0.8590	---	0.0114	0.9428
	Secondary glide	3	0.5567	0.4633	---	0.0148
	Secondary pool	18	0.3369	0.3177	0.2288	---
Age 1 & 2	Primary glide	19	---	0.0398	0.2939	0.2262
	Primary pool	55	0.8973	---	0.0023	0.4116
	Secondary glide	10	0.8911	0.9556	---	0.0264
	Secondary pool	29	0.1413	0.0412	0.1837	---
All Ages	Primary glide	25	---	0.0278	0.7739	0.0022
	Primary pool	67	0.7325	---	0.0939	0.2355
	Secondary glide	19	0.6178	0.7825	---	0.0122
	Secondary pool	45	0.0439	0.0284	0.1998	---

Intrinsic potential

Approximately 95% of the surveyed stream length had a value of intrinsic potential equal to or greater than 0.75 (Figure 23), which is within the range considered as high intrinsic potential in other studies (Burnett et al. 2007; Busch et al. 2011).

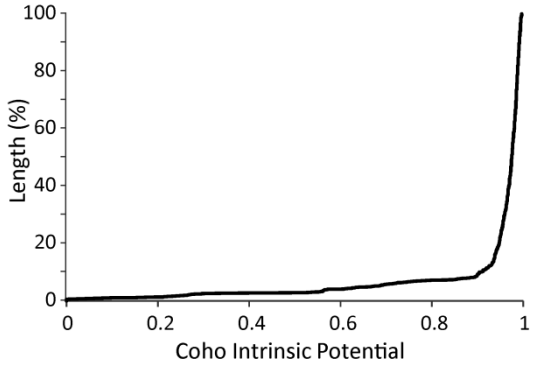

Figure 23. Cumulative distribution of coho salmon intrinsic potential for 54.8 km of surveyed habitat in primary channels of the Nome River and its tributaries. Intrinsic potential was modeled according to Burnett et al. (2007) from the ALOS PRISM 2.5-m DEM-delineated stream layer.

That such a large percentage of stream length was modeled as high intrinsic potential results because values of the three component attributes (mean annual flow, stream gradient, and stream constraint) were highly suitable for coho salmon over the surveyed length. To illustrate, approximately 90% of the field-surveyed length had stream gradients of less than 1.5% (Figure 24a), which corresponded to values exceeding 0.75 for the stream gradient index used in calculating intrinsic potential (Figure 24b).

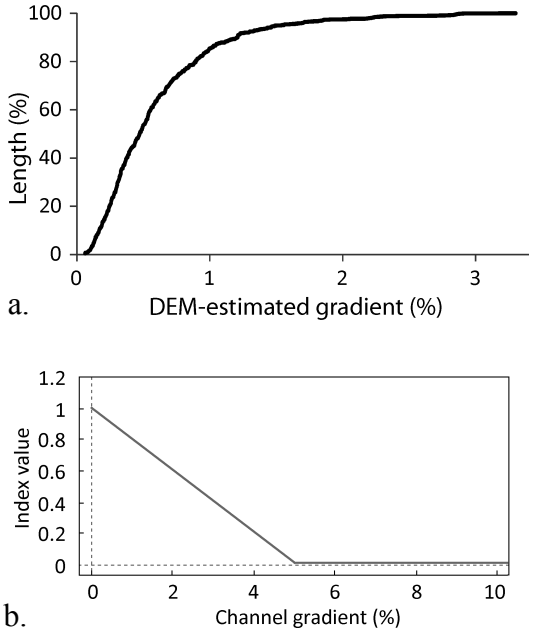

Figure 24. Plot of a) the cumulative distribution of stream gradient for 54.8 km of surveyed length in primary channels of the Nome River and its tributaries, and b) the relationship between values of stream gradient and index scores used to calculate intrinsic potential for coho salmon (Burnett et al. 2007).

Although the range of gradients was narrow for surveyed streams in the Nome River basin, we found that the percentage of channel length (Figure 25a) and total length of channel (Figure 25b) in slow-water habitat unit types (pools and glides) varied inversely with DEM-based channel gradient. Slow-water unit types comprise the majority of very-low-gradient channels (< 0.01 gradient).

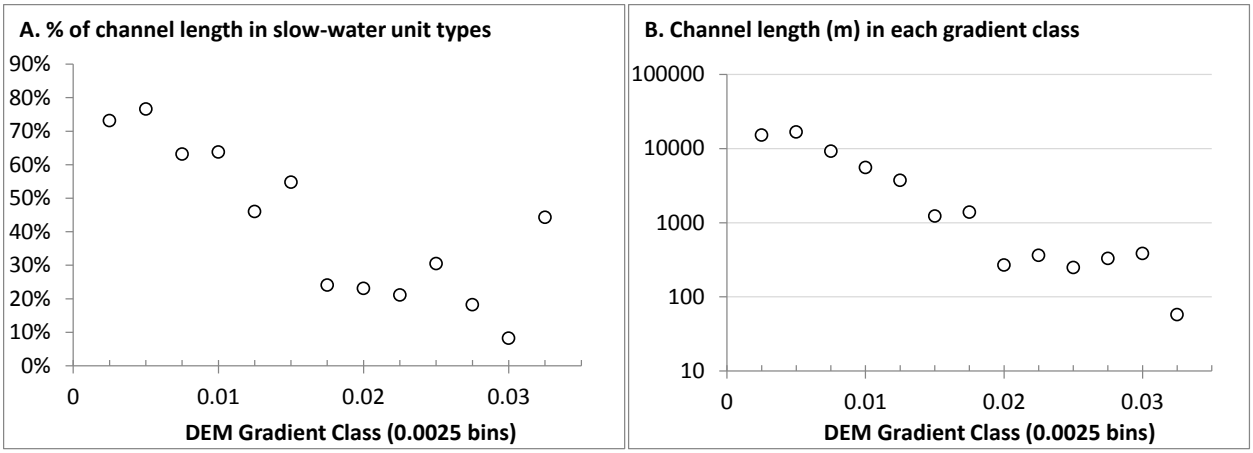

Figure 25. Channel units surveyed in primary channels of the Nome River basin grouped by gradient classes estimated from the ALOS PRISM 2.5-m DEM plotted against: a) the proportion of channel length in slow-water units (pools and glides); and b) the total channel length in each gradient class. Units with DEM gradients exceeding 0.03 included less than 100 m of channel length, less than the 500-m length scale used to estimate channel gradient from the DEM.

VII. DISCUSSION

Terrain Data

Our research demonstrates the feasibility of creating highly accurate, high-resolution digital elevation models over a large area of the AYK from ALOS PRISM satellite data. This stems largely from the availability in PRISM of full swath data for three independent viewing geometries (backward, nadir, and forward), which is unique compared to other optical stereo satellite data. By combining multiple swaths of the PRISM imagery, we derived for the Nome River basin a final seamless ortho-rectified optical image mosaic (8 bit amplitude nadir imagery) and a 2.5-m DEM mosaic (32-bit floating-point elevations). The status of the Alaska Satellite Facility as the Americas ALOS Data Node allowed us to obtain the Japanese Space Agency (JAXA)-supported DOGS-AP software. This software includes a stereo matching technique that takes full advantage of the triplet images and redundancy between backward-nadir and forward-nadir geometries when generating PRISM DEMs and ortho imagery. By combining the backward-nadir and forward-nadir correlations, the software produces DEMs of greater accuracy than two-view stereoscopic methods that have been the standard.

We developed processing algorithms that bypassed the graphical user interface of the DOGS-AP software and automated PRISM DEM production. We also automated production of PRISM mosaics by developing Perl programming language scripts for: 1) the tie-point .matching; 2) automated culling through statistical assessment; 3) bundle adjustment using all input swaths; 4) determining optimal affine transforms for each input swath; and 5) combining results into seamless mosaics. However, manual cloud masking of each PRISM DEM was still required prior to mosaic processing.

The ALOS PRISM 2.5-m DEM was much more accurate than either the available NED 60-m DEM or the ALOS PALSAR 10-m DEM we derived. The final PRISM DEMs have a vertical accuracy of 5 meters expressed as the linear error at a 95% probability level (LE95) with postings at 2.5 m or 5 m that meets the U.S. Geological Survey (USGS) defined National Map Accuracy Standards for Alaska. The LE95 was derived from the measured RMSE (Maune et al. 2007) in Table 6.

Our use of high quality differential Global Positioning System (GPS) data for geodetic control points improved the planimetric accuracy of the DEMs. The vertical accuracy of PRISM DEMs for the Nome River basin was similar to that of PRISM DEMs for Death Valley National Park, U.S. (R. Guritz, unpublished data), an area of southern California resembling the Nome River basin in terrain variability and sparse vegetation. Accuracies of the southern California DEMs were nearly identical when evaluated with LiDAR data (15 cm LE95 at 1-m posting) and with satellite laser altimetry data (ICESat), the data source we used to evaluate the Nome River basin DEMs. Thus, the ICESat data provide a reliable and economical means to evaluate DEM accuracies over large, remote regions of the AYK region.

Unlike our DEMs, the National Elevation Data for Alaska do not meet National Map Accuracy Standards, and only recently have other data accurate enough to do so become available for limited areas of the state. These data were developed through the Alaska Statewide Digital Mapping Initiative (SDMI). The SDMI (www.alaskamapped.org) is coordinating a multi-year, program, to provide high-resolution digital elevation data and ortho-imagery for all of Alaska. The program is jointly funded by the state and federal governments, with estimated costs for the statewide DEMs between $55,000,000 and $75,000,000 (Maune 2009). To date, 5-m resolution DEMs have been delivered from aircraft-based Interferometric Synthetic Aperture Radar (IFSAR) sensors for large regions of south central Alaska and some of the AYK region. In 2011, IFSAR DEM costs were roughly $35 per km^2 (USGS 2012). Projects also have been undertaken to develop 1.2-m-resolution DEMs from aircraft-based LiDAR sensors for a variety of areas including the Kenai Peninsula, Matanuska-Susitna Borough, and the proposed gas line corridor south from Prudhoe Bay (Department of Geological and Geophysical Surveys, http://www.dggs.alaska.gov); only the latter includes any of AYK region. Given the high acquisition and processing costs, LiDAR data are unlikely to be a viable source of

DEMs for much of the AYK region; estimates for LiDAR-derived DEMs range from $100 to $200 per km^2, depending upon the region and amount of post processing desired (USGS 2012).

Until the SDMI digital elevation data become available for the AYK region, ALOS PRISM data are a relatively low-cost source of DEMs and ortho-imagery with accuracies and resolutions that should be sufficient to benefit fisheries management. The software we developed for producing the final PRISM DEM and ortho imagery kept costs low, approximately $5 per km^2 for the Nome River basin. Using methods developed for the Nome River basin, ALOS PRISM DEMs have also been produced for fisheries management in the Slana River. In May of 2011, JAXA terminated agreements with each of the foreign partner data nodes, including the Americas ALOS Data Node at ASF. This decision supports changing their data archive and distribution to a commercial vendor-based system and preparing for future missions including ALOS2 planned to launch in early 2013. Costs for DEMs produced using ALOS or ALOS2 data for non-research applications are not known at this time. However, DEM products can be requested through JAXA, the new commercial vendors, and possibly ASF from their archive of ALOS PALSAR and PRISM data to support research activities in Alaska evaluated on a case-by-case basis. Inquiries can be directed to Scott Arko (saarko@alaska.edu).

In addition to ALOS PRISM, various sources of satellite-generated DEMs and/or ortho-imagery are or will soon be available for the AYK region. Such products range in resolution, accuracy, and cost but are relatively inexpensive compared to aircraft-based sources. Included among these sources are the Advanced Spaceborne Thermal Emission and Reflection Radiometer (ASTER) Global Digital Elevation Model Version 2 (GDEM V2), which can be obtained for free at a 30-m posting; SPOT 5 ortho-imagery at 2.5-m resolution is being obtained as part of the SDMI and SPOT 5HRS DEMs, produced by correlation of stereo-photo pairs, can be purchased for about $4 per km^2 at a 10-m posting; GeoEye-1 (GeoEye-2 in 2013) can provide stereo-photo pairs with up to 0.5 m resolution for generating ortho-imagery and DEMs; and the Tandem-X mission will generate in 2014 a global DEM from X-band SAR Interferometry at 12-m postings, but published prices are not yet available for these commercially offered products.

Stream Network with Hydrogeomorphic Attributes

For the Nome River and its tributaries, we combined the newly created DEMs and field data to delineate a stream network with 14 modeled hydrogeomorphic attributes that can influence salmon habitat. Data for the hydrogeomorphic attributes are available for each channel node in the stream network. When compared to other common tools for delineating streams from DEMs, ArcHydro (Maidment 2002) and HEC-GeoHMS (USACE 2000), our algorithms (Miller et al. 2003, Clarke et al. 2008) produced the most spatially and structurally accurate networks (Peñas et al. 2011). Differences in accuracy were most pronounced with higher-

resolution DEMs because this is when results from the three stream delineation algorithms most diverge (Peñas et al. 2011).

Of the different sources of digital elevation data we examined, the highest resolution ALOS PRISM-derived 2.5-m DEMs yielded a stream network that best represented the spatial location and extent of channels visible on the ortho-rectified optical imagery and the summer TerraSAR-X images. None of the DEMs produced a stream network that accurately represents all of the meandering and anastomosing channels in the broad, low-gradient valleys of the Nome River basin. Although the 2.5-m horizontal resolution of the DEM resolved the valleys and many valley-floor features, DEMs with sub-meter horizontal resolution and vertical precision will be necessary to delineate all stream channels or characterize channel banks and terraces. By linking the flow paths inferred from the PRISM DEM to a water mask developed from the PRISM optical imagery, we enhanced the quality of the final delineated stream network, particularly along the mainstem of the Nome River. We capitalized on relatively high contrast between wet and dry areas in the PRISM optical imagery to develop the water mask; however, this will be impractical in heavily forested areas. Difficulties when delineating streams in flat areas have been recognized (Wang and Yin 1998; Peñas et al. 2011) and solutions other than increasing DEM resolution have been explored (Zhang and Huang 2009). Adding the capacity to incorporate a water mask in methods that were developed for areas of relatively high topographic relief (Miller et al. 2003; Clarke et al. 2008), allowed us to delineate a stream network for the Nome River basin that faithfully followed primary channels on the 1:100,000 NHD.

Our methods vary the contributing-area threshold necessary to initiate a stream channel and so consistently represented many small channels that are not mapped on the NHD. Thus, for the Nome River basin, the final ALOS PRISM 2.5-m DEM-delineated streams extend to contributing areas as small as 0.004 km^2 in steep, dissected terrain, but may not initiate a stream until the contributing area exceeds 1.0 km^2 in low-gradient, undissected terrain. This helps minimize delineation of artifact channels in low-gradient areas. The final stream network includes the entire extent of channels that support salmonids in the Nome River basin. By contrast, Luck et al. (2010) used a 50-km^2 initiation threshold when delineating stream networks for Alaska from Shuttle Radar Topography Mission (SRTM) 60-m DEMs. Their stream network, based on such a large stream initiation threshold, should include rivers with drainage areas similar to the Nome River and Osborne Creek but likely omits smaller tributaries where anadromous salmonids have been observed (e.g., Gaboury et al. 2005). Because field measurements at locations where channels initiate were unavailable for the Nome River basin, as is true for most areas, the upstream extent of streams in our final stream network was solely based on characteristics of the DEM. Streams were delineated as far upslope as the PRISM 2.5-m DEM would allow and the stream network undoubtedly includes channels with seasonal and ephemeral flow and likely some unchannelized areas. To classify DEM-traced channels based on flow regime, if this is ever

desired for the Nome River basin, will require field data collection (e.g., Olson and Brouillette 2006; Clarke et al. 2008; McCleary 2011).

Because the final stream network was delineated by tracing flow directions inferred from DEMs, the flow path to any point in the channel network or in the basin can be followed upstream from a stream mouth. This capacity allows identification of floodplain and hillslope areas that are linked by surface flow to each channel node and was critical to modeling several of the hydrogeomorphic attributes. Thus, several subsequent data processing steps could be automated and greatly simplified, including associating valley-floor attributes, such as off-channel habitat area, to channel locations and summarizing field or modeled data (e.g., habitat abundance) for any specified portion of the stream network.

The 14 hydrogeomorphic attributes that are linked to the stream network can inform ecological, hydrological, and geomorphological research, analysis, and modeling. Such hydrogeomorphic attributes have been generated elsewhere (e.g., Davies et al. 2007; Benda et al. 2007) and used over large areas to model channel morphology, channel dynamics, and stream habitats (e.g., Wohl and Merritt 2005; Miller and Burnett 2008; Busch et al. 2011; Whited et al. 2013). Ability to model channel gradients from DEMs has proven particularly useful in Alaska for characterizing salmonid habitats (Wissmar et al. 2010). Despite our field- and DEM-estimated channel gradients being statistically significantly correlated with one another, the correlation was less than in other studies (e.g., Davies et al. 2007; Clarke et al. 2008; Wissmar et al. 2010). The most likely explanation is that the field and DEM estimates in these other studies were considered over a much wider range of channel gradients (0% to exceeding 15%) than in the Nome River basin (0% to 4%). Even so, we were able to resolve channel gradients with the ALOS PRISM DEM across this entire range, yet less reliably at the lowest gradients.

Although channel gradient and many of the other hydrogeomorphic attributes were derived with existing approaches (e.g., Burnett et al. 2007; Clarke et al. 2008), we developed new methods for attributes that describe channel configuration from the valley width and water mask based on the DEM-delineated valley floor. Such coarse-scale features of floodplain habitat complexity may be more important to salmon than suggested from fine-scale measures obtained in the field but by necessity in only in a few selected sites (Luck 2010). The attributes of water-mask area per channel length and edge length per channel length indicate availability of off-channel and complex edge habitats, which are important to rearing juvenile salmonids (e.g., Nickelson et al. 1992; Beechie et al. 1994; Bradford et al. 2001; Bradford et al. 2009). Where valley-width- and water-mask-based estimates are important correlates with observed fish distributions or abundances, then further effort may be warranted to determine consistency with estimates from field or other of independent datasets.

The methods we developed can be applied to delineate stream networks for a variety of uses throughout the AYK wherever DEMs are available. Such stream networks can benefit fisheries management in many ways, including as we demonstrated for the Nome River basin, by providing a bridge between DEM-derived topography and field data. Delineated streams can help to address other mapping needs in Alaska as identified through a user survey of governmental agencies, non-governmental organizations, academia, native groups, and private industries (Alaska Statewide Digital Mapping Initiative 2008). Approximately 75% of survey respondents, more than for any other feature type (e.g., land cover, buildings, roads), indicated the need for hydrography to support modeling and analysis across a range of interests that encompass watershed management, water quality management, floodplain management, sea-level change, and safe operations of float planes.

Classifying Open Water as an Indicator of Potential Overwintering Habitat

Discontinuation of the RADARSAT data and poor resolution in the PALSAR data focused our classification efforts on the TerraSAR-X data, thereby substantively increasing the challenges and time required to process data. Documentation for the ASF prototype MapReady (v 2.2.5, 23 May 2009) software indicated TerraSAR-X data was experimentally supported. However, the capability for terrain correcting and geo-coding TerraSAR-X data was not fully functional until version 3.1.22 was released on 21 December 2012. After that date, we began creating SPAN images with PolSARPro from 24 dual polarization TerraSAR-X datasets.

The close match between the water mask from the ALOS PRISM optical imagery and the river network on the SPAN image from summer provides evidence that terrain correcting and geo-coding of the SAR imagery were successful. This is necessary to focus classification efforts on areas covered by the water mask, as is typically done (e.g., Gauthier et al. 2006; Mermoz et al. 2009) and so better distinguish areas in the SPAN imagery as open water, ice over water, and frozen to the bottom. Terrain correcting and geo-coding enabled us to assemble a time series of geo-referenced SPAN images, reflecting the high accuracy of the ALOS PRISM 2.5-m DEM in minimizing geometry differences between ascending and descending data and in correcting for layover affects in the SAR data due to terrain height and look direction. Although we plan to classify SPAN images only for dates corresponding to field data collection in late March and early April of 2009, the time series should help distinguish between dark areas of open water and of ice because many of the frozen areas appeared brighter in previous images earlier in the freezing process.

Given the ability to visually identify open water and ice in the SPAN images from TerraSAR-X data, we are optimistic about developing a statistical model for classification. Ice and water have been classified from SAR

data in larger rivers (e.g., Mermoz et al. 2009a, 2009b), and in one case with direct relevance to salmonid management. In the Tanana River, persistent areas of open water, thought to be associated with groundwater upwelling, were distinguished from ice in C-band SAR imagery and directly related to numbers of spawning chum salmon (Wirth et al. 2012). A portion of the data we collected during the winter at the 72 field sites will inform a supervised classification of the SPAN images; the rest will be used to assess the accuracy of classified images.

Although user's accuracies from SAR classifications of open water can be very high, exceeding 90% (Mermoz et al. 2009a, 2009b), several hurdles remain to developing a usable classification for the Nome River. For example, the X-band SAR may not penetrate snow as readily as the longer wavelength, coarser resolution C-band, and so distinguishing classes of open water and ice may be challenging where snow is present. In addition, past classifications of open water / ice were for much larger rivers than the Nome River. The 3-m resolution of the TerraSAR-X data should be small enough for classifying the mainstem Nome River given that the mean wetted widths of pools range from 13 m to 45 m. But tributary pools, including those in Osborne Creek, have mean wetted widths $\leq$ 5 m. We may be able to overcome this and other problems by combining SAR data with DEM-derived terrain data and field data on ice classes. To illustrate, no open water was found at any of our mainstem field sites with drainage areas < 146 km^2 and so this threshold may offer a coarse screen to exclude the tributaries as open water during winter. Now that the time series of SPAN images from the TerraSAR-X data is geo-referenced to the rest of our data, we will develop and test the classification for open water over the next few months. This may offer a basis for identifying potential spawning or overwintering rearing habitat (e.g., Levings and Lauzier 1991; Wirth et al. 2012).

Relating Juvenile Coho Salmon to Hydrogeomorphic and Landscape Characteristics

The new technique we developed for associating field data to nodes in a DEM-derived stream network affords efficiency in data processing and flexibility in data analysis. The stream layer for the Nome River basin was written to a GIS vector file with a record for each geo-referenced primary channel unit containing tabular data for all summer and winter field attributes and all DEM-derived hydrogeomorphic attributes. Summer field data from the sample of secondary and alcove units were geo-referenced to the stream layer by snapping a GPS point to the nearest primary channel node. Such data could be directly linked to secondary channels and alcoves when mapped in a stream network. If ever of interest for the Nome River, secondary channels and alcoves from the water mask can be added to the DEM-derived stream network. All data are documented, processed for quality control, and available through the Watershed Explorer on the NetMap site (http://earthsystems.net/NomeRiver). Although stored in a channel-node structure at the resolution of the DEM, the data can be summarized for analysis at any coarser spatial resolution.

Juvenile coho salmon did not appear to be randomly distributed at any spatial resolution we considered in the Nome River basin. At the micro-habitat scale, juvenile coho salmon were observed primarily along stream margins and only occasionally in mid-channel habitat, which as Bradford et al. (1997) summarized, is typical in larger rivers. Juvenile coho using stream margins were often concentrated around the bank dens of beaver. The link between beaver ponds and juvenile coho salmon rearing is well established (e.g., Nickelson et al. 1992). Bank denning activities of beaver are thought to exert less influence on freshwater ecosystems (Collen and Gibson 2000), and potential relationships to coho salmon have not been widely studied. Of all stream segments surveyed, only Buster Creek contained beaver dams in the primary channel, but bank dens were common particularly in the mainstem. At the channel-unit scale for primary channels in the mainstem, the distribution of fish of all age classes, but especially of age 2, was patchy and heavily influenced by the many units with zero counts. Snorkel counts, however, were not spatially auto-correlated for age-2 fish and only weakly so at small spatial scales (< 300 m) for age-0 and age-1 fish. This obviates the need to account for spatial autocorrelation, thus simplifying subsequent statistical modeling to relate juvenile coho salmon to hydrogeomorphic and landscape characteristics. Cumulative counts of age-0 and age-1 fish increased gradually over the downstream most 23 km of the mainstem Nome River and then increased sharply over the next 3 km upstream. Beyond this distance, age-1 fish were rarely observed. The longitudinal distribution of age-0 fish coincides with reports of salmon spawning habitat concentrated on the Nome River between Osborne Creek and Hobson Creek (Gaboury et al. 2005). Approximately 75% of the counted age-2 fish were seen in the downstream-most 5 km of snorkeled habitat in the Nome River. At the stream-segment scale in the mainstem, each age class occurred in each stream segment but densities were generally greater for age-0 fish in upstream segments and of age-2 fish in downstream segments. At the tributary scale, we saw juvenile coho salmon only in Osborne Creek and Darling Creek. Juvenile coho salmon have been captured during previous summers in the other Nome River tributaries though were more widely distributed in June than in August (Gaboury et al. 2005). Taken with this, our findings suggest that juvenile coho salmon may have begun moving downstream toward overwintering habitats before the August survey but fewer or more narrowly distributed spawners could help explain differences in juvenile distributions between the two studies.

Among channel-unit types, densities of juvenile coho salmon were much greater in slow-water than fast-water habitats, but snorkelers observed no fish in many of the slow-water habitats. Despite much of the primary channel in the Nome River being in fast-water habitats, we found juvenile coho salmon in only two snorkeled riffles. Higher densities of each age class were seen in beaver ponds than in other habitat types. However, only five beaver ponds were snorkeled due to human health concerns and visibility issues. Beaver ponds are important for juvenile coho salmon, particularly during winter (e.g., Nickelson et al. 1992; Rosell et al. 2005), but may warm and dry during summer becoming less suitable habitat (Dolloff 1987). Considering all

other snorkeled slow-water habitats, glides in secondary channels supported the lowest densities of all three age classes, indicating relatively poor summer rearing quality. Densities in secondary channel pools were higher than in primary channel pools only for age-0 fish. Except for age-1 fish, densities in primary channel pools and glides did not differ. Results when comparing fish densities among age classes and among habitat types depended on whether units with zero counts were included or excluded. This suggests that age-specific and habitat-specific differences in fish abundance may arise from factors affecting whether or not fish occupy a unit as well as those affecting abundance in occupied units.

Consequently, statistical tools are needed to model relationships between these seriously zero-inflated juvenile coho salmon data and hydrogeomorphic and landscape characteristics in the Nome River basin. Two promising classes of models we plan to explore are Poisson regression to directly predict counts (e.g., Kirkby 2013) and hurdle modeling or modified hurdle modeling that uses logistic regression to predict presence/absence followed by linear regression to predict density (e.g., Steel et al. 2012). Modeling the three age classes separately exacerbates the "zero challenge" but may allow identification of potentially important differences in habitat use among life-history stages. However, we will likely explore modeling age-1 and age-2 fish together as a "pre-smolt" class, given that densities were similar in both slow-water habitat types (pools and glides) and that the majority of these fish are expected to smolt the following spring. Due to small sample sizes for secondary channels/alcoves and how juvenile coho salmon were distributed, we will focus modeling on pools and glides in primary channels of the Nome River and Osborne Creek. The strong correspondence between results for linear and areal density of juvenile coho salmon, fish counts that were uncorrelated with unit area, and the fact that stream length is generally considered an appropriate measure of habitat abundance for coho salmon (Bradford 1997) lead us to use the linear metric in any subsequent modeling of fish density.

More juvenile coho salmon were observed than any other age class or species of fish in the Nome River basin, which was consistent with the high intrinsic potential we modeled throughout the basin. Almost all stream reaches had a high intrinsic potential, and thus the model developed for western Oregon (Burnett et al. 2007) had limited utility in the Nome River basin. It may, however, be useful for distinguishing among streams for the capacity to provide high-quality rearing habitat when applied over a broader area of Norton Sound or of the AYK, where values of the component attributes (mean annual flow, stream gradient, and stream constraint) are more likely to vary beyond the range that is highly suitable for coho salmon. Despite a narrow range of gradients for surveyed streams in the Nome River basin, the channel length in slow-water habitat unit types varied inversely with DEM-derived channel gradient. This relationship may be helpful for identifying high-capacity stream reaches over a finer spatial resolution as an alternative to the intrinsic potential model. Similarly, pool density and DEM-derived gradients were correlated in southeast Alaska, but this was over a wider range of channel gradients (Wissmar et al. 2010) than occur in the Nome River.

The realized quality, as opposed to the capacity, of habitat in the Nome River depends on various abiotic and biotic factors. Neither large wood nor boulders are common in streams of the Nome River basin, and thus habitat quality largely depends on the complexity of channels and their margins. In primary channels of the mainstem, approximately half of all habitat units identified in the field were complex, defined as containing an entrance or an exit to a secondary channel or alcove. Approximating this are the two metrics of channel complexity we derived from the water mask, which will be used in our statistical modeling of juvenile coho salmon. As potential predators of juvenile coho salmon, adults of one species or another were seen in every Nome River stream segment. Presence of adults may have influenced the suitability and use of habitats by juvenile coho salmon and will be considered in statistical models. Densities of juvenile coho salmon in the Nome River were relatively low compared with the few estimates we could find for other streams at higher latitudes (e.g., Bradford et al. 1997; Rosenfeld et al. 2000; Wissmar et al. 2010). This could be because habitat quality in the Nome River is poor; the basin does rank relatively high among Norton Sound river basins regarding the potential for human effects on streams. It may also be because our detection probabilities for observing juvenile coho salmon while snorkeling were low. Thus, our estimates may not be comparable with those obtained in other basins or by other methods.

VIII. REFERENCES

Alaska Statewide Digital Mapping Initiative Project Planning SDMI User Survey Report Project Needs, User Preferences, and Potential Partnerships, www.alaskamapped.org .

Andrew, M.E., and M.A. Wulder. 2011. Idiosyncratic responses of Pacific salmonid species to landcover fragmentation and scale. Ecography 34:780-797doi: 10.1111/j.1600-0587.2010.06607.x

Anlauf, K. J., D. W. Jensen, K. M. Burnett, E. A. Steel, K. Christiansen, J. C. Firman, B. E. Feist, and D. P. Larsen. 2011. Explaining spatial variability in stream habitats using both natural and management-influenced landscape predictors. Aquatic Conservation: Marine and Freshwater Ecosystems, DOI: 10.1002/aqc.1221

Atwood, D. K., R. M Guritz, R. R. Muskett, C. S. Lingle, J. M. Sauber, and J. T. Freymueller. 2007. DEM control in Arctic Alaska with ICESat laser altimetry. IEEE Transactions on Geoscience and Remote Sensing 45:3710-3720.

AYK SSI (Arctic-Yukon-Kuskokwim Sustainable Salmon Initiative). 2006. Arctic-Yukon-Kuskokwim salmon research and restoration plan. Bering Sea Fishermen's Association, 705 Christensen Drive, Anchorage, Alaska.

Beechie, T., E. Beamer, and L. Wasserman. 1994. Estimating coho salmon rearing habitat and smolt production losses in a large river basin, and implications for habitat restoration. North American Journal of Fisheries Management 14:797–811.

Benda, L., D. Miller, K. Andras, P. Bigelow, G. Reeves, and D. Michael. 2007. NetMap: A new tool in support of watershed science and resource management. Forest Science 53: 206-219.

Bisson, P. A., K. Sullivan, and J. L. Nielsen. 1988. Channel hydraulics, habitat use, and body form of juvenile coho salmon, steelhead and cutthroat trout in streams. Transactions of the American Fisheries Society. 117:262-273.

Bottom, D. L., and K. K. Jones. 1990. Species composition, distribution, and invertebrate prey of fish assemblages in the Columbia River Estuary. Progress in Oceanography 25: 243-270.

Bradford, M. J. 1997. Empirical review of coho salmon smolt abundance and the prediction of smolt production at the regional level. Transactions of the American Fisheries Society 126:49–64.

Bradford, M. J., J. A. Grout, and S. Moodie. 2001. Ecology of juvenile Chinook salmon in a small nonnatal stream of the Yukon River drainage and the role of ice conditions on their distribution and survival. Canadian Journal of Zoology 79:2043–2054.

Bradford, M. J., A. von Finster, and P. A. Milligan. 2009. Freshwater life history, habitat, and the production of Chinook salmon from the upper Yukon basin. Pages 19–38 *in* C. C. Krueger and C. E. Zimmerman, editors. Pacific salmon: ecology and management of western Alaska's populations. American Fisheries Society, Symposium 70, Bethesda, Maryland.

Burnett, K. M. 2001. Relationships among juvenile anadromous salmonids, their freshwater habitat, and landscape characteristics over multiple years and spatial scales in the Elk River, Oregon. Doctoral dissertation, Oregon State University, Corvallis, Oregon.

Burnett, K. M., G. H. Reeves, S. E. Clarke, and K. R. Christiansen. 2006. Comparing riparian and catchment influences in stream habitat in a forested, montane landscape. Pages 175-197 *in* R. M. Hughes, L. Wang, and P. W. Seelbach, editors. Landscape influences on stream habitats and biological assemblages. American Fisheries Society, Symposium 48, Bethesda, Maryland.

Burnett, K. M., G. H. Reeves, D. J. Miller, S. Clarke, K. Vance-Borland, and K. Christiansen. 2007. Distribution of salmon-habitat potential relative to landscape characteristics and implications for conservation. Ecological Applications 17:66-80.

Busch, D. S., M. Sheer, K. Burnett, P. McElhany, and T. Cooney. 2011. Landscape-level model to predict spawning habitat for lower Columbia River fall Chinook salmon (*Oncorhynchus tshawytscha*). River Research and Applications, doi: 10.1002/rra.1597

Clarke, S. E., and K. M. Burnett, 2003. Comparison of digital elevation models for aquatic data development. Photogrammetric Engineering and Remote Sensing 69:1367-1375.

Clarke, S. E., K. M. Burnett, and D. J. Miller. 2008. Modeling streams and hydrogeomorphic attributes in Oregon from digital and field data. Journal of the American Water Resources Association 44:459-477.

Collen, P., and R. J. Gibson. 2000. The general ecology of beavers (*Castor* spp.), as related to their influence on stream ecosystems and riparian habitats, and the subsequent effects on fish–a review. Reviews in Fish Biology and Fisheries 10:439-461.

Daly, C., R. P. Neilson, and D. L. Phillips. 1994. A statistical topographic model for napping climatological precipitation over mountainous terrain. Journal of Applied Meteorology 33:140-158. (http://www.climatesource.com/docs/csguid.pdf; http://www.climatesource.com/ak/fact_sheets/fact_precip_ak.html)

Davies, J. R., K. M. Lagueux, B. Sanderson, and T. J. Beechie, 2007. Modeling stream channel characteristics from drainage-enforced DEMs in Puget Sound, Washington, USA. Journal of the American Water Resources Association 43:414-426.

Dolloff, C. A.1987. Seasonal population characteristics and habitat use by juvenile coho salmon in a small southeast Alaska stream. Transactions of the American Fisheries Society 116:829-838

ESRI. 1998. Shapefile technical description: An ESRI white paper—July 1998. ESRI press, Redlands http://www.esri.com/library/whitepapers/pdfs/shapefile.pdf

Frissell C. A., W. J. Liss, C. E. Warren, and M. D. Hurley. 1986. A hierarchical framework for stream habitat classification: viewing streams in a watershed context. Environmental Management 10:199-214.

Fullerton, A. H., S. T. Lindley, G. R. Pess, B. E. Feist, E. A. Steel, and P. McElhany. 2011. Human influence on the spatial structure of threatened Pacific salmon metapopulations. Conservation Biology 25: 932–944. DOI: 10.1111/j.1523-1739.2011.01718.x

Gaboury, M. N., R. B. Murray, R. C. Bocking, and M. J. Nemeth. 2005. Development and application of a salmon habitat restoration framework on the Nome River watershed, Alaska. Final report prepared for the Arctic-Yukon-Kuskokwim Sustainable Salmon Initiative by LGL limited environmental research associates and LGL Alaska Research Associates, Inc. Anchorage, Alaska.

Ganio, L. M., C. E. Torgersen, and R. E. Gresswell. 2005. A geostatistical approach for describing spatial pattern in stream networks. Frontiers in Ecology and Environment 3:138-144.

Gauthier, Y., F. Weber, S. Savary, M. Jasek, L. M. Paquet, and M. Bernier. 2006. A combined classification scheme to characterise river ice from SAR data. EARSeL eProceedings 5(1):77-88.

Hall, J. E., D. M. Holzer, and T. J. Beechie, 2007. Predicting river floodplain and lateral channel migration for salmon habitat conservation. Journal of the American Water Resources Association 43(3):786-797. DOI: 10.1111/j.1752-1688.2007.00063.x

Hankin, D. G., and G. H. Reeves. 1988. Estimating total fish abundance and total habitat area in small streams based on visual estimation methods. Canadian Journal of Fisheries and Aquatic Sciences 45:834-844.

Hawkins, C. P., J. L. Kershner, P. A. Bisson, M. D. Bryant, L. M. Decker, S. V. Gregory, D. A. McCullough, C. K. Overton, G. H. Reeves, R. J. Steedman, and M. K. Young. 1993. A hierarchal approach to classifying stream habitat features. Fisheries 18:3-12.

Huusko, A., L. Greenberg, M. Stickler, T. Linnansaari, M. Nyk nen, T. Vehanen, S. Koljonen, P. Louhi, and K. Alfredsen. 2007. Life in the ice lane: the winter ecology of stream salmonids. River Research and Applications 23:469–491. doi: 10.1002/rra.999

Kirkby, K. M. S. 2013. Distribution of juvenile salmonids and stream habitat relative to 15-year-old debris-flow deposits in the Oregon Coast Range. Master's thesis, Oregon State University, Corvallis, Oregon.

Lawson, P. W., E. Bjorkstedt, M. Chilcote, C. Huntington, J. Mills, K. Moore, T. E. Nickelson, G. H. Reeves, H. A. Stout, and T. C. Wainwright. 2005. Identification of historical populations of coho salmon (*Oncorhynchus kisutch*) in the Oregon Coast evolutionarily significant unit. Review draft, Oregon Northern California Coast Technical Recovery Team, NOAA/NMFS/NWFSC, 129 pp.

Lee, D. C., J. R. Sedell, B. E. Rieman, R. F. Thurow, and J. E. Williams. 1997. Broadscale assessment of aquatic species and habitats. General Technical Report PNW-GTR-405 (Vol. 3), U.S. Department of Agriculture, Forest Service, Pacific Northwest Research Station, Portland, Oregon.

Leopold, L. B., M. G. Wolman, and J. P. Miller, 1964. Fluvial processes in geomorphology. Dover Publications, New York, New York.

Levings, C. D., and R. B. Lauzier. 1991. Extensive use of the Fraser River basin as winter habitat by juvenile Chinook salmon (*Oncorhynchus tshawytscha*).Canadian Journal of Zoology 69:1759–1767.

Lindley, S. T., R. S. Schick, A. Agrawal, M. Goslin, T. E. Pearson, E. Mora, and J. G. Williams. 2006. Historical population structure of Central Valley steelhead and its alteration by dams. San Francisco Estuary and Watershed Science 4(1):

Lister D. B., and H. S. Genoe. 1970. Stream habitat utilization by cohabiting underyearlings of Chinook *Oncorhynchus tshawytscha*) and coho (*O. kisutch*) salmon in the Big Qualicum River, British Columbia. Journal of the Fisheries Research Board of Canada 27:1215-1224.

Luck, M., N. Maumenee, D. Whited, J. Lucotch, S. Chilcote, M. Lorang, D. Goodman, K. McDonald, J. Kimball, and J. Stanford. 2010. Remote sensing analysis of physical complexity of North Pacific Rim rivers to assist wild salmon conservation. Earth Surface Processes and Landforms (www.interscience.wiley.com) DOI: 10.1002/esp.2044

Maidment, D. R. 2002. Arc Hydro: GIS for water resources with CDROM (Vol. 220). ESRI press, Redlands, California.

Maune, D. F. 2009. Digital elevation model (DEM) data for the Alaska Statewide Digital Mapping Initiative (SDMI). Dewberry, 8401 Arlington Blvd, Fairfax, Virginia 22031-4666.

McCleary, R. J. 2011. Landscape organization based on application of the process domain concept for a glaciated foothills region. Doctoral dissertation. University of British Columbia. Vancouver, British Columbia, Canada.

Menard, J., J. Soong, and S. Kent. 2011. 2009 Annual Management Report Norton Sound, Port Clarence, and Kotzebue. Alaska Department of Fish & Game, Fishery Management Report, No. 11-46, Anchorage, Alaska.

Mermoz, S., Allain, S., Bernier, M., & Pottier, E. 2009a. Investigation of Radarsat-2 and Terrasar-X data for river ice classification. In Geoscience and Remote Sensing Symposium, 2009 IEEE International, IGARSS 2: II-29.

Mermoz S., S. Allain, M. Bernier, E. Pottier, and I. Gherboudj. 2009b. Classification of river ice using polarimetric SAR data. Canadian Journal of Remote Sensing 35:460-473. 10.5589/m09-034

Miller, D. J. 2003. Programs for DEM analysis. Landscape dynamics and forest management, General Technical Report RMRS-GTR-101CD. USDA Forest Service, Rocky Mountain Research Station, Fort Collins, Colorado.

Miller, D. J., and K. M. Burnett. 2008. A probabilistic model of debris-flow delivery to stream channels, demonstrated for the Coast Range of Oregon, USA. Geomorphology 94:184–205.

Miller et al. 2003 missing

Montgomery, D. R., and J. M. Buffington. 1997. Channel-reach morphology in mountain drainage basins, *Geological Society of America Bulletin*, *106*(5), 596-611.

Nemeth, M. J., B. Bocking, and S. Kinneen. 2004. Development of habitat-based escapement goals for coho salmon in Norton Sound drainages. Annual report prepared for the Norton Sound Fishery Disaster Relief Fund by LGL Alaska Research Associates and Norton Sound Economic Development Corporation, Anchorage, Alaska

Nemeth, M. J., B. Bocking, and S. Kinneen. 2005. Freshwater habitat as a predictor of coho salmon smolt production in two Norton Sound rivers: an initial study to support the development of habitat-based escapement goals. Annual report prepared for the Norton Sound Fishery Disaster Relief Fund by LGL Alaska Research Associates and Norton Sound Economic Development Corporation, Anchorage, Alaska.

Nemeth, M. J., B. C. Williams, R. C. Bocking, and S. N. Kinneen. 2009. Freshwater habitat and coho salmon production in two rivers: an initial study to support the development of habitat-based escapement goals in Norton Sound, Alaska. *In* C. C. Krueger and C. E. Zimmerman, editors. 2009. Pacific salmon: ecology and management of western Alaska's populations. American Fisheries Society Symposium 70, Bethesda, Maryland.

Nickelson, T. E., J. D. Rodgers, S. L. Johnson, and M. F. Solazzi. 1992. Seasonal changes in habitat use by juvenile coho salmon (*Oncorhynchus kisutch*) in Oregon coastal streams. Canadian Journal of Fisheries and Aquatic Sciences 49:783-789.

Norton Sound Scientific Technical Committee (NTSSC). 2002. Research and restoration plan for Norton Sound salmon. 125 p.

Nowacki, G., P. Spencer, M. Fleming, T. Brock, and T. Jorgenson. 2001. Ecoregions of Alaska: 2001. U.S. Geological Survey Open-File Report 02-297 (map).

Olson, S. A., and M. C. Brouillette. 2006. A logistic regression equation for estimating the probability of a stream in Vermont having intermittent flow. U.S. Geological Survey Scientific Investigations Report 2006-5217.

Parks, B., and R. J. Madison. 1985. Estimation of selected flow and water-quality characteristics of Alaskan streams. Water-Resources Investigations Report 84-4247, U.S. Geological Survey, Anchorage, Alaska.

Peñas, F. J., F. Fernández, M. Calvo, J. Barquín, and L. Pedraz. 2011. Influence of data sources and processing methods on theoretical river network quality. Limnetica 30:197-216

Rabus, B., M. Eineder, A. Roth, and R. Bamler. 2003. The shuttle radar topography mission–a new class of digital elevation models acquired by spaceborne radar. ISPRS Journal of Photogrammetry and Remote Sensing 57:241–262.

Reeves, G. H., F. H. Everest, and T. E. Nickleson. 1989. Identification of physical habitats limiting the production of coho salmon in western Oregon and Washington. General Technical Report PNW-GTR-245. U.S. Department of Agriculture, Forest Service, Pacific Northwest Research Station, Portland, Oregon.

Rodgers, J. F., M. F. Solazzi, S. L. Johnson, and M. A. Buckman. 1992. Comparison of three techniques to estimate juvenile coho salmon populations in small streams. North American Journal of Fisheries Management 12:79-86.

Rosell, F., O. Bozer, P. Collen, and H. Parker. 2005. Ecological impact of beavers *Castor fiber* and *Castor canadensis* and their ability to modify ecosystems. Mammal Review 35:248–276. doi: 10.1111/j.1365-2907.2005.00067.x

Rossi, R. E., D. J. Mulla, A. G. Journel, and E. H. Franz. 1992. Geostatistical tools for modeling and interpreting ecological spatial dependence. Ecological Monographs 62:277-314.

Sheer, M. B., and E. A. Steel. 2006. Lost watersheds: barriers, aquatic habitat connectivity, and salmon persistence in the Willamette and Lower Columbia River basins. Transactions of the American Fisheries Society 135:1654-1669.

Simpson, J. J., G. L. Hufford, M. Fleming, J. S. Berg, and J. B. Ashton. 2002. Long-term climate patterns in Alaskan surface temperature and precipitation and their biological consequences. IEEE Transactions on Geosciences and Remote Sensing 40:1164–1184. (http://www.climatesource.com/docs/csguid.pdf; http://www.climatesource.com/ak/fact_sheets/fact_precip_ak.html)

Smith, H. 1997. Nome River water control structures. BLM-Alaska Open File Report 62. U.S. Department of the Interior, Bureau of Land Management, Anchorage, Alaska.

South, L. M. 2010. Remote sensing-GIS-based approach to identify and model spawning habitat for fall chum salmon in a sub-Arctic, glacially-fed river. Master's thesis. University of Alaska, Fairbanks, Alaska.

Steel, E. A., B. E. Feist, D. Jenson, G. R. Pess, M. B. Sheer, J. Brauner, and R. E. Bilby. 2004. Landscape models to understand steelhead (*Oncorhynchus mykiss*) distribution and help prioritize barrier removals in the Willamette Basin, OR, U.S.A. Canadian Journal of Fisheries and Aquatic Sciences 61:999–1011.

Steel, E. A., D. W. Jensen, K. M. Burnett, K. Christiansen, J. C. Firman, B. E. Feist, K. J. Anlauf, and D. P. Larsen. 2012. Landscape characteristics and coho salmon (*Oncorhynchus kisutch*) distributions: explaining abundance versus occupancy. Canadian Journal of Fisheries and Aquatic Sciences 69:457-468.

Takaku, J., and T. Tadono. 2009. PRISM on-orbit geometric calibration and DSM performance. IEEE Transactions on Geoscience and Remote Sensing 47:4060-4073.

Thompson, W. L., and D. C. Lee. 2000. Modeling relationships between landscape level attributes and snorkel counts of Chinook salmon and steelhead parr in Idaho. Canadian Journal of Fisheries and Aquatic Sciences 57:1834-1842.

U.S. Army Corps of Engineers [USACE]. 2000. HEC-HMS hydrologic modelling system user's manual. Hydrologic Engineering Center, Davis, California. 178 pp.

U. S. Geological Survey [USGS]. 2012. Appendix F - Final Report of the National Enhanced Elevation Assessment. Submitted by Dewberry. March 29, 2012. Pp 671-687.

Wang, X., and Z.-Y. Yin. 1998. A comparison of drainage networks derived from digital elevation models at two scales. Journal of Hydrology 210:221–241.

Whited, D. C., J. S. Kimball, M. S. Lorang, and J. A. Stanford. 2013. Estimation of juvenile salmon habitat in Pacific Rim rivers using multiscalar remote sensing and geospatial analysis. River Research Applications 29:135–148. doi: 10.1002/rra.1585

Williams, B. C., M. J. Nemeth, and C. Lean. 2010. Abundance and marine survival of coho salmon smolts from the Nome River, Alaska, 2006-2009. Report prepared for the Arctic-Yukon-Kuskokwim Sustainable Salmon Initiative by LGL Alaska Research Associates, Inc. and Norton Sound Economic Development Corporation. 52 p.

Wirth L., A. Rosenberger , A. Prakash , R. Gens , F. J. Margraf, and T. Hamazaki. 2012. A remote-sensing, GIS-based approach to identify, characterize, and model spawning habitat for fall-run chum salmon in a sub-Arctic, glacially fed river. Transactions of the American Fisheries Society 141:1349-1363.

Wissmar, R. C., R. K. Timm, and M. D. Bryant. 2010. Radar-derived digital elevation models and field-surveyed variables to predict distributions of juvenile coho salmon and Dolly Varden in remote streams of Alaska. Transactions of the American Fisheries Society 139:288-302.

Wohl, E., and D. Merrit. 2005. Prediction of mountain stream morphology. Water Resources Research 41:W08419, doi: 10.1029/2004SR003779.

Woll, C., A. Prakash, and T. Sutton. 2011. A case-study of in-stream juvenile salmon habitat classification using decision-based fusion of multispectral aerial images. Applied Remote Sensing Journal 2:37-46.

Zhang, H. and G. Huang. 2009. Building channel networks for flat regions in digital elevation models Hydrological Processes 23:2879–2887 DOI: 10.1002/hyp.7378

IX. DELIVERABLES

1. Full-mosaic 10-m resolution DEMs for the Nome River basin from four pairs of Phased Array L-Band Synthetic Aperture Radar (PALSAR) fine-beam data with interferometry.
2. Full-mosaic 2.5-m resolution DEMs for the Nome River basin from three swaths of the ALOS-Panchromatic Remote-sensing Instrument for Stereo Mapping (PRISM) triplet stereo imagery
3. Digital stream network for the Nome River basin modeled from the final PALSAR-derived DEM mosaic.
4. Digital stream network for the Nome River basin modeled from the final PRISM-derived DEM mosaics.
5. GIS map of a water mask in Esri shapefile format of the Nome River and its tributaries, derived from ALOS PRISM 2.5-m ortho-image mosaic.
6. GIS maps, in Esri shapefile format, of polygons delineating Nome River basin valley floor areas on the ALOS-PRISM 2.5-m DEM at or below: 1) the channel centerline elevation; 2) one wetted channel depth elevation above the channel centerline elevation; 3) three wetted channel depth elevations above the channel centerline elevation; and 4) five wetted channel depth elevations above the channel centerline elevation.
7. Digital stream network, along with a large suite of modeled hydrogeomorphic characteristics, for the Nome River basin modeled from the final 2.5-m PRISM-derived DEM mosaics and the PRSIM ortho- image mosiac.

8. NetMap terrain characterization for the Nome River basin from the final the final 2.5-m PRISM-derived DEM mosaics.

9. Dataset collected at 72 sites along the Nome River identified in the field as open water, ice over water, frozen to the bottom, and water over ice. Data are documented, processed for QA/QC, and available in Excel spreadsheet and Esri shapefile formats. (Summer 2009)

10. Ice classification from SAR data. (Summer 2013)

11. Dataset of 1) habitat characteristics and 2) valley characteristics collected in the field at the habitat-unit scale for 49 km of the Nome River and 14 km of the tributaries (Osborne Creek, Lillian Creek, Buster Creek, Darling Creek, HooDoo Gulch, Sampson Creek, Hobson Creek, Rocky Mountain Creek, Sulfur Creek, and Christian Creek); also 3) relative fish abundances for juvenile coho salmon by size class, for adult coho, chum, pink, and sockeye, as well as for Dolly Varden, whitefish, and grayling (>100 mm) from snorkel surveys in 193 Nome River habitat units and in 114 tributary habitat units. Data are documented, processed for QA/QC, and available in an Excel spreadsheet. (Summer 2009)

12. Dataset on fish scales and length-at-age for 332 juvenile coho salmon collected from minnow traps at 34 sampling locations throughout the basin. All data are documented, processed for QA/QC, and available in an Excel spreadsheet. (Summer 2009)

13. Guritz, R., D.J. Miller, and K.M. Burnett. 2009. Mapping Nome River Salmon Habitat using PRISM, PALSAR, and TerraSAR-X data. Presentation to at the 3rd ALOS Joint PI Symposium, Kona, Hawaii, November 9-13. http://www.asf.alaska.edu/content/pi_symp/Guritz_R._softtools.pdf

14. Guritz, R., D.J. Miller, and K.M. Burnett. 2009. Study of the Nome River Salmon Habitat using PRISM, PALSAR, and TerraSAR-X data. Presentation at the 36th Annual Meeting of the Alaska Chapter of the American Fisheries Society, Fairbanks, AK, November 3-5.

15. Burnett, K.M., and K. Vance-Borland. 2010. Landscape predictors of coho salmon. Presentation at the Arctic-Yukon-Kuskokwim Sustainable Salmon Initiative mini-symposium to report on project status and findings, Nome, AK, March 11.

16. Guritz, R., D.J. Miller, and K.M. Burnett. 2010. Advances in mapping and modeling salmon habitat using PRISM, PALSAR, and TerraSAR-X data. International Geoscience and Remote Sensing Society, 30th Annual meeting, July 25-30, 4-p abstract will be published in the proceedings.

17. Burnett, KM. 2008. Landscape predictors of coho salmon. Alaska Sustainable Salmon Fund Semiannual Performance Report.

18. Burnett, KM. 2009. Landscape predictors of coho salmon. Alaska Sustainable Salmon Fund Semiannual Performance Report.

19. Burnett, KM. 2009. Landscape predictors of coho salmon. Alaska Sustainable Salmon Fund Semiannual Performance Report.

20. Burnett, KM. 2010. Landscape predictors of coho salmon. Alaska Sustainable Salmon Fund Semiannual Performance Report.

21. Burnett, KM. 2010. Landscape predictors of coho salmon. Alaska Sustainable Salmon Fund Project Completion Report – Phase 1 of 2.

22. Burnett, KM. 2011. Landscape predictors of coho salmon. Alaska Sustainable Salmon Fund Project Completion Report.

X. PROJECT DATA

1. Full-mosaic 10-m resolution DEMs for the Nome River basin from four pairs of Phased Array L-Band Synthetic Aperture Radar (PALSAR) fine-beam data with interferometry.
2. Full-mosaic 2.5-m resolution DEMs for the Nome River basin from three swaths of the ALOS-Panchromatic Remote-sensing Instrument for Stereo Mapping (PRISM) triplet stereo imagery
3. Digital stream network for the Nome River basin modeled from the final PALSAR-derived DEM mosaic.
4. Digital stream network for the Nome River basin modeled from the final PRISM-derived DEM mosaics.
5. GIS map of the Nome River and its tributaries from directly interpreting ALOS PRISM 2.5-m ortho-image mosaic.
6. Digital stream network, along with a large suite of modeled hydrogeomorphic characteristics, for the Nome River basin modeled from the final 2.5-m PRISM-derived DEM mosaics and the PRSIM ortho- image mosiac.
7. NetMap terrain characterization for the Nome River basin from the final the final 2.5-m PRISM-derived DEM mosaics.
8. Dataset collected at 72 sites along the Nome River identified in the field as open water, ice over water, frozen to the bottom, and water over ice. Data are documented, processed for QA/QC, and available in an Excel spreadsheet. (Summer 2009)
9. Feasibility assessment for ice classification from SAR data.
10. Dataset of habitat characteristics collected in the field at the habitat-unit scale for 49 km of the Nome River and 14 km of the tributaries (Osborne Creek, Lillian Creek, Buster Creek, Darling Creek, HooDoo Gulch, Sampson Creek, Hobson Creek, Rocky Mountain Creek, Sulfur Creek, and Christian Creek). Data are documented, processed for QA/QC, and available in an Excel spreadsheet. (Summer 2009)
11. Dataset of relative fish abundances for juvenile coho salmon by size class, for adult coho, chum, pink, and sockeye, as well as for Dolly Varden, whitefish, and grayling (>100 mm) from snorkel surveys in 193 Nome River habitat units and in 114 tributary habitat units. All data are documented, processed for QA/QC, and available in an Excel spreadsheet. (Summer 2009)
12. Dataset of valley characteristics collected in the field at the reach scale for 49 km of the Nome River and 14 km of the tributaries (Osborne Creek, Lillian Creek, Buster Creek, Darling Creek, HooDoo Gulch, Sampson Creek, Hobson Creek, Rocky Mountain Creek, Sulfur Creek, and Christian Creek). All data are documented, processed for QA/QC, and available in an Excel spreadsheet. (Summer 2009)
13. Dataset on fish scales and length-at-age for 332 juvenile coho salmon collected from minnow traps at 34 sampling locations throughout the basin. All data are documented, processed for QA/QC, and available in an Excel spreadsheet. (Summer 2009)

XI. ACKNOWLEDGEMENTS

This project would not have been possible without the help of many individuals and organizations. The Fisheries Research and Development Program of the Norton Sound Economic Development Corporation (NSEDC) provided logistical and personnel support for winter and summer field sampling. Charlie Lean of NSEDC, in particular, provided direction and local knowledge concerning the Nome River, natural history of Nome River salmon, and guidance concerning winter sampling. We also thank Kevin Keith and Sye Larsen of NSEDC for assisting with winter fieldwork. Summer field sampling required a large team of surveyors and we thank: Loretta Ellenburg and Bruce Hansen of the USFS Pacific Northwest Research Station; Steve Crawford, Robert Kirchner, Justin Priest, and Ben Williams of LGL Alaska Research Associates; and Adrian Barr, Kevin Keith, and Reba Lean of NSEDC. This project was funded by the Arctic-Yukon-Kuskokwim Sustainable Salmon Initiative with additional support from Norton Sound Economic Development Corporation, U.S. Forest Service, and U.S. Geological Survey. The American Recovery and Reinvestment Act of 2009 provided additional funding for the project. Use of trade, product, or firm names is for descriptive purposes only and does not imply endorsement by the U.S. Government.

XII. APPENDICES

Rick Guritz, Remote Sensing Analyst with the University of Alaska Fairbanks, acquired satellite data then generated and evaluated the DEMs. Dan Miller, Senior Scientist with Earth Systems Institute, extracted the water mask, delineated stream networks, and derived hydrogeomorphic attributes.

Christian Zimmerman, Research Fishery Biologist at the USGS Alaska Science Center (ASC), and Matt Nemeth, Fishery Biologist at LGL Alaska Research Associates, Inc. (LGL), collected elevation and location data in the field for 16 geodetic control points

Rick Guritz, Ken Vance-Borland, Spatial Analyst at Oregon State University, and Kelly Burnett, Research Fish Biologist with the USFS, wrote a successful proposal to the German Aerospace Center (DLR) to acquire TerraSAR-X polarimetric StripMap radar images (3-m resolution).

Rebecca Flitcroft, Ken Vance-Borland, and Kelly Burnett developed the field data-collection protocol with input from Rick Guritz and others on the team. Christian Zimmerman, Matt Nemeth, and NSEDC personnel (Kevin Keith, Sye Larson, and Charlie Lean) collected data in the Nome River during March 25 – 28, 2009 and April 8-10, 2009.

Rebecca Flitcroft, Ken Vance-Borland, Matt Nemeth, Christian Zimmerman, and Kelly Burnett developed the field data-collection protocol with input from Dan Miller and others on the team. Matt Nemeth and Kelly Burnett supervised field crew training and data collection 13 - 24 August 2009. Field crews were from the USFS Pacific Northwest Research Station (Loretta Ellenburg and Bruce Hansen), LGL (Steve Crawford, Robert Kirchner, Justin Priest, and Ben Williams), and the NSEDC (Adrian Barr, Kevin Keith, and Reba Lean).

Christian Zimmerman and Matt Nemeth designed the database structure and then entered and conducted QA/QC for all winter field data. Loretta Ellenburg, Bruce Hansen, and Kelly Burnett designed the database structure for summer habitat and snorkeling data. Loretta Ellenburg and Bruce Hansen entered, catalogued, and conducted QA/QC for all summer habitat and snorkeling data. Matt Nemeth and Justin Priest designed the database structure and then entered and conducted QA/QC for all minnow trapping data.

Mark Meleason, Statistician with Oregon State University; Nicholas Som, Statistician with US. Fish and Wildlife Service; Rebecca Flitcroft and Kelly Burnett initiated statistical modeling of relationships between juvenile coho salmon, habitat data, hydrogemorphic variables, and landscape characteristics.